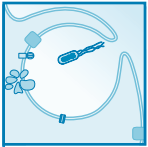


VOLTAGE-GATED PROTON CHANNELS: MOLECULAR BIOLOGY, PHYSIOLOGY, AND PATHOPHYSIOLOGY OF THE H_V FAMILY

Thomas E. DeCoursey

Department of Molecular Biophysics and Physiology, Rush University Medical Center, Chicago, Illinois



DeCoursey TE. Voltage-Gated Proton Channels: Molecular Biology, Physiology, and Pathophysiology of the H_V Family. *Physiol Rev* 93: 599–652, 2013; doi:10.1152/physrev.00011.2012.—Voltage-gated proton channels (H_V) are unique, in part because the ion they conduct is unique. H_V channels are perfectly selective for protons and have a very small unitary conductance, both arguably manifestations of the extremely low H⁺ concentration in physiological solutions. They open with membrane depolarization, but their voltage dependence is strongly regulated by the pH gradient across the membrane (ΔpH), with the result that in most species they normally conduct only outward current. The H_V channel protein is strikingly similar to the voltage-sensing domain (VSD, the first four membrane-spanning segments) of voltage-gated K⁺ and Na⁺ channels. In higher species, H_V channels exist as dimers in which each protomer has its own conduction pathway, yet gating is cooperative. H_V channels are phylogenetically diverse, distributed from humans to unicellular marine life, and perhaps even plants. Correspondingly, H_V functions vary widely as well, from promoting calcification in coccolithophores and triggering bioluminescent flashes in dinoflagellates to facilitating killing bacteria, airway pH regulation, basophil histamine release, sperm maturation, and B lymphocyte responses in humans. Recent evidence that hH_V1 may exacerbate breast cancer metastasis and cerebral damage from ischemic stroke highlights the rapidly expanding recognition of the clinical importance of hH_V1.

I.	DEFINITIONS AND BACKGROUND	599
II.	HISTORY: KEY DISCOVERIES	602
III.	THE GENE: PHYLOGENETIC DIVERSITY	604
IV.	THE PROTON CHANNEL MOLECULE	605
V.	KEY PROPERTIES OF H_V1	610
VI.	PHYSIOLOGICAL ROLES: DIVERSE...	626
VII.	ROLES IN MAMMALIAN AND HUMAN...	630
VIII.	ROLES IN INNATE IMMUNITY	634
IX.	MANIFESTATIONS IN THE KO MOUSE...	639
X.	HUMAN MUTATIONS	640
XI.	FUTURE DIRECTIONS	640

I. DEFINITIONS AND BACKGROUND

A. What Are Voltage-Gated Proton Channels?

Voltage-gated proton channels encompass a family of proton specific ion channels that open and close with a probability that depends strongly on both membrane potential and the pH gradient across the membrane. In this review, “proton channel” or “H_V1” (see sect. IIIB) designates the voltage-gated proton channel. Proton conduction is also a feature of a large number of other biologically important molecules. Proton conduction in inorganic systems is an important topic as well, for example, in hydrogen fuel cell

membranes (147, 265, 401). This review will focus on the voltage-gated proton channel; other molecules will be included when they have directly relevant or heuristic properties.

A number of distinctive if not unique properties are shared by every voltage-gated proton channel studied to date by voltage clamp. These include 1) proton specific conduction; 2) opening in response to membrane depolarization, increased pH_o, and decreased pH_i; 3) extremely small unitary conductance; 4) strong temperature dependence of both conduction and gating; and 5) the absence of inactivation. The proton selectivity is thought to be perfect (proton specificity); no evidence that other ions can permeate has been presented (104). The extraordinary modulation of the voltage-dependent gating process by pH appears to be a universal feature of these channels; increasing pH_o or decreasing pH_i by one unit shifts the entire proton conductance g_H-V relationship by 40 mV to more negative voltages (74, 104). The single-channel conductance is very small, ~10³ times smaller than most ion channels (75); this property likely reflects the fact that the proton concentration is 10⁶ smaller than the concentration of the main ions in physiological solutions (104). The temperature dependence of both conductance and gating kinetics is greater than almost all other ion channels, strongly suggesting extraordinary complexity of both permeation and gating (54, 112, 269, 270). The

lack of inactivation (113) has practical consequences, in that decay of proton current invariably indicates that H^+ flux is large enough to change pH significantly, thereby decreasing the driving force ($V-E_H$). A final property that once helped to define proton currents, but is no longer universal, is high sensitivity to inhibition by Zn^{2+} , Cd^{2+} , and other polyvalent metal cations. Although most proton channels studied to date share high metal sensitivity, recent expansion of the H_V1 phylogenetic tree has revealed several species with weak Zn^{2+} sensitivity (432, 462, 489). Because Zn^{2+} sensitivity in hH_V1 is determined almost entirely by two histidine residues (360, 416), and the capacity to be inhibited by Zn^{2+} confers no obvious evolutionary advantage, it is entirely possible that some voltage-gated proton channels may lack a metal binding site altogether.

This field has always been blessed with abundant reviews; in fact, at last count, the ratio of original studies to reviews was just 1.64. Recent reviews, most of which focus on more restricted areas than the present one, include References 62, 102, 103, 105, 106, 110, 123, 143, 254, 302, 354, 496. A series of focused reviews on proton channels is available online in *Wiley Interdisciplinary Reviews: Membrane Transport and Signaling* (60, 121, 156, 323, 357, 420).

B. How Are Protons Transported Through Membranes?

Protons rarely permeate biological membranes on their own. Despite a large literature that demonstrates that the permeability of protons through membranes is several orders of magnitude higher than that of other cations (96, 104, 196, 198), in practical terms, the flux of protons through biological membranes is dwarfed by the flux ascribable to proton transporters. Nearly all proton movement across biological membranes is mediated by specialized membrane proteins designed to transport protons in an orderly and highly regulated manner.

A large number of important molecules contain proton transport pathways that are essential to the function of the molecule. In many of these, the conduction pathway does not cross the entire membrane and is coupled to other functions of the molecule. These include bioenergetic molecules in the mitochondrial electron transport chain, photosynthetic molecules, proton pumps, and ATP synthases that use the energy from ATP to pump protons or use the electrochemical energy stored in a proton gradient to generate ATP, and numerous others (45, 167, 223, 277, 477, 523). Despite the requirement that protons move to specific locations at precise times in these molecules, it does not necessarily follow that the pathway used by protons is (or needs to be) perfectly selective for protons. For example, the reaction center of *Rhodobacter sphaeroides* has a proton pathway that leads to the secondary quinone (Q_B). Mutation of two Asp residues in the middle of the proton path-

way severely restricts proton conduction, but this property can be “rescued” by any of several small weak acids that act inside the pathway (483). With the assumption that the mutations do not alter the rest of the molecule, the proton channel in the reaction center is evidently not selective for protons at least up to the point of these mutations, which is presumably where the weak acids do their job.

Selectivity is conceptually more clear-cut, and experimentally more accessible for molecules that transport protons all the way across membranes. **TABLE 1** lists a number of these molecules. Here the question is whether any other ions can follow the same pathway. Electrophysiological measurements can be done according to well-established approaches. Under voltage-clamp conditions, the reversal potential of the current that flows through the molecule of interest is determined under various ionic conditions. The reversal potential is then compared with the Nernst potential calculated for the ionic conditions. If multiple ionic species are present, the Goldman-Hodgkin-Katz voltage equation (184, 216, 221) can be used for this purpose (e.g., *Eqs. 1* and *2* below). Absolute measurements are complicated by several factors: voltage offsets, “leak” currents that reflect current pathways that are extraneous to the molecule of interest, liquid junction potentials (24, 375), etc. It may be preferable, or more convenient, to evaluate the change of reversal potential when solutions are changed. In the case of voltage-gated proton channels, the reversal potential typically changes by nearly the amount predicted by the Nernst equation when pH is changed, but does not change when other ions are replaced, leading to the conclusion that this channel is specific (perfectly selective) for protons (104, 362).

C. Proton Conduction in Water and in Proteins

Four unique and crucial aspects of the diffusion of protons are 1) the rapid transfer of protons between water molecules, 2) the equivalence of the three protons in H_3O^+ , 3) the tiny size of the proton itself, and 4) the delocalization of protons in a hydrogen bonded array. Proton transfer normally occurs at hydrogen bonds (179, 230, 289, 365, 399, 434), although proton transfer in the absence of hydrogen bonds was reported recently in π -stacked structures (183). Because of its special conduction mechanism, proton mobility in water is about five times greater than that of other ions. Another consequence is that the proton can negotiate pathways that other ions cannot even consider. A large number of biologically important molecules have taken advantage of the special properties of protons to create proton-selective pathways through proteins and across membranes.

The facility of proton conduction reflects the nature of proton conduction in water, namely, the Grotthuss mechanism

Table 1. Reported selectivity of various proton conducting molecules

Channel	Ratio	Reference Ion	Criterion	Key Residue(s)	Reference Nos.
Voltage-gated H ⁺ H _V 1	$>2 \times 10^8$	P_D/P_{TMA}	V_{rev}	Asp ¹¹² (hH _V 1)	107, 362
	$\geq 10^7$	P_H/P_{TMA}	V_{rev}	Asp ⁵¹ (kH _V 1)	74, 114, 462
	$\geq 10^6$	$P_H/P_{Cs,K,Na}$	V_{rev}		124, 187, 250
	$\geq 1.8 \times 10^6$	P_H/P_{Cl}	V_{rev}		187
<i>Elodea</i> H ⁺	10^8 to 10^9	P_H/P_K	V_m	—	328
Channelrhodopsin-2	$3-6 \times 10^6$	P_H/P_{Na}	V_{rev}	Glu ⁹⁰	32, 142
Channelrhodopsin-1	High	P_H/P_{Na}	V_{rev}	Glu ¹⁶²	364
M ₂ (full length)	10^7	P_H/P_K	Flux		331
	10^4 to 10^6	P_H/P_K	Flux		288
M ₂ (residues 22–62)	3.6×10^5	P_H/P_K	Flux	His ³⁷	402
BM ₂	High	P_H/P_K	V_{rev}	His ¹⁹	310, 345
TRP-ML1	10^4 to 10^6	P_H/P_{Cs}	V_{rev}	—	467
TRPM7	High	P_H/P_{NMDG}	V_{rev}	Asp ¹⁰⁵⁴	242, 386
Sour taste cell proton current	High	P_H/P_{Na}	V_{rev}		67
Sugar sensor SGLT3	High	P_H/P_{Na}	V_{rev}	Glu ⁴⁵⁷	36
Arachidonic acid-induced, EAAT4 glutamate transporter	High	P_H/P_{Na}	V_{rev}	—	152
Colicin A	1.2×10^4	P_H/P_K	V_{rev}	—	459
Mutant aquaporin	$8-34 \times 10^3$	P_H/P_K	I	R195V, R195S	295, 524
Taste receptor	4×10^3	P_H/P_K	V_{rev}	—	261
TRPV1	87–1,127	P_H/P_{Cs}	V_{rev}		205, 509
Na ⁺ (V-gated)	252–274	P_H/P_{Na}	V_{rev}		346, 347
Gramicidin A	43–344	P_H/P_{Na}	V_{rev}		363
Synthetic proton channel (LSLLLSL) ₃	>40	g_H/g_{Li}	i_H detection	none	283
Na ⁺ (amiloride sensitive)	7–25	P_H/P_{Na}	V_{rev}		181, 394
ASIC1a	≥ 5	P_H/P_{Na}	V_{rev}	—	69

Permeability ratios were determined from measured V_{rev} values using the Goldman-Hodgkin-Katz (GHK) equation (216), from the assumption that membrane potential V_m measurements reflect a diffusion potential generated by the cations present, from detection of single-channel currents i_H , from I using the GHK current equation, or from flux estimates. D, deuterium; NMDG, *N*-methyl-D-glucamine. It should be noted that despite the lower limits given in this table, there is no evidence that H_V1 is less than perfectly selective.

(93, 94), traditionally envisioned as protons hopping from one water molecule to the next. The crucial distinction from the conduction of other ions is that H⁺ (and OH[−]) are part of the bulk solvent, and their diffusion is facilitated by taking short-cuts “through” water molecules (90). The proton in water is essentially always attached to a water molecule, forming a hydronium ion, H₃O⁺ (31, 87). Eigen and colleagues emphasized the stability of the H₉O₄⁺ complex (the Eigen cation) consisting of the hydronium ion and its first hydration shell, within which the proton is delocalized (140, 141, 517). Hydrogen bond rearrangement among second shell waters was considered rate determining for proton transport, with the result being structural diffusion (*Strukturwanderung*) or drift of the entire H₉O₄⁺ complex (140, 141, 517). This view was further refined by Agmon, who proposed that that the rate-limiting step involves breaking a second shell hydrogen bond (5, 317); and that proton mobility results from alternating isomerization between H₉O₄⁺ (the “Eigen cation”) and H₅O₂⁺ [the “Zundel cation,” which incidentally was first conceived by Mau-

rice L. Huggins (229, 230), and shortly thereafter by Lattimer and Rodebush (279)]. The current view, espoused by Agmon, Voth, and co-workers (316) has evolved a bit further. Protons in water exist mainly as Eigen cations, with the Zundel cation existing only as a transition state. Cleavage of a second shell hydrogen bond correlates with partner swapping during the “special pair dance,” the lurid details of which should be read in their original, unexpurgated format (316), whereas successful proton transfer is a somewhat slower process.

In a narrow, presumably single-file channel, geometric constraints preclude Eigen cation formation, and protons can only move in a linear path from one water to the next (59, 452). Intriguingly, a “linearized” Eigenesque cation, manifested as the extra proton delocalizing over two water molecules in the channel, was observed in *ab initio* simulations of such a virtual channel (452). Also in contrast to proton transfer in bulk water, breaking a hydrogen bond is not a necessary precondition to proton transfer in a water wire

(452). In any case, essential features of HBC or Grotthuss conduction are that protons are transferred via hydrogen bond rearrangement (179, 230, 279) and that the identity of the conducted proton may change with each proton transfer event (31, 90). One proton enters the channel, and a different proton emerges from the other end, as evident in **FIGURE 1**.

Proton conduction through channels differs from that of all other ions. Nagle and Morowitz (365) proposed hydrogen-bonded chain (HBC) conduction to explain how proton selective conduction might be achieved in membrane proteins (**FIGURE 1**). Any combination of water molecules and amino acid side chains capable of forming a hydrogen bonded chain that spans the membrane, even if not simultaneously or continuously, comprises a potential pathway for proton permeation. A “water wire” is a special case, in which the entire chain consists of water molecules. The gramicidin channel is a classical example of a water wire; it contains a single-file row of 8–12 water molecules (292). A water wire enables proton conductance, but does not enforce proton selectivity. In fact, gramicidin channels are nonselective among cations, although their proton permeability and conductance (normalized to permeant ion concentration) considerably exceeds that of all other ions (219, 363) (**TABLE 1**). The higher conductance of gramicidin to protons reflects the Grotthuss mechanism in which, unlike ordinary cations, a proton does not have to wait for water in the pore to move out of the way, it hops across or through the water molecules.

A novel variant of adventitial proton permeation was proposed for nonselective endplate channels. The possibility that protons might hop by a Grotthuss-like mechanism

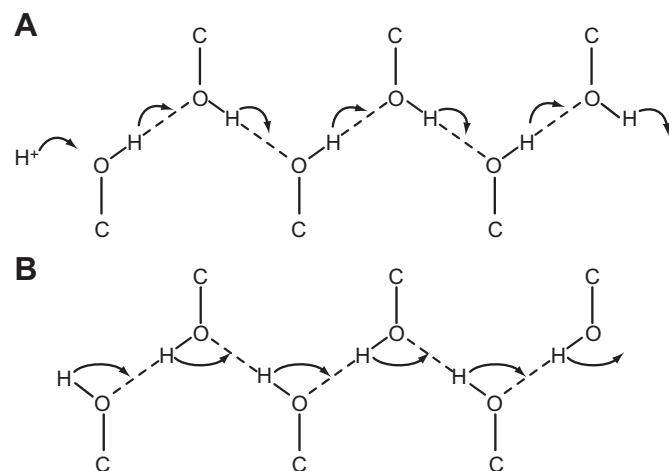


FIGURE 1. The hydrogen bonded chain (HBC) mechanism for proton conduction through proteins. Shown are hydroxyl groups forming a continuous HBC. *A*: each proton hops one position along the chain, with the final group releasing a proton into the distal solution. *B*: after the transfer, the chain is not able to accept another proton from the proximal side until all the groups have reoriented. Permeation of OH⁻ occurs when a proton leaves the distal end of the HBC (neutralizing OH⁻ to form H₂O), and the defect migrates by retrograde H⁺ hopping. [Redrawn from Nagle and Morowitz (365).]

through the channel when it is occupied by NH₄⁺ was proposed to explain anomalously large permeability to NH₄⁺ (484). Charge transported by H⁺ in this way would be indistinguishable electrophysiologically from that carried by NH₄⁺.

II. HISTORY: KEY DISCOVERIES

The idea of a voltage-gated proton channel was first proposed by Woody Hastings and colleagues in 1972 (161). A number of bioluminescent marine dinoflagellates such as the evocatively named *Noctiluca (miliaris) scintillans* (95) or *Gonyaulax polyedra* (39, 161) emit light in response to mechanical stimulation. The triggering mechanism involves an action potential in the tonoplast, the membrane enclosing a large central vacuole. The action potential activates a proton conductance (373), which mediates rapid proton flux from the vacuole at pH 3.5 (374) into small vesicles called scintillons that contain luciferin and luciferase (161, 202, 438). The scintillons are the sources of the light flashes (132), which result from activation of luciferase by low pH (266, 438). Nearly 40 years after the existence of voltage-activated proton channels in dinoflagellates was conceived, a bona fide proton channel gene was identified in a nonbioluminescent dinoflagellate, *Karlodinium veneficum* (462).

A decade after Hastings' groundbreaking proposal, elegant studies of snail (*Helix aspersa*) neurons by Roger Thomas and Bob Meech revealed direct voltage-clamp evidence for voltage-gated proton channels (492). Byerly, Meech, and Moody (53) characterized the main biophysical properties of proton currents in another snail, *Lymnaea stagnalis*, emphasizing that proton channels were distinct from other known ion channels. Perhaps because proton currents resemble delayed rectifier K⁺ currents (sigmoid activation during depolarization, exponential deactivation on repolarization, faster gating at large positive or negative voltages; qualitatively similar inhibition by divalent cations, superficially similar inhibition by weak bases), many casual observers suspected that proton currents passed adventitiously through other channels, or even through the phospholipid bilayer membrane itself without the benefit of a protein pathway. Despite exhaustive evidence to the contrary (113), this notion was not completely dispelled until the proton channel gene was finally identified in 2006 (416, 432).

Studying *Helix pomatia*, Doroshenko, Kostyuk, and Martynyuk (130) reinforced the important observations of Byerly et al. (53) in *Lymnaea stagnalis*, that lowering pH_i shifted the g_H-V relationship dramatically negatively, while decreasing pH_o shifted the curve positively. Studying *Ambystoma* (salamander) oocytes, Mike Barish and Christiane Baud (22) found that amphibia have similar voltage-gated proton currents. Martyn Mahaut-Smith (314) showed that proton currents in *Helix* neurons were 80 times more sen-

sitive to inhibition by Zn^{2+} than were Ca^{2+} currents. A decade after their discovery in snail neurons, proton currents were identified in mammalian cells, rat alveolar epithelial cells (99). The exodus from the realm of phylogenetic exotica into the anthropocentric mainstream was completed 2 years later, when proton currents were reported in human cells (33, 111, 263) and cell lines (124).

In the lull before stormy attempts to identify a proton channel gene, the number of cells and species expressing proton channels mushroomed, the properties of proton channels were systematically explored, and progress toward understanding functions continued. The number of species with proton currents confirmed by voltage-clamp increased from 2 in 1984, to 5 by 1994 (113), then 11 by 2003 (104), to at least 2 dozen species with genes highly homologous to hH_V1 in 2008 (106). At latest count, there are at least 37 high confidence H_V1 homologs in assorted species (FIGURE 2), along with quite a few other probable but lower confidence homologs (S. M. E. Smith, personal communication). It was determined that the dependence of gating on pH_i and pH_o could be expressed simply in terms of the pH gradient (ΔpH), with a 40-mV shift of the g_{H^+} -V relationship for a one unit change in ΔpH (74). Astonishingly, this “Rule of

Forty” continues to hold true even for a large series of mutant proton channels (415). The conductance and gating kinetics of proton channels were found to vary more strongly with temperature than almost any other ion channel (54, 76, 112, 269, 270). Deuterium was shown to permeate proton channels just 50% as well as protons (107). The unitary conductance was found to vary with pH_i but not pH_o and was estimated to be ~ 15 fS at physiological pH (75). A crucial discovery that shed light on functions of proton currents in phagocytes was the observation of profoundly enhanced gating under conditions when NADPH oxidase was active (19). The proposal by Henderson, Chappell, and Jones that voltage-gated proton channels exist in human neutrophils where they serve to compensate charge for the electrogenic activity of NADPH oxidase (208–210) was confirmed by demonstrations that human neutrophils have voltage-gated proton channels (111), that NADPH oxidase is electrogenic (442), and that NADPH oxidase is inhibited by depolarization (120).

The *Sturm und Drang* of the decade beginning in 1995 during which the $gp91^{phox}$ component of NADPH oxidase was proposed to be a voltage-gated proton channel (207) and contradictory evidence was presented, is recounted in detail elsewhere (p. 548–552 of Ref. 104; p. 2555–2556 of Ref. 102; see also Refs. 103, 119, 123, 211, 319, 338) and will not be revisited here. In 2006, authentic proton channel genes were identified in human (416), mouse, and the sea squirt *Ciona intestinalis* (432). The properties of the gene products in heterologous expression systems mirrored native proton currents in nearly every respect, including all of the peculiar or unique properties summarized above. One subtle difference that remains unexplained is that the absolute position of the g_{H^+} -V relationship is generally somewhat more negative at any given ΔpH for heterologously expressed than for native proton channels (355). Nevertheless, there is no doubt that these genes code for the same voltage-gated proton channels that we know and love.

To date, no more than one gene has been reported in any species. A suggestion that four classes of proton channels might exist (98, 137), which was based mainly on substantial differences in gating kinetics, most likely simply reflects genetic differences among species (cf. FIGURES 2 AND 5). No proton currents have been detected in any cell type studied from the *Hvcn1* knockout mouse, including neutrophils, monocytes, microglia, granulocytes, alveolar epithelial cells, and B lymphocytes (61, 105, 145, 334, 391, 417, 525), suggesting that the single *Hvcn1* gene codes for mH_V1 proton channels in all murine tissues. Knockdown by siRNA eliminated proton currents in the JME human airway epithelial cell line (233). A mutation of hH_V1 resulting in the substitution of Met^{91} with Thr^{91} was detected in genetic material from a single individual and shown to shift the g_{H^+} -V relationship positively by 20–30 mV in a heterologous expression system, decreasing the likelihood of chan-

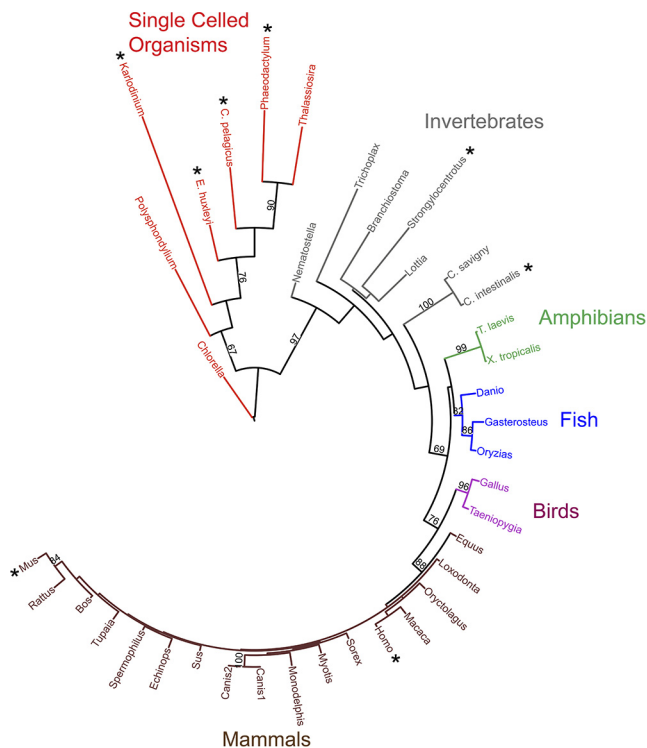


FIGURE 2. Phylogenetic tree of 37 known and predicted proton channels. Branch length indicates the evolutionary distance between sequences. This maximum likelihood phylogenetic tree was constructed from a multiple sequence alignment of the voltage sensing domain (VSD) portion of 37 H_V1 s using 100 bootstraps. The eight H_V1 genes that have been confirmed by heterologous expression and electrophysiological recording are starred. Bootstrap values >60 are shown; these numbers indicate the probability that the branch is genuine. [From Smith et al. (462).]

nel opening (233). Long and short isoforms resulting from the same $\text{hH}_{\text{V}1}$ gene, *HVCN1*, have been observed in human B lymphocytes and related cells (61); whether they exhibit different properties is currently under investigation (333).

Discovery of the proton channel gene predictably opened floodgates of interest in proton channels, which in this specific case was greatly amplified by the unexpected and astoundingly cool properties of the gene product. The proton channel protein was found to resemble the voltage sensing domain (VSD) of other voltage-gated ion channels, suggesting the possibility of exploiting $\text{hH}_{\text{V}1}$ to study voltage-gating mechanisms. Progress has occurred at an unprecedented pace, with the discovery that the channel is a dimer (259, 286, 497) rapidly followed by descriptions of the *Hvcn1* knockout mouse (61, 145, 334, 391, 417, 525), and the appearance of evidence that the protomers that comprise the dimeric channel interact cooperatively during gating (185, 359, 360, 498). Recently, the selectivity filter was identified and found to be fundamentally identical in the human channel $\text{hH}_{\text{V}1}$ (362) and a dinoflagellate $\text{kH}_{\text{V}1}$ (462).

Homology models of the channel molecule have been produced (267, 360, 415, 521) based largely on its similarity to K^+ channel VSD for which crystal structures exist. As yet, no structure of the entire proton channel exists, although the structure of the C terminus (carboxyl or COOH terminus) has been reported (172, 296).

III. THE GENE: PHYLOGENETIC DIVERSITY

A. Phylogeny: Which Species Have Proton Channels?

The phylogenetic tree in **FIGURE 2** includes 37 likely or confirmed proton channels and reveals that $\text{H}_{\text{V}1}$ channels are extremely widely distributed. With the assumption that the putative $\text{H}_{\text{V}1}$ s all turn out to be genuine, four or more kingdoms within the domain Eukaryota are represented: Plantae (*Chlorella*, a green algae), Protista (*Polysphondylium*, a slime mold, dinoflagellates, diatoms, and phytoplankton), and Animalia (the rest). The slime mold *Polysphondylium* may also be categorized in Amoebozoa, if one accepts this as a separate kingdom. There is a probable $\text{H}_{\text{V}1}$ in the Fungi kingdom (gi 322694380 gb EFY86211.1 in *Metarhizium acridum*, a virulent fungus), that was not included in **FIGURE 2** because the sequence may not be full-length (S. M. E. Smith, personal communication). Some might consider *Trichoplax* a poor excuse for membership in the Animalia kingdom. If one prefers the newfangled supergroup classification of eukaryotes (3, 17, 49, 398), then four or five of the five, six, seven, or eight supergroups are represented: Unikonta (or Opisthokonta), Al-

veolata, Stramenopiles, Plantae (or Archaeplastida), and Haptophytes+Cryptophytes. It has been suggested that the tendency of higher plants to generate a large inwardly directed H^+ gradient that is used to drive co- and counter-transport would make expression of an outwardly directed proton channel pointless (488). Eight $\text{H}_{\text{V}1}$ genes have been expressed heterologously and shown to encode bona fide proton channels: human (416), mouse, the sea squirt *Ciona intestinalis* (432), the purple sea urchin *Strongylocentrotus purpuratus* (Y. Okamura, personal communication), two phytoplankton species *Coccolithus pelagicus* spp *braarudii* and *Emiliania huxleyi* (489), the dinoflagellate *Karlodinium veneficum* (462), and the diatom *Phaeodactylum tricornutum* (488). Proton currents have been identified in cells from several other species, although the corresponding gene is not yet listed in the GenBank. Species awaiting gene identification or confirmation that the identified gene, when expressed, does in fact generate proton currents, include *Helix aspersa* (492), *Lymnaea stagnalis* (53), *Rana esculenta* (232), *Rana pipiens* (193), *Tritonia diomedea* (522), *Ambystoma mexicanum* (25), Chinese hamster (72), rat (99), rabbit (384), and cow (429).

The branch length in the tree in **FIGURE 2** reflects the extent of differences from the other proteins. It is evident that mammalian $\text{H}_{\text{V}1}$ s are closely similar to each other, whereas invertebrate $\text{H}_{\text{V}1}$ s vary substantially, and $\text{H}_{\text{V}1}$ s in unicellular organisms have extremely divergent sequences. One might predict that divergent sequences ought to manifest divergent properties and functions. This prediction appears to be borne out for the *Karlodinium* proton channel, $\text{kH}_{\text{V}1}$, which occupies the longest branch in the phylogenetic tree. In fact, $\text{kH}_{\text{V}1}$ differs dramatically from all other proton channels thus far characterized in exhibiting substantial inward current (see sect. VIA).

B. Nomenclature

No systematic nomenclature for proton channels yet exists. Part of the reason for this may be that only one gene per species has yet been identified. The official gene name approved by the HUGO Gene Nomenclature Committee (HGNC) is italicized by convention, and the protein may be given the same name, but not italicized. To maximize confusion, the human gene is *HVCN1*, the rat or mouse gene is *Hvcn1*, and in some other species (*Ciona*, *Xenopus*) it is *hvcn1*. The first groups to identify proton channel genes called the human gene product (i.e., the protein coded by *HVCN1*) $\text{H}_{\text{V}1}$ (416), the mouse product mVSOP , and the *Ciona intestinalis* protein CiVSOP (432). The H in $\text{H}_{\text{V}1}$ is for the conducted ionic species, H^+ , not for human, so the human variant should be called $\text{hH}_{\text{V}1}$. The V subscript means the channel is activated by voltage, and 1 indicates that it is the first isoform in the species. The VSOP nomenclature designates Voltage-Sensor-Only Protein, historically arising from its discovery in the course of a search

for VSP (voltage sensing phosphatase) homologs and from the fact that the VSOP closely resembles the VSD (voltage sensing domain) of many other voltage-gated ion channels, but strikingly lacks an explicit pore domain (cf. **FIGURE 3**). Despite the descriptive appeal of VSOP, we reluctantly suggest that mH_V1 and CiH_V1 should replace the original abbreviations for mouse and *Ciona* proton channels. **TABLE 2** summarizes some properties of confirmed and selected suspected proton channel proteins and suggests a unified nomenclature. The prefix indicates the species, listed either as one lowercase letter (common name) or two letters (genus and species) followed by H_V1 (e.g., hH_V1 and HsH_V1 are equivalent). We believe that the V (voltage-gated) should be an uppercase subscript, but journal editors (present company excluded!) and lazy authors will likely have the last word and change this into a lowercase “v,” just as they have enforced incorrect nomenclature onto the F_oF_1 -ATPase field. To postpone the time when we run out of letters to designate species, genus and species can be used, for example, the channel in *Coccolithus pelagicus* is CpH_V1 (489).

The human *HVCN1* gene has an alternative initiation site at Met²¹, which generates a “short form” channel comprising 253 amino acids instead of 273 (the first 20 are missing).

The suggested name for this splice variant would have the format hH_V1_{v2} (splice variant 2) according to the HUGO Guidelines for Human Gene Nomenclature (510). However, this cumbersome name would have two “v”s that mean different things (voltage and variant). So, for the present, it is listed in **TABLE 2** as hH_V1_s , with the long form implicit as the default meaning of hH_V1 . Thus far, hH_V1_s has been identified only in human B lymphocytes and related cells (61, 62).

IV. THE PROTON CHANNEL MOLECULE

There is no evidence that any accessory proteins are required to associate with the H_V1 molecule in order for it to function. Proton conduction was observed when the hH_V1 channel protein was purified and reconstituted into liposomes (287).

Common features of proton channels include four predicted transmembrane (TM) segments (S1-S4) (416, 432), intracellular N- and C-terminal domains (>50 residues), and short linkers between TM helices, with high homology in the S2-S3 linker. However, the recently identified dinoflagellate (*Karlodinium*) proton channel has a long S1-S2 linker of 68 residues. Proton channels in chordates (includ-

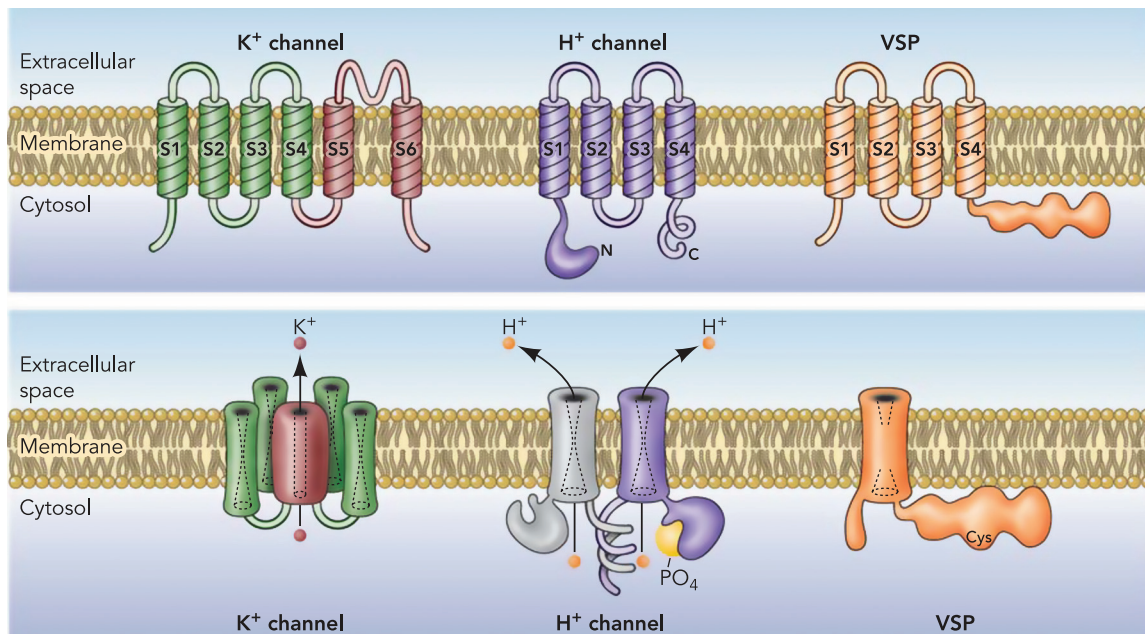


FIGURE 3. Architectural features of K^+ channels, H^+ channels, and voltage-sensing phosphatases (VSP). The top row shows the monomers from which the final oligomer (bottom row) is constructed. K^+ channels are tetramers of subunits that each contain six membrane-spanning regions, of which S1-S4 comprise the voltage sensing domain (VSD) and S5-S6 form the pore. S5-S6 regions from each subunit together form a single central pore, which is surrounded by four VSDs (bottom panel). H_V1 contains S1-S4 regions that are quite similar to the K^+ channel VSD, but lacks a pore domain (416, 432). The proton channel is a dimer held together by coiled-coil interactions in the C-terminal domain, in which each monomer has its own conduction pathway (259, 286, 497). Phosphorylation of Thr²⁹ in the intracellular N terminus converts the channel from “resting mode” to “enhanced gating mode” (117, 335, 352). The VSP has similar S1-S4 regions but lacks conduction. It senses membrane potential and modulates phosphatase enzyme activity accordingly (348, 349). [From DeCoursey (105).]

Table 2. Nomenclature and protein features of selected members of the voltage-gated proton channel (H_V1) family

Proposed Name	Protein GI Number	Protein Identity, %	Organism	Molecular Mass, Da	Length, amino acids
hH_V1	34783432	100	<i>Homo sapiens</i> (human)	31,683	273
hH_V1_s	374834170	92.7	(Short form; "isoform 2")	29,415	253
PaH _V 1	297692952	96.7	<i>Pongo abelii</i> (Sumatran orangutan)	31,756	275
MmH _V 1	380790623	93.8	<i>Macaca mulatta</i> (rhesus monkey)	31,554	273
pH _V 1	194042948	88.0	<i>Sus scrofa</i> (wild pig)	31,863	272
AmH _V 1	301754531	86.8	<i>Ailuropoda melanoleuca</i> (giant panda)	31,749	271
cH _V 1	296478571	86.2	<i>Bos taurus</i> (cow)	31,872	272
dH _V 1	345790859	85.3	<i>Canis lupus familiaris</i> (dog)	31,216	268
fH _V 1	355695395	82.8	<i>Mustela putorius furo</i> (ferret)	31,404	268
EcH _V 1	338727680	79.0	<i>Equus caballus</i> (horse)	33,309	288
mH_V1	109809757	78.0	<i>Mus musculus</i> (mouse)	31,242	269
rH _V 1	109497399	68.1	<i>Rattus norvegicus</i> (Norway rat)	33,737	294
OcH _V 1	291406960	58.5	<i>Oryctolagus cuniculus</i> (rabbit)	43,090	391
GgH _V 1	71897219	53.5	<i>Gallus gallus</i> (chicken)	27,599	235
LaH _V 1	344297427	50.0	<i>Loxodonta africana</i> (elephant)	50,727	455
XtH _V 1	56789050	45.6	<i>Xenopus (Silurana) tropicalis</i> (Western clawed frog)	26,575	230
XIH _V 1	56788929	43.6	<i>Xenopus laevis</i> (African clawed frog)	26,596	230
DrH _V 1	50539752	40.9	<i>Danio (Brachydanio) rerio</i> (zebrafish)	27,110	235
CIH_V1	118344228	26.1	<i>Ciona intestinalis</i> (transparent sea squirt)	38,501	342
CsH _V 1	358341603	22.7	<i>Clonorchis sinensis</i> (Chinese liver fluke)	34,088	305
SpH_V1	187282419	22.3	<i>Strongylocentrotus purpuratus</i> (purple sea urchin)	37,483	328
EhH_V1	JGI:631975	18.1	<i>Emiliana huxleyi</i> (coccolithophore)	37,389	339
PtH_V1	219120098	16.1	<i>Phaeodactylum tricornutum</i> (diatom)	38,582	338
CvH _V 1	307105313	16.0	<i>Chlorella variabilis</i> (green alga)	50,746	480
CpH_V1	304359300	15.2	<i>Coccolithus pelagicus</i> (coccolithophore)	36,281	325
kH_V1	351694294	14.6	<i>Karlodinium veneficum</i> (dinoflagellate)	27,624	248

Characteristics of proton channel proteins are shown. The protein sequence identification (GI) numbers are from the NCBI database, the *E. huxleyi* number (JGI) is from the Joint Genome database, <http://www.jgi.doe.gov/>. Identity with the human protein is for full-length protein sequences, obtained from the "needle" option at <http://www.ebi.ac.uk/Tools/emboss/align/> (EMBL-EBI). The isotopically averaged molecular mass of a monomer is given using Protein Calculator v 3.3 (<http://www.scripps.edu/~cdputnam/protcalc.html>). Species for which the expressed gene product has been confirmed in voltage-clamp studies to function as a proton channel are in **bold** and include human (416), human Short form hH_V1_s (333), mouse and *Ciona* (432), purple sea urchin *Strongylocentrotus* (Y. Okamura, personal communication), two coccolithophores (489), a diatom *Phaeodactylum tricornutum* (488), and *Karlodinium* (462).

ing *Ciona intestinalis*) appear to be dimeric (185, 259, 286, 497), mainly due to a coiled-coil region in the C terminus that holds the dimer together (172, 185, 259, 286, 296, 359, 360, 497). Assembly of parallel α -helical coiled-coil dimers was confirmed in the crystal structure of the hH_V1 C terminus (172, 296). H_V1 in several unicellular organisms (*Karlodinium veneficum*, a dinoflagellate, and *Phaeodactylum tricornutum*, a diatom) lack predicted coiled-coil regions (462), and thus are presumably monomeric. Another proposed function of the C terminus is to direct localization of H_V1 to the membrane (296). Fujiwara et al. (172) proposed that the C terminus influences channel activation by direct mechanical interaction with the S4 segment.

TABLE 2 is arranged in descending order according to protein identity with hH_V1. The bold entries, many of which differ

drastically from hH_V1, have been confirmed by heterologous expression and voltage-clamp characterization. Notably, many of these congregate near the bottom of the table, illustrating and confirming the high diversity among confirmed H_V channels (which is also apparent in **FIGURE 2**).

A. Modularity of the VSD

The discovery of H_V1 as well as the VSP family of voltage-sensitive phosphatases (**FIGURE 3**) strengthens the idea that the VSD and the pore domains of voltage-gated ion channels can be considered modular (268, 329, 330, 376). Attaching four VSDs to an ion channel pore domain confers voltage sensitivity to channel opening and closing. A VSD attached to an enzyme (a phosphatase) confers voltage sen-

sitivity on enzyme activity (348, 349). The proton channel is essentially a free-standing VSD; both the C and N termini can be truncated, and the remaining molecule still opens and closes in a voltage- and pH-dependent manner, and is still proton selective (185, 259, 360). The “paddle motif,” comprising parts of the S3b and S4 helices, has been shown to be modular in the sense that large segments are transferable among hH_V1, CiVSP, and K_V2.1 without loss of channel function (9).

The phylogram in **FIGURE 4** illustrates the relationships between VSD from voltage-gated H⁺ channels, mostly eukaryotic K⁺, Na⁺, and Ca²⁺ channels as well as voltage-sensing phosphatases (VSP) and a group of membrane proteins without a known function, C15orf27. Only the VSD (S1–S4 TM segments) was considered in this analysis. Given the exclusion of the pore domains from the analysis, it is surprising that channels of distinct selectivity fall mainly on distinct branches. The selectivity filter is logically located in the pore domain, yet the VSDs separate according to selectivity! Evidently, ion selectivity is important enough evolutionarily that once introduced, it was retained. The VSDs of cation channels were “dragged along” as ion pores with

different selectivity evolved, because mixing and matching between pores and VSDs is rare to nonexistent (S. M. E. Smith, personal communication). The H_V1/C15orf27/VSP group is phylogenetically distinct from eukaryotic K_V and Na_V/Ca_V channels. The H_V1 family members occupy their own branch. As we will discuss later (**FIGURE 5**), despite these VSDs existing in separate branches, they do share a number of intriguing key residues that seem to indicate a universality of voltage-gating mechanisms.

B. Amino Acid Sequence Reveals Parallels With the VSD of Other Voltage-Gated Ion Channels

It came as a complete surprise that the proton channel molecule (**FIGURE 3**) so closely resembled the VSD of other voltage-gated ion channels (416, 432). There are certainly a number of differences, but there is substantial overall similarity, especially in the S4 segment, which contains most of the charged residues that have been shown to act as voltage sensors in K⁺ channels. A BLAST search reveals strong similarities of H_V with voltage-gated sodium and calcium channels and a somewhat more distant relationship with voltage-gated potassium channels.

FIGURE 5 shows amino acid sequence logos for the four TM domains of 37 known or putative H_V1 family members, and for comparison, analogous logos for the C15orf27 family, the VSP family, and a selection of K_V channels. At any given position, the frequency of appearance of a residue is indicated by letter height. Where only a single letter appears, that amino acid is completely conserved in all members of the group. Of particular interest are residues that are conserved among all H_V1 sequences, but not other VSD-containing molecules. For example, Glu¹¹⁹ (hH_V1) appears promising at first in being almost perfectly conserved among H_V1, but it is replaced by Gly⁵⁸ in kH_V1 (top row in **FIGURE 5**), and thus is not indispensable for any function that kH_V1 can perform. Asp¹⁸⁵ (hH_V1), on the other hand, is highly conserved among H_V1 (sometimes being conservatively replaced by Glu), but is absent in all other VSDs. It participates in an external charge cluster in open hH_V1 channels (267). Several amino acids are conserved among all types of VSDs, and one expects that they must serve similar functions in all families, and furthermore that these functions are essential to the ability of any VSD to respond to voltage. For example, acidic residues corresponding to Glu¹⁵³ (in S2) and Asp¹⁷⁴ (in S3) in hH_V1 are thought to serve as counter charges that stabilize cationic charges in S4 in K_V channels (35, 284, 396, 448, 493). Ramsey et al. (415) showed that mutations that neutralize either of these two residues in hH_V1 shifted the g_H-V relationship strongly negatively. If we view changes in the position of the g_H-V relationship as reflecting the relative stability of closed and open states, a negative shift indicates a more stable open state of the mutants. Evidently, these acidic groups nor-

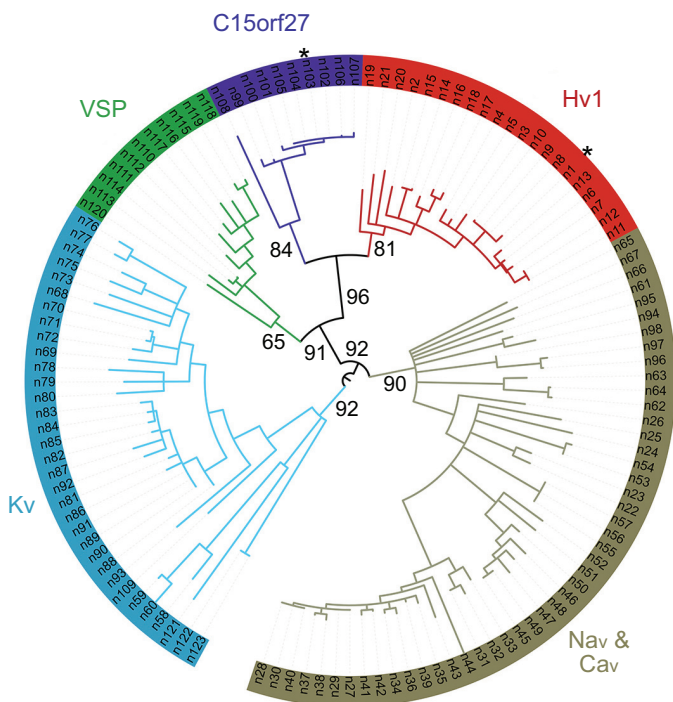


FIGURE 4. Phylogenetic relationship between the proton channel (H_V1) family and other VSD-containing proteins. Unrooted phylogram from a maximum likelihood analysis of 122 VSDs shows that H_V1 sequences appear on a branch distinct from other VSDs. The phylogenetic analysis was performed on VSD sequences only and did not include the cation channel pores or N and C termini. Sequences are color coded: K_V, voltage-gated K⁺ channel; Na_V, voltage-gated Na⁺ channel; Ca_V, voltage-gated Ca²⁺ channel; VSP, voltage-sensitive phosphatase; C15orf27, protein of unknown function. Branches with likelihood support values [a measure of confidence in a branch's appearance in a tree] <0.50 are collapsed. [From Musset et al. (362).]

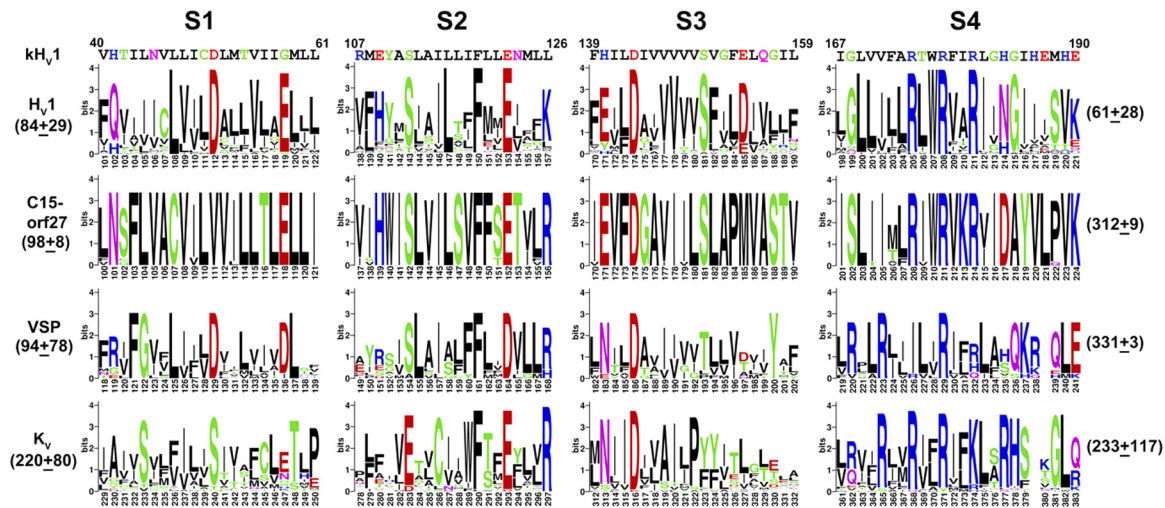


FIGURE 5. Sequence logos derived from alignment of the primary sequences of the four TM segments of the *Karlodinium* proton channel, kH_{V1} (top row) with the TM segments of 37 members of the H_{V1} family, 15 of C15orf27, 15 of VSP, and 13 K_V channels. The letter height (single letter amino acid abbreviations) in the sequence logos shows the proportion of all sequences with a particular amino acid at that position. The overall height of the stack indicates information content (439) or sequence conservation at that position (88). The mean (\pm SD) numbers of amino acids in the N and C termini are given to the left and right, respectively. The examples numbered for each family are hH_{V1} , human C15orf27, CiVSP, and *Shaker* for K_V . [From Smith et al. (462).]

mally stabilize the closed state of hH_{V1} . Another universally conserved position is Phe¹⁵⁰ in hH_{V1} . The corresponding Phe residue in K_V channels is thought to form a hydrophobic seal, or external boundary of a “gating charge transfer center” through which the S4 cationic charges move successively during channel opening (486). Just internal to Phe¹⁵⁰, Glu¹⁵³ and Asp¹⁷⁴ complete the gating charge transfer center in hH_{V1} . The extent to which S4 may move in H_{V1} the way it does in K_V channels is a very important and as yet unresolved question that is discussed below.

All four families of VSD-containing molecules in **FIGURE 5** (as well as Na_V and Ca_V channels) have highly conserved Arg or Lys residues in S4, which are considered to be crucial elements of the voltage sensing device. The precise numbers and positions of these cationic residues vary. Proton channels have three Arg residues in S4, and these occur with fixed spacing, RxWRxxR. In fact, the WRxxR pattern is one of the proposed signatures of H_V that was used to identify a dinoflagellate H_V , kH_{V1} (462). The extent to which these charged residues in S4 comprise the voltage sensor of H_V and are analogous to those in other channels is discussed below.

A few of the \sim 100 amino acids in the intracellular N terminus (amino or NH_2 terminus) of hH_{V1} (not shown in **FIGURE 5**) have been assigned specific functions. A phosphorylation site at Thr²⁹ in hH_{V1} (352) that is thought to be responsible for enhanced gating of proton channels in activated phagocytes, is conserved in most species, exceptions being *Ciona*, *Karlodinium*, and *Strongylocentrotus*. Although phagocytes are absent in the unicellular *Karlodinium*, *Ciona* has phagocytic amoebocytes (463) and the sea urchin *Strongylocentrotus* has nutritive phagocytes (200), and both

species have the Nox2 NADPH oxidase isoform [*Ciona* Nox: NP_001121595, *Strongylocentrotus* Nox: NP_001073020]. Also located in the intracellular N terminus is the site of the first identified human mutation of hH_{V1} , Met⁹¹ (233). As discussed below (**FIGURE 28**), the M91T mutation alters the position of the g_H -V relationship at any given Δ pH. It is intriguing that, together with Thr²⁹ (hH_{V1}), two locations in the N terminus distinctly alter gating, which one would expect to involve mainly the TM segments. In the absence of structural information, the mechanism by which the N terminus interacts with the voltage gating machinery can only be speculated.

The crucial selectivity filter element in the middle of the S1 TM segment, Asp¹¹² in hH_{V1} (362) and Asp⁵¹ in kH_{V1} (462), is universally conserved, without even a conservative Glu substitution. Although Glu can replace Asp at this position without loss of selectivity (362, 462) and the Δ pH dependence of gating is also preserved, D112E mutation of hH_{V1} altered gating kinetics, and thus has distinct functional consequences that may explain why evolution settled on Asp (362).

Functions for the other conserved residues in H_V are less well defined or unknown. It was suggested that Asn²¹⁴ might act as the selectivity filter of the hH_{V1} proton channel (496), based on loss of current in the N214R mutant, abolition of current in N214C treated with the thiol modifying reagent MTSET, and attenuation of WT H^+ current by internally applied guanidinium ions (497). The corresponding N264C mutant in Ci H_{V1} conducted current that was abolished by MTSET (185). In some alignments with the K^+ channel VSD, this Asn residue corresponds with the position of the fourth Arg, which is absent in H_V . Tombola et al. (497) proposed that in the open state of the

channel, the small polar Asn would move up to the constriction that was previously occluded by the larger Arg residues, where it would allow protons but no other ions to pass. However, the Okamura group found that in the murine mH_V1, the equivalent N→R mutation (N210R) did not abolish current (428). Similarly, both N214R and N214D mutants of hH_V1 have been found to be proton selective (362, 428). Finally, kH_V1, EhH_V1, and CpH_V1 all have His in this position (462, 489). In summary, a number of polar and charged residues at this position are compatible with proton selectivity. An even more compelling argument against Asn²¹⁴ (in hH_V1) being the selectivity filter is that truncation of the C terminus between R2 and R3 (i.e., removing Asn²¹⁰ altogether) did not abolish proton conduction (428).

Of the two His residues that contribute to Zn²⁺ sensitivity in hH_V1 (360, 416), His¹⁴⁰ is widely conserved, and the somewhat more critical His¹⁹³ is conserved in 13 mammals and birds, but Asp or Glu appear at the corresponding position in most aquatic species (*Ciona*, *Danio*, *Strongylocentrotus*, *Xenopus laevis* and *Xenopus tropicalis*, *Saccoglossus*, *Trichoplax*, *Branchiostoma*) with the exception of *Nematostella* which has Asn. It is tempting to speculate that the lower sensitivity to Zn²⁺ predicted for the latter species might reflect a desire on their part to survive despite higher levels of ambient polyvalent metal cations. However, the current levels of heavy metals in sea water are too low to impair proton channel function significantly (76 nM Zn²⁺, 112 nM Ni²⁺, 14 nM Cu²⁺, 1 nM Cd²⁺, 21 pM La³⁺; Ref. 500), even were the channels directly exposed to sea water.

C. Are Eutherian Voltage-Sensitive Phosphoinositide Phosphatases Proton Channels?

Very recent evidence (476) suggests that human orthologs of VSPs might function as proton channels. TPTE (Transmembrane Phosphatase with Tensin homology) and its paralog TPTE2 contain a VSD. These proteins appear to express preferentially in Golgi and not in plasma membranes, so they cannot easily be studied electrophysiologically. However, chimerae comprising the S3-S4 TM segments of human TPTE/TPTE2 spliced into zebra fish (*Danio rerio*) Dr-VSP were expressed at the plasma membrane and generated voltage-gated proton current. Intriguingly, a His residue at the inner end of the S4 segment appeared crucial to proton conduction; introducing His at the corresponding position in Dr-VSP also produced proton current (476).

D. Dimeric Expression

In 2008, three groups reported a variety of evidence all pointing to the proton channel existing as a dimer (259,

286, 497), at least when the protein is expressed heterologously. **FIGURE 6A** illustrates that when H_V1 is tagged with green fluorescent protein, the fluorescence intensity decays irreversibly in two discrete steps (497). FRET measurements are consistent with dimer formation (259). Although Western blots exhibit monomeric protein, reducing conditions or use of cross-linking agents revealed dimers (259, 286). By taking precautions to limit the extent of disruption of oligomers by high temperature, detergent, and proteases, Petheő et al. (404) demonstrated distinct dimers in Western blots from human neutrophil and eosinophil membranes, confirming that the native proton channel also prefers to go through life with a partner.

The dimer is held together mainly by coiled-coil interactions of the intracellular C terminus (259, 286, 497), possibly with some contribution from N-terminal interaction (185, 259, 497). Lee et al. (286) proposed that the outer ends of the S1 region also interact in the dimer. The channel can be forced to exist as a monomer, by removal of the C terminus by mutation (259, 360) or by constructing a chimera using the C terminus from a monomeric protein such as CiVSP (497). The monomer still functions as a voltage-gated proton channel, showing that each monomer has its own conduction pathway. This observation raises the question why the channel assembles as a dimer, when it can apparently function as a monomer.

Proton channels in human, mouse, and *Ciona intestinalis* appear to be dimers (259, 286, 359, 360, 497). The *Karlorhinium* channel kH_V1 is suspected to be a monomer based on indirect evidence: the kH_V1 C terminus lacks any predicted coiled-coil domain, activation is exponential, and Zn²⁺ is a very weak inhibitor (462).

The physiological purpose of dimerization is not yet clear. Perhaps it is something as mundane as stabilizing the protein in the membrane (359). Another possibility is that the cooperative gating that occurs in the dimer (see sect. VD2)

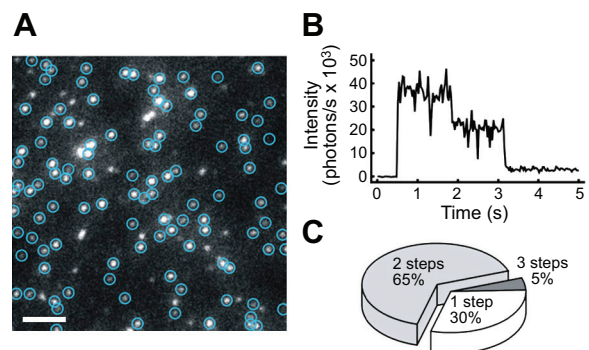


FIGURE 6. Photobleaching of GFP-tagged hH_V1 occurs in two distinct irreversible steps, indicating that the channel exists mainly as a dimer. **A:** blue circles indicate individual channels that were followed over time. **B:** time course of fluorescence intensity of one spot (i.e., channel). **C:** illustrates that most channels bleached in two steps. [From Tombola et al. (497), with permission from Elsevier.]

confers some physiological advantage over the simpler gating of the monomer. Channel opening in the dimer is slower, compared with the monomer (172, 259, 359, 360, 497), but more steeply voltage dependent; the gating charge is twice as large in the dimer as in the monomer: 6 versus 3 e_0 in CiH_V1 (185) or 4 versus 2 e_0 in mH_V1 (172). In phagocytes (see sect. VIII), an important function of proton channels is to limit the extent of depolarization that results from the electrogenic activity of NADPH oxidase. This enzyme is active during phagocytosis, and depending on the stimulus, its activity may persist for a few seconds or up to hours (118). In this setting, it is likely more important that the proton channel has steep voltage dependence than that it activates extremely rapidly (360). The steep voltage dependence reduces the extent of depolarization that is required to open enough H⁺ channels to compensate the electron current, thereby limiting the propensity of NADPH oxidase to inhibit its own activity (120, 351).

E. Models of Dimeric Association

Three proposals for the location of the dimer interface have been suggested. Lee et al. (286) observed crosslinking when Cys residues were introduced at the outer end of the S1 segment, leading to the proposal that the two S1 helices face each other at the dimer interface (FIGURE 7A). A very different interface was required to explain the stronger effects of Zn²⁺ in WT dimeric hH_V1 than in monomeric (C-truncated) hH_V1 (360). The two His residues in hH_V1 that are responsible for high-affinity Zn²⁺ binding, His¹⁴⁰ and His¹⁹³ (416), appear likely to form a high-affinity binding site only at the interface between monomers in the dimer (360), if the S2 and S3 segments from each protomer approach each other closely (FIGURE 7B). Because Zn²⁺ ap-

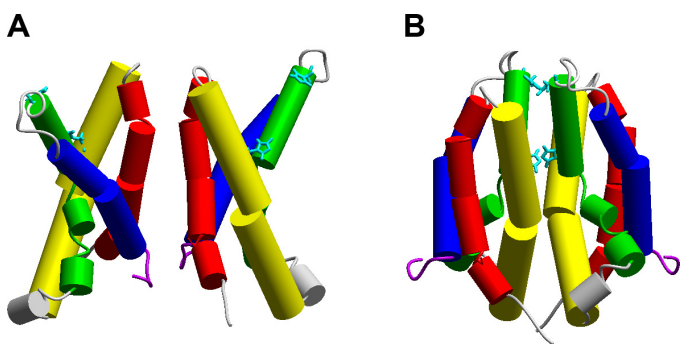


FIGURE 7. Possible dimer interfaces for hH_V1. *A*: cross-linking between Cys residues introduced at several positions on S1 (red) led to this dimer model (286). *B*: competition between H⁺ and Zn²⁺ for a high-affinity binding site led to an alternative model. Apposition of S2 (yellow) and S3 (green) segments allows the Zn²⁺ binding residues His¹⁴⁰ and His¹⁹³ to approach each other closely enough to form potential bidentate Zn²⁺ binding sites. A recent study proposed that the C terminus and the S4 helix form a single rigid helix through which the C termini mediate cooperative gating and that any direct interaction within the TM region is inconsequential to this process (172). [From Musset et al. (359).]

pears to prevent channel opening (71), Zn²⁺ binding at this interface may prevent channel opening, perhaps by preventing the dimer orientation in FIGURE 7A that might allow channel opening.

A very different model was proposed recently by Fujiwara et al. (172). Based on intricate studies of the thermostability of various constructs of mH_V1, they concluded that direct interaction between the TM domains in the dimer is not responsible for cooperative gating. Instead, the coiled-coil interaction that links the dimer also directly influences gating by mechanical interaction mediated by a continuous extended rigid alpha helix encompassing both C terminus and the S4 segment. When mutations interfered with the coiled-coil interaction or when the C-terminal coiled-coil domains were effectively “disconnected” from the S4 segments by inserting a flexible linker, cooperative gating was prevented, as judged by the criteria of activation kinetics corroborated by effective gating charge measurements. Recently, subtle mutations in the C-terminal coiled-coil domain were shown to result in the channel assembling as a trimer or tetramer (173), indicating that there is substantial latitude in the interface among H_V1 protomers required for function. The dimeric channel exhibited much more distinct sigmoidicity in activation than other oligomeric forms, however, suggesting that cooperative gating is favored by a specific interface.

V. KEY PROPERTIES OF H_V1

A. Minuscule Unitary Conductance

It was recognized early that proton channels have a very small conductance. Byerly and Suen (54) could not see single-channel currents in excised patches of membrane from snail neurons and concluded that the single-channel currents were too small to resolve. Nor did they detect an increase in current noise (variance) at voltages where proton current was activated, most likely because the rapid gating kinetics in *Lymnaea* required filtering at 1 kHz. A study of human eosinophil membrane patches was facilitated by the much slower gating kinetics of hH_V1. Cherny et al. (75) could just detect single-channel currents of 7–16 fA near $V_{\text{threshold}}$ in occasional favorable patches. The low frequency range of gating kinetics enabled filtering at 10–20 Hz without loss of signal, but another factor was high seal resistance (up to ~ 5 T Ω), which is the most critical variable in optimizing the signal-to-noise ratio in the low frequency range (291). More useful information was obtained by analysis of current variance. At voltages where proton current was activated, the variance was greater by a factor of 100-fold or more than the background measured at sub-threshold voltages (75). By analysis of current variance, both unitary conductance and the maximal P_{open} could be determined. Single-channel conductance increased as pH_i decreased: 38 fS at pH_i 6.5, 140 fS at pH_i 5.5, ~ 220 fS at

pH_i 5.0, and ~400 fS at pH_i 4.1, but was independent of pH_o. The maximal P_{open} during large depolarizations was ~0.95 at pH_i ≤ 5.5, decreasing to 0.75 at pH_i 6.5. Extrapolated to physiological pH_i 7.2 gives 15 fS at 20°C, which scales to 78 fS at 37°C (75). The dependence on pH_i but not pH_o is consistent with H⁺ (not OH⁻) being the conducted ion. That the unitary conductance is 3 orders of magnitude smaller than most ion channels mainly reflects the low concentration of permeating ions (104); in most cells, [H⁺] is ~10⁶ smaller than [K⁺] or [Na⁺].

B. Extraordinary Temperature Dependence

Byerly and Suen (54) compared H⁺ and K⁺ currents in *Lymnaea* neurons and found that the H⁺ conductance increased much more strongly with temperature. The Q₁₀ (the change for a 10°C increase in temperature) of the H⁺ conductance is 2–3 in a variety of cells and species (54, 76, 112, 269), and increases at lower temperatures (112, 269). Higher values, up to 5.3 at <20°C, were observed in excised patches, which might be less subject to proton depletion artifacts (112). The strong temperature dependence has been interpreted as evidence that the conduction pathway is not a simple water wire, that the rate-limiting step occurs during permeation, and that the pathway includes at least one titratable group (76, 112, 269).

Gating kinetics exhibit even stronger temperature dependence than conductance (76, 112, 269, 416). Analyzed in terms of a delay followed by an exponential rise for current activation and single exponential decay for deactivation, all three parameters (delay, τ_{act} and τ_{tail}) had identical Q₁₀ values of 6–9 (E_a 30–38 kcal/mol) (112). In contrast, most ion channel gating processes have Q₁₀ near 3. The similarity of Q₁₀ for these processes is consistent with a channel having multiple subunits that undergo an identical, complex conformational change during opening, with the reverse transition in one subunit being sufficient to terminate conduction (112). Intriguingly, the hH_V1 dimer expressed heterologously exhibits gating kinetics with a Q₁₀ as large as native proton currents (360, 416), but the Q₁₀ of the C-terminal truncated construct of hH_V1 (presumed to be monomeric) is only half as large (360), suggesting that the coop-

erative gating of the dimer is more demanding energetically than the monomer. For mH_V1, WT and C-truncated constructs have similar Arrhenius slopes, perhaps reflecting species differences that were detected in the C terminus crystal structures (172).

C. Perfect Selectivity

A defining property of voltage-gated proton channels is their essentially perfect selectivity (i.e., specificity) for protons. Specificity is vitally important for proton channels because the physiological concentration of protons is ~10⁶ lower than that of K⁺ or Na⁺, in and around cells. Without specificity, H_V1 currents would be contaminated by lesser ions. In other words, if under physiological ionic conditions, the relative permeability defined by the Goldman-Hodgkin-Katz equation (Eq. 1) $P_{\text{H}}/P_{\text{Na}}$ were <10⁶, the conductance would reverse closer to E_{Na} than to E_{H} , and would be barely recognizable as a proton conductance. That estimates of the relative permeability of the voltage-gated proton channel can be as low as 10⁶ is the result of these being conservative “worst-case” estimates (76, 109, 116, 124, 187, 250, 436); as will be seen below, the true selectivity is much greater.

There are two ways to evaluate the selectivity of ordinary ion channels, by conductance or by permeability. In principle, selective conductance could be determined by substituting another ion for protons on one side of the membrane, and determining how much current that ion carries. It is not possible to remove protons, because all aqueous solutions have a finite proton concentration, not to mention the complications arising from the ΔpH dependence of gating (see sect. VE). H⁺ currents can be recorded even at pH_i 8.5, where the permeating ion concentration is just ~3 nM (107). Therefore, the only way to quantify selectivity is by relative permeability. Permeability to protons is determined by measuring the reversal potential (V_{rev}) in solutions containing different ions, and comparing it with the Nernst potential for H⁺ (E_{H}). One can calculate from deviations between V_{rev} and E_{H} the relative permeability of other ions present in the solution using the Goldman-Hodgkin-Katz voltage equation (184, 216, 221)

$$V_{\text{rev}} = \frac{RT}{F} \log \frac{P_{\text{Cl}^-}[\text{Cl}^-]_i + P_{\text{K}^+}[\text{K}^+]_o + P_{\text{Na}^+}[\text{Na}^+]_o + P_{\text{H}^+}[\text{H}^+]_o}{P_{\text{Cl}^-}[\text{Cl}^-]_o + P_{\text{K}^+}[\text{K}^+]_i + P_{\text{Na}^+}[\text{Na}^+]_i + P_{\text{H}^+}[\text{H}^+]_i} \quad (1)$$

where R , T , and F have their usual meanings, P_{X} is the permeability to ion X, and $[\text{X}]_i$ and $[\text{X}]_o$ indicate internal and external concentrations of ion X. This equation shows that the permeability of each ion, combined with its concentration, determines how large an effect it will have on V_{rev} . When this calculation is carried out, the true proton

selectivity of H_V1 is underestimated even when the resulting values of $P_{\text{H}}/P_{\text{X}}$ are 10⁷ to 10⁸ (74, 107, 114), because the assumption that deviation from E_{H} reflects permeation of other ions is almost certainly incorrect. In numerous studies (104), when liquid junction potentials are carefully corrected, there is no detectable change in V_{rev} when the pre-

dominant cation or anion is replaced, including small or very large ions. Studies encompassing a wide range of pH tend to indicate that the deviation of V_{rev} from Nernst increases with ΔpH , and does not depend on specific pH (74, 124, 187, 250, 303). Thus deviations of V_{rev} from E_H most likely reflect imperfect control over pH, rather than selectivity for other ions. Anyone who has carefully measured V_{rev} of voltage-gated proton channels knows that the result obtained depends strongly on careful minimization of pH changes due to H^+ current during the prepulse, as well as residual pH changes from pulses applied minutes earlier (22, 99, 108, 113, 124, 187, 232, 250, 341, 355, 441).

Additional evidence for perfect proton selectivity was obtained recently by measuring V_{rev} after reducing the ionic strength by isotonic sucrose dilution (362), which classically defines whether a channel is cation or anion selective (23). Reducing the ionic strength in the bath solution decreases the concentrations of all ions present, with the exception of H^+ and OH^- , which are held constant by buffering. If a channel is cation or anion selective, V_{rev} will shift negatively or positively at low ionic strength, respectively (23). For proton channels, even dilution of the ionic strength to 90% sucrose, 10% salt did not change V_{rev} , supporting proton selectivity, because pH remains constant while all other ion concentrations are reduced. Until evidence is produced that another ion can permeate, the presumption will remain that voltage-gated proton channels are proton specific.

The precise mechanism by which perfect proton selectivity is achieved is not yet clear. Conventional ion channels have an aqueous pore that is thought to include a narrow region in which water or ions are constrained to move in single file and interact with the pore wall (216). Ion selectivity may result from steric factors, i.e., how well the dehydrated ion fits the pore (264), and electrostatic effects, e.g., negative charges in the pore wall promote cation selectivity. Permeation requires the ion to travel the length of the pore. For ordinary ions, permeation also requires that any water molecules or other ions in a single-file region of the pore must also permeate to clear the pathway. But protons are not ordinary ions, as will be discussed next.

1. Mechanisms of proton selectivity: the hydrogen-bonded chain

According to the classical proposal of Nagle and Morowitz (365, 366), if one or more of the elements in a HBC is a titratable group, the channel could be proton selective. If permeation occurs only by sequential protonation/deprotonation of one or more sites, proton selectivity is ensured. Before the hH_V1 gene was identified, a number of properties of proton currents were determined, all of which seemed consistent with the proton conduction pathway being more complex than a simple linear row of water molecules, as is found in gramicidin channels. In fact, comparison of the

permeation properties of voltage-gated proton channels with those of proton conduction through gramicidin became a paradigm (106). Thus, compared with gramicidin, the reduction of proton current in heavy water (D_2O) was greater in voltage-gated proton channels (7, 78, 107), the temperature dependence of the proton conductance was much greater (7, 77, 112, 269), and the proton selectivity was tremendously greater than for gramicidin (104, 363). A natural explanation was that the conduction pathway through H_V1 included at least one titratable residue (113). In practice, identifying such a residue proved to be elusive. Ramsey et al. (415) systematically mutated 33 amino acids, including all ionizable residues in or near all four putative TM segments of hH_V1 , but identified no single mutation that abolished proton conduction.

Before continuing, one might ask whether experimental evidence exists to support the prediction that a HBC that includes one or more titratable residues can be proton selective. We will examine several examples that may clarify the extent to which this is the case, and then return to the selectivity filter of the voltage gated proton channel.

2. Histidine as a selectivity filter

Perhaps the clearest example of a single titratable residue producing proton selectivity is found in mutants of the VSD of traditional voltage-gated ion channels. In an elegant series of studies, Dorine Starace, Enrico Stefani, and Pancho Bezanilla individually mutated each of the four key Arg residues that are known to sense membrane potential in the S4 segment of the *Shaker* K^+ channel VSD (469–471). The S4 segment is thought to move outward through the membrane upon depolarization, resulting in channel opening, but normally the VSD does not itself conduct current. The view that emerges from these and many other studies is that in the closed channel the outermost Arg (R1) is retracted toward the inner side of the membrane and is positioned at a constriction or focal point of what is essentially an hour-glass of water molecules. The advantage of this architectural feature is that the membrane electrical field is concentrated across a small distance (35, 65, 471, 529). Upon depolarization, S4 slides outward and the four Arg residues ratchet past the constriction so that in the fully open state, the fourth Arg (R4) resides at the constriction. In the native protein, no current flows past the constriction in open or closed states of the VSD “gating pore.” When R1 was mutated to histidine, the VSD became a proton channel that was conductive at negative voltages (470). When R4 was mutated to histidine, a proton-selective current was observed at depolarized voltages at which the central K^+ pore opens (469). These results are explained beautifully if the constriction is so narrow that there is aqueous access on both sides and if the presence of a histidine residue precisely at the constriction enables protonation on one side and deprotonation on the other, resulting in proton-selective current. When R2 or R3 were mutated to histidine, the

molecule behaved as a proton carrier, with the histidine being protonated and shuttling protons across the constriction during random, stochastic gating movements that are most probable in the middle voltage range where transitions between open and closed states occur frequently (471). When R1 was mutated to residues other than histidine, voltage-gated nonselective cation current was observed (494). Finally, the I287H mutation in the S2 segment and I241H in S1 also produce proton current (57). The combined evidence strongly suggests that a single histidine residue at a narrow point in an otherwise aqueous pore can produce proton selectivity.

In the Na_v1.4 skeletal muscle Na⁺ channel VSD, a comparable mutation to the outermost Arg in S4, R666H, results in a proton-selective conductance (473), which causes hypokalemic periodic paralysis (248, 464). Surprisingly, guanidinium⁺ was reported to permeate this mutant, although Na⁺ permeation was undetectable (464), suggesting that the proton selectivity is not absolute (but for an alternative explanation, see sect. VC5). Similarly, the analogous mutation in the Na_v1.5 cardiac muscle Na⁺ channel VSD to the outermost Arg in S4, R219H, causes anomalous inward H⁺ leak current as well as dilated cardiomyopathy and related electrical problems (188).

A second, rather different example of histidine facilitating proton transfer is found in the active-site cavity of human carbonic anhydrase II (CA-II), which has a turnover rate near 10⁶ s⁻¹ (457). During catalysis of CO₂ to HCO₃⁻, a proton is generated that is exported through the active-site cavity into bulk solution, a distance of ~15 Å (150). The catalytic rate of CA-II is limited by the proton transfer step (472). Located midway between the active site and the surface of the enzyme, His⁶⁴ is thought to shuttle these protons (472, 499). The H64A mutant still functions in catalysis, but in the absence of buffer, proton transfer dependent turnover is reduced 20-fold (499). This kinetic defect can be overcome by derivatives of imidazole and pyridine as proton acceptors/donors, which rescue catalysis (11, 499). The imidazole side chain of His⁶⁴ appears to alternate between two orientations, pointing towards the reaction center or outward toward bulk solution (159, 367). Finally, micromolar Cu²⁺ and Hg²⁺ inhibited the native enzyme but not the H64A mutant, and Hg²⁺ was found to bind to His⁶⁴ (151). Together, these results strongly suggest that in the native enzyme, His⁶⁴ acts as an efficient proton shuttle (499). Additional evidence that histidine shuttles protons effectively comes from the least efficient carbonic anhydrase isoform, CA-III. In this enzyme, Lys occupies the position of His⁶⁴ in CA-II. Replacing Lys⁶⁴ in CA-III with His increases the catalytic rate severalfold, as does simple addition of imidazole buffer (241). Intriguingly, replacing Lys⁶⁴ in CA-III with either Asp or Glu increased the internal proton transfer rate 20-fold (411), indicating that in this enzyme, Asp and Glu transfer protons even more efficiently than

His. However, despite its considerable facilitation of proton transfer, His⁶⁴ does not act as a selectivity filter. Catalysis requires rapid translocation of both CO₂ and HCO₃⁻ (substrate and product, or vice versa in the reverse reaction) between the reaction center and the external solution during each reaction cycle. The nonselectivity of the CA-II proton channel likely reflects its geometry. Rather than being a narrow, single-file cylinder like the archetypal gramicidin A channel, the side chain of His⁶⁴ is ~8 Å from that of Gln⁹², directly across the active-site cavity (456). Clearly, proton selectivity requires a narrow lumen in addition to a titratable group.

The third example is the proton channel for which the selectivity mechanism has been most widely studied and debated, the influenza A virus M₂ channel (FIGURE 8). The M₂ channel is a homotetramer of 96-amino acid monomers, that is strongly proton selective (79, 301, 344), but recently was shown to have detectable permeability to other cations (288, 331, 402). The precise value obtained for P_H/P_K (TABLE 1) is lower (10⁴ to 10⁵) at low pH_i and when low pH_i is maintained for an extended period of time (seconds to minutes) (W. F. DeGrado, personal communication). The key residue His³⁷ mediates activation of the conductance (i.e., channel opening) at low pH (511) and also is essential to the proton selectivity (504). The arrangement of the tetramer results in all four His³⁷ pointing towards each other in the conduction pathway. The pore is thought to be narrow and water-filled, with a constriction at the tetrad of His³⁷ residues (406). Two main schools of thought surround the selectivity mechanism of the M₂

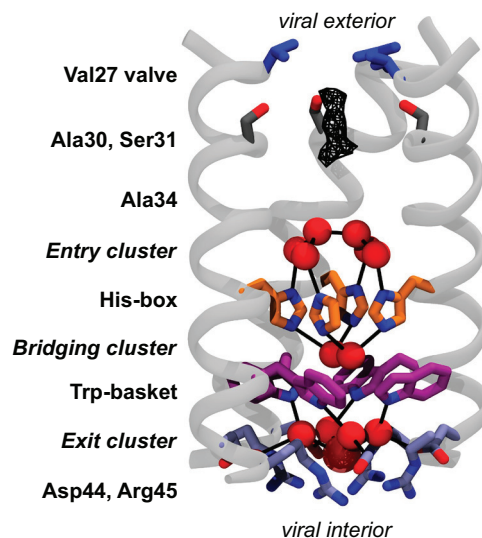


FIGURE 8. Molecular anatomy of the M₂ proton channel transmembrane domains. Three of the four monomers that form the channel are shown as gray ribbons. The tetrad of His³⁷ residues are orange; red spheres are water molecules. The “entry cluster” comprises six waters, four of which are hydrogen bonded to the His³⁷. The two waters in the “bridging cluster” are also hydrogen bonded to the His. The permeating proton is thought to be delocalized among the His box and associated water clusters. Black lines indicate hydrogen bonds. [From Acharya et al. (2).]

channel: the “frozen water” model and the “histidine shuttle” model. Sansom and colleagues proposed that immobilized water would allow protons, but presumably no other ions to permeate (165, 431). Intriguingly, two-dimensional infrared spectroscopy indicates that water in the M_2 channel is immobilized (icelike) at high pH, but “melts” at low pH, becoming more liquid and capable of conducting protons (178). Pinto et al. (406) proposed that the outwardly directed imidazole nitrogen of neutral His³⁷ is protonated, creating a charged species. Subsequent deprotonation of the inwardly directed ring nitrogen releases a proton to the inside, followed by a ring flip (His tautomerization) to restore the deprotonated nitrogen to the proximal side. This mechanism is strongly reminiscent of the HBC hop-turn mechanism (FIGURE 1). This hypothesis was supported by a “chemical rescue” study in which proton conduction was restored in three His³⁷ mutants (H37G, H37S, H37T) by addition of imidazole (504). Thus H37G was a poorly selective cation channel, but proton permeation and selectivity increased with the introduction of imidazole (504). Several studies have modeled M_2 conduction and concluded that obligatory successive proton transfer and release by His³⁷ can account quantitatively for experimental data (225, 253, 282, 450, 537). Protonation of the His³⁷ tetrad is supported by the high in situ pK_a values, with the first through fourth being 8.2, 8.2, 6.3, and <5.0 [somewhat lower estimates were obtained with different membrane composition (226)]; the third protonation event “activates” the conductance (227, 408). Charge is stabilized in the “His box” (FIGURE 8) either by low barrier hydrogen bonds between the His³⁷ (227, 450) or through the formation of numerous dipolar interactions involving carbonyl-bound waters and water-mediated aromatic interactions (2, 225). In the latter mechanism, the conducted proton is delocalized among the four His³⁷ and nearby waters (2). Strong evidence for the His³⁷ shuttle mechanism was provided by NMR measurement showing rapid interchange between protonated and deprotonated states of imidazole nitrogens (226). The latter mechanism does not eliminate any possibility of a role for water; a water molecule might transiently invade the His cluster, and assist passage of the proton from a more outwardly focused to inwardly focused nitrogen. Only very sophisticated experiments or calculations will be able to discriminate among these possibilities.

A fourth example arises from the surprising recent discovery that although the *Ciona intestinalis* VSP (FIGURE 3) displays no channel-like activity, the human equivalents, TPTE and TPTE2, appear to function as proton channels (476). TPTE (but not TPTE2) has even lost its phosphatase activity, which suggests that some evolutionary advantage is conferred by its residual proton channel function. Because these molecules traffic to Golgi and not plasma membranes in mammalian expression systems, their proton channel function was examined in chimerae of S3-loop-S4 from TPTE or TPTE2 inserted into DrVSP (*Danio rerio*,

zebra fish VSP). Proton conduction was abolished by mutation of a single His residue near the inner end of S4. Furthermore, the DrVSP was transformed from nonconducting to proton channel activity by inserting His at the corresponding location, R171H (476).

In addition to, or perhaps as a consequence of, the ability of His to shuttle protons, a role in buffering protons has been suggested in H⁺-ATPases. In one of two H⁺ half-channels in the *E. coli* ATP synthase, His²⁴⁵ may capture protons near the channel entrance, by virtue of having a pK_a near physiological pH (129). Intriguingly, H245C is dysfunctional, but H245C + D119H (a “second site suppressor” mutation) restores function (502), suggesting that His and not Asp can serve this function. A comparable role of capturing protons has been suggested by R. Fillingame for Lys in the H⁺-ATPase of alkalophilic bacteria (214), where the higher pK_a of Lys would be required to buffer protons at high ambient pH. In addition to Lys, several nearby amino acids in combination help to capture and translocate protons: Glu, Gly, and Arg. The cationic charge of the conserved and required Arg keeps the proton from overstaying its welcome (214, 507).

3. Mechanisms of proton selectivity: the frozen water hypothesis

The suggestion that water immobilized inside the M_2 pore might enable proton-selective conduction was mentioned above. Another channel we will consider is a synthetic channel (LSLLLSL)₃; this channel is proton selective despite altogether lacking formal charges (283). Selectivity was evaluated by the ability to detect single-channel currents; thus the value given in TABLE 1 is a lower limit. It is generally considered that proton selectivity in this case results from water molecules that are confined in the narrow pore, whose mobility is predicted by molecular dynamics (MD) calculations to be greatly restricted (418). MD simulations of a narrow cylindrical hydrophobic pore indicate that when the diameter is reduced to 4 Å, the water molecules are confined to single-file and proton conduction is increased by an order of magnitude over wider pores (43). Intriguingly, increasing the diameter slightly to 5 Å allows a Zundel (or Huggins) cation (H₃O₂⁺) to lodge sideways in the pore (43), possibly blocking conduction. MD simulations support the possibility of the frozen water mechanism for the (LSLLLSL)₃ channel, but result in a maximal conductance for H⁺ that is just ~1,120 times greater than for K⁺, pointing to the possibility that this channel may conduct other cations (526).

4. Other proton-selective channels

A large number of molecules conduct protons with less than perfect selectivity. TABLE 1 lists proton-conducting molecules for most of which estimates exist of the relative per-

meability of protons and other ions. Some provide clues to how proton selectivity might be achieved. For example, the human TRPM7 channel is proton selective, and it loses conduction when Asp¹⁰⁵⁴ is mutated to Ala, whereas the D1054E mutant conducted well. A nearby Glu¹⁰⁵² appears also to contribute to proton conduction, and these two acidic groups comprise the proposed selectivity filter of this channel (386). Where possible, key residues that are crucial to proton selectivity are listed in **TABLE 1**. There appear to be a preponderance of Asp and Glu residues, although His occurs as well.

An unusual case is aquaporin, which normally does not conduct protons or any other ions. In rat aquaporin 1, mutating a single Arg¹⁹⁵ residue to valine (28, 524) or to serine (295) results in proton conduction with moderately high selectivity (**TABLE 1**). The Arg¹⁹⁵ is located at the narrowest part of the channel, the “selectivity filter” with a diameter of 2 Å, which ensures single-filing of waters. The R195V mutation appears to eliminate electrostatic repulsion and, in addition, increases the diameter to an extent that in R195S, two waters could squeeze through the constriction (69, 295). These mutants appear to be examples of narrow pores in which a specific arrangement of amino acids enables preferential H⁺ permeation presumably across a water wire, while discouraging, but not completely excluding other ions.

Another interesting case is channelrhodopsin-2, which conducts H⁺ much better than other monovalent cations, but its selectivity doubles during the photocycle (32). Other molecules with a preference for protons, but who are not perfectly faithful (and whose degree of infidelity has not been quantified), include an H⁺-coupled oligopeptide transporter OPT3 (153), diphtheria toxin channels (430), H⁺-induced current through a sugar transporter SGLT1 (36) and a proton-coupled folate transporter SLC46A1 (501), Semliki Forest virus envelope protein (437), and a serotonin transporter (58).

A distinction could be made between proton-conducting channels and proton binding sites. The binding selectivity for protons can be quite impressive, e.g., $>10^9$ for H⁺ over Na⁺ for F-type ATPases (262). ATP synthases (H-ATPases) may be driven by Na⁺ or H⁺ gradients. The proton-coupled variety binds H⁺ with high specificity at a conserved Asp or Glu residue. Selectivity of binding exceeds 10^8 because the pump is driven by H⁺, but not Na⁺ when their concentrations differ by $>10^8$ (200 mM Na⁺ at pH 9) (410). Remarkably, given specific geometry and other interacting residues, Glu can also form a Na⁺-selective site. Krah et al. (262) point out that given its pK_a, glutamate intrinsically binds H⁺ selectively in solution with <100 μM affinity, but binds Na⁺ negligibly. Size restriction and a hydrophobic local environment also enhance H⁺ over Na⁺ specificity (262). The MotB

component of the flagellar motor transduces a proton gradient into flagellar rotation. Crucial to this process is Asp³² (in *E. coli*), which binds protons and transfers them through the proton channel (538). Of 15 substitutions, only D32E preserved function (538).

5. Mechanism of proton selectivity of hH_V1

The proposal that Asn²¹⁴ might act as the selectivity filter of the hH_V1 proton channel (496) was discussed previously (see sect. IVD). The selectivity mechanism of the voltage-gated proton channel was reevaluated recently, by comparing hH_V1 with C15orf27 (**FIGURE 4**), a structurally similar molecule of no known function that lacks measurable conductance in heterologous expression systems (362). Five key candidate residues (Asp¹¹², Asp¹⁸⁵, Asn²¹⁴, Gly²¹⁵, and Ser²¹⁹) were swapped between molecules to attempt to abolish conduction in hH_V1 and induce it in C15orf27. Four of the five hH_V1 mutants retained H⁺-selective conduction, but D112V lacked clear current, suggesting that Asp¹¹² was crucial to proton conduction. In a series of Asp¹¹² mutants, most (D112A, D112N, D112S, D112H, D112F) still conducted current, but with substantially reduced proton selectivity. In fact, ionic strength reduction experiments showed that all were anion selective! As illustrated in **FIGURE 9**, lowering the external ionic strength by dilution with isotonic sucrose shifted V_{rev} positively, indicating anion selectivity. Sucrose dilution lowers the concentrations of all external ions, except H⁺ and OH⁻, which are still buffered. The reversal potential V_{rev} will shift negatively for a cation-selective channel and positively for an anion-selective channel (23). Anion permeation was confirmed by replacing CH₃SO₃⁻ with Cl⁻ (**FIGURE 10**) which shifted V_{rev} negatively, demonstrating Cl⁻ permeability for all mutants, except D112E. Thus a single amino acid substitution converted the proton specific hH_V1 into an anion channel!

In view of the above examples of His shuttling protons (see sect. VC2), perhaps the most surprising result was that D112H conducted Cl⁻, apparently in contrast with the proton-selective Arg→His mutants of the K⁺ channel VSD (469–471). The explanation may be revealed by the consequence of neutralization of the key residue. When Asp¹¹² is neutralized, the result in almost all cases is a nonselective anion channel. In contrast, when R1 of the K⁺ channel VSD is neutralized by mutation, the result is a nonselective cation channel (495). Although in both systems a His residue is positioned at a likely constriction, the residue that was replaced by His could hardly be more different, acidic Asp or basic Arg. There are at least two ways to interpret this phenomenology. One possibility is that the hH_V1 channel leading up to Asp¹¹² may exclude cations, and the role of Asp¹¹² would be the exclusion of anions. Alternatively, Asp¹¹² in the open channel may interact with one or more cationic groups, for example an S4 Arg residue (267). A conserved Arg residue

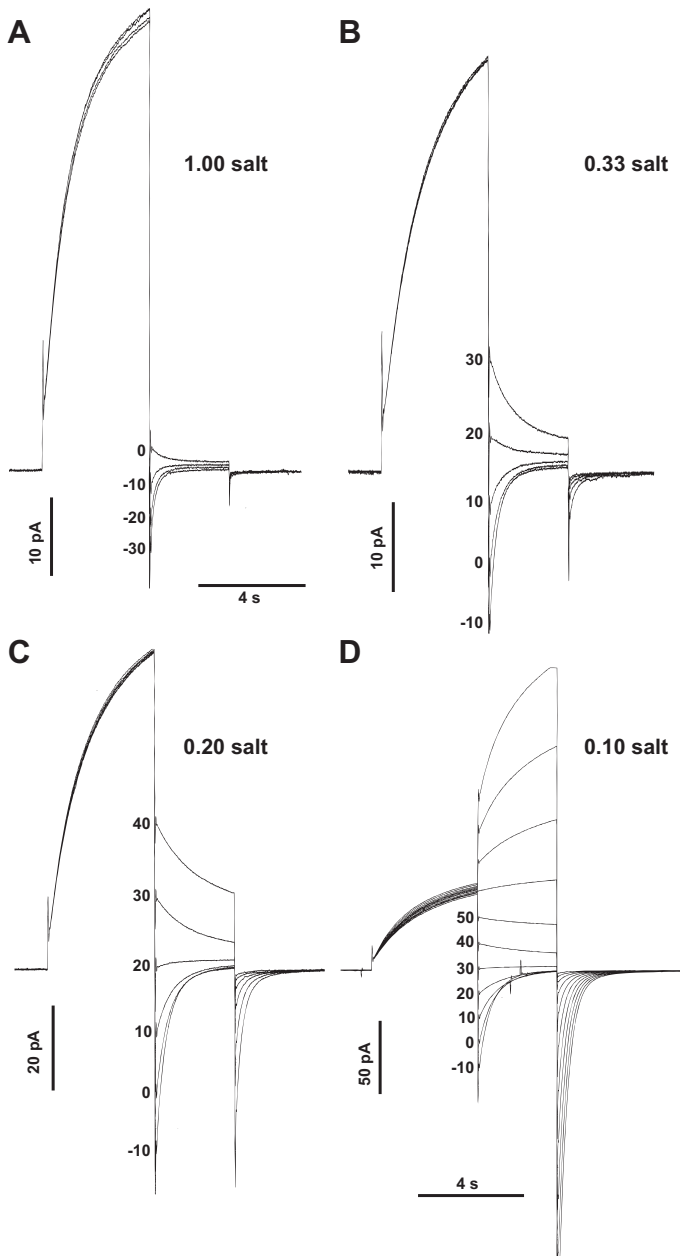


FIGURE 9. Ionic strength dilution with isotonic sucrose reveals that the D112A/D185M mutation of hH_v1 results in anion selectivity. Tail current reversal potential measurements are shown at several levels of dilution of the bath solution. Bath and pipette solutions contained ~130 mM TMA⁺ CH₃SO₃⁻ at pH 7.0 and 5.5, respectively. The control V_{rev} (A) is far from E_{T+} , which is -87 mV, but not significantly different from that in D112A mutants (362). Dilution of the external solution shifts V_{rev} progressively positively. [Unpublished data by Deri Morgan, from a study reported in Musset et al. (362).]

in several types of H⁺-ATPases is thought to lower the pK_a of the crucial Asp residue transiently to promote H⁺ release during transport (47, 155). When Asp¹¹² is neutralized, this would leave uncompensated positive charge, which would result naturally in anion selectivity. From this perspective, the anion selectivity of the D→H mutants seems not paradoxical, but predictable.

In previous studies, the anion versus cation selectivity of nonselective receptor-activated channels could be switched by mutating one (63, 252) or a few amino acids (175, 195). In some cases, the principle mechanism of charge selectivity appears to be simply electrostatics, a negatively charged channel selects for cations, and vice versa (252). Carland et al. (63) found that mutating a Pro in a human GABA receptor channel to anionic Glu produced a cation-selective channel, whereas mutating it to cationic Arg resulted in anion selectivity.

A contribution of Arg²¹¹ to the proton selectivity of hH_v1 was proposed recently (30). Most R211x mutants, when expressed in amphibian oocytes, appeared to be permeable to guanidinium⁺ (CH₆N₃⁺ or, informally, Gu⁺) when applied at 100 mM at pH 8, because outward currents were observed in all 15 mutants studied, but no current was seen in the WT channel. This effect was reported only at pH 8, not at lower pH. However, in a mammalian expression system, robust outward currents are clearly evident in both R211A (FIGURE 11A) and WT channels (FIGURE 11B) at symmetrical pH 8 with 100 mM GuCl. Perhaps the selectivity of the human channel, hH_v1, is altered when it is

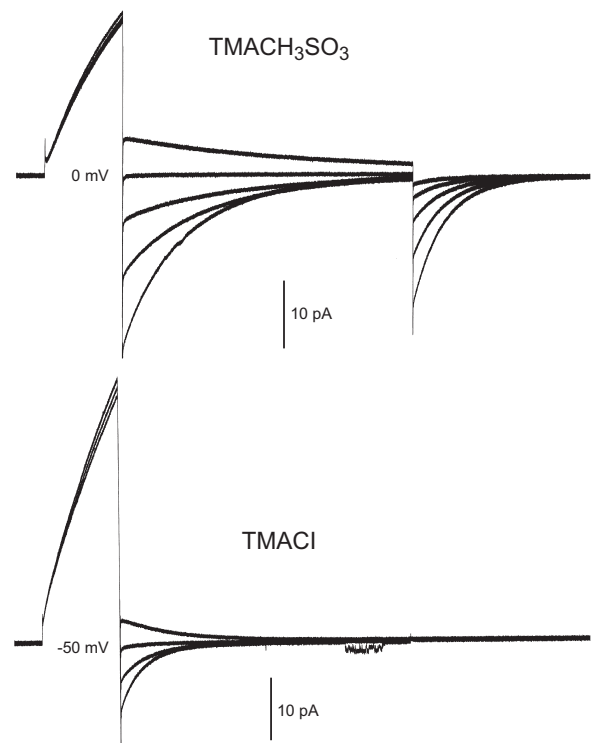


FIGURE 10. Identification of the selectivity filter of hH_v1. The replacement of Asp¹¹² by serine converts the human proton channel hH_v1 into an anion channel. Tail current measurements at symmetrical pH 5.5 with ~130 mM TMA⁺ CH₃SO₃⁻ in pipette and bath (top) and after bath replacement with TMA⁺ Cl⁻ (bottom) reveal that V_{rev} shifted nearly -50 mV, indicating higher permeability to Cl⁻ than to CH₃SO₃⁻. In each, a 4-s depolarizing prepulse activated the conductance, then the voltage was stepped back to a range of voltages in 10-mV increments to determine the zero current potential, V_{rev} . [Unpublished figure by Deri Morgan, from a study reported in Musset et al. (362).]

expressed in *Xenopus laevis* oocyte membranes at high pH. The apparent Gu^+ permeation of R211S may parallel the anomalous Gu^+ permeability of the R666H mutant of the Na_V channel VSD (464), which is predominantly proton selective (473) and is not detectably permeable to other monovalent cations (464). The rationale for using Gu^+ was that it resembles the side chain of Arg, which passes through the “gating pore” repeatedly during normal channel opening. Despite the elegance of this scenario, and given that GuCl is a chaotropic agent that efficiently denatures proteins and interferes with hydrogen bonds (148), it is important to determine whether Gu^+ permeation signals a general loss of selectivity, or is anomalous. Several considerations indicate that Gu^+ does not permeate by a normal mechanism: 1) Gu^+ is a notorious protein denaturing agent, 2) Gu^+ is not a physiological ion, 3) no physiological ions permeate WT H_V1 , 4) cations smaller or larger than Gu^+ do not permeate, and 5) Gu^+ drastically alters gating. The R211H mutant, for example, is not detectably permeable to K^+ , Na^+ , Li^+ , TMA^+ , or Cl^- (361). The mechanisms by which Gu^+ denatures proteins are under debate, but include replacing waters that are bound by proteins, reorganizing local water networks, and altering or disrupting hydrogen bonds between water and the protein (148, 326). One may envision Gu^+ “tunneling” its way through the channel by local denaturation, rather than being conducted by the normal route. That Gu^+ permeation is anomalous is shown directly by the fact that Gu^+ dramatically alters gating. At symmetrical pH with 100 mM Gu^+ , the open conformation of the R211S construct is stabilized; its g - V relationship was shifted ~ 100 mV more negative than during H^+ permeation (30). This is an exceptionally dramatic “permeant ion effect” compared with those observed in other ion channels (171,

449, 481, 503). In any case, Arg^{211} is not required for proton selectivity because truncation of the C terminus of mH_V1 between the second and third Arg in S4 did not abolish proton conduction (428).

The dinoflagellate proton channel kH_V1 , despite fairly major differences from hH_V1 and only 15% amino acid identity, has an analogous selectivity filter at Asp^{51} in the middle of the S1 helix. As in hH_V1 , the $\text{Asp} \rightarrow \text{Glu}$ mutation preserves H^+ specificity, and neutralizing mutations produce anion selectivity (462). The similarity of the effects of mutations suggest that this is a general property of voltage-gated proton channels, and consequently, must serve a specific function. Given that only the WT hH_V1 or kH_V1 channels and their $\text{Asp} \rightarrow \text{Glu}$ mutants were perfectly proton selective, proton selectivity evidently requires a carboxylic acid at a critical location in the pathway. Nevertheless, the precise mechanism of selectivity remains unclear. Existing evidence does not establish with certainty that the conduction mechanism involves successive protonation and deprotonation of the carboxyl group during H^+ permeation. It is conceivable that the acid (Asp or Glu) creates a local environment in which structured or trapped water molecules mediate proton conduction.

6. Can H^+ and OH^- currents be distinguished?

It is surprisingly difficult to distinguish H^+ and OH^- permeation through a channel. Under all conditions, these ions have identical Nernst potentials, and they also share equal and opposite concentration gradients. Furthermore, their flux has identical effects on pH on both sides of the membrane. For example, voltage-gated proton currents extrude protons and increase pH_i , which can be detected with pH-sensing dyes. However, OH^- influx, which would be driven identically by the same electrochemical potential, would similarly increase pH_i . Permeation of OH^- in frog skeletal muscle has been concluded from measurements at pH 10 (505), where protons are scarce. Similarly, $(\text{C}_6\text{F}_5)_2\text{Hg}$ acts as an electrogenic OH^- carrier, with conductance proportional to $[\text{OH}^-]$ from pH 6–9 (38). Channels that allow OH^- efflux (or H^+ influx) are also found in freshwater algae, *Chara* spp. (309). In these channels, OH^- efflux seems more plausible because transport is insensitive to pH_o where H^+ would be the substrate if it were the conducted species. The pH near the outer membrane surface also rapidly increases to 10.0–10.5 or higher during transport, which translates to 30–100 pM H^+ as substrate (309). In contrast, pH_i is 8.1–8.4, so as substrate $[\text{OH}^-]$ would be 1.3–2.5 μM (309). Intriguingly, the H^+/OH^- channels of *Chara* were shown recently to be inhibited by Zn^{2+} (8).

The strongest experimental evidence supporting H^+ (rather than OH^-) permeation through WT H_V1 is the increase in

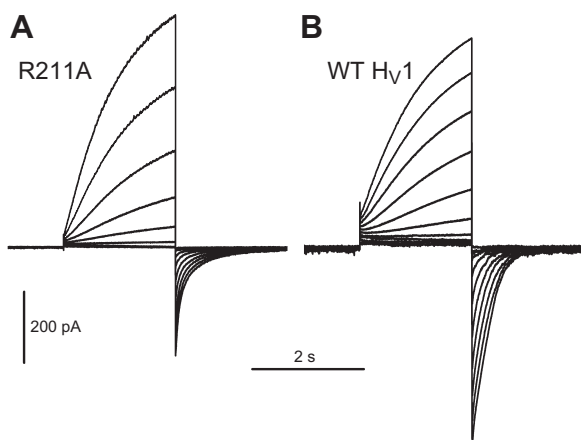


FIGURE 11. Guanidinium (Gu^+) is not an effective blocker of hH_V1 . Families of currents in COS-7 cells expressing R211A (A) and wild-type hH_V1 channels (B) during pulses applied in 10-mV increments up to +50 mV from a holding potential of -40 mV. Both cells were studied in whole cell configuration in symmetrical solutions containing 100 mM GuCl at pH 8.0. (Unpublished data by Vladimir V. Cherny.)

single-channel conductance when pH_i is decreased, combined with the lack of dependence on pH_o . Lowering pH_i from 6.5 to 4.1 increased the unitary conductance progressively from 38 to 400 fS (75). Changes in pH_o had no effect; if OH^- were the permeant species, one would expect sensitivity of the unitary conductance to pH_o but not to pH_i . The deuterium isotope effect on conductance is substantially larger than for proton/deuterium conduction through gramicidin channels (7, 78), the archetypal water-filled pores (292), which also indirectly supports H^+ rather than OH^- permeation, at least OH^- permeation by hydrodynamic diffusion (104, 107).

The distinction between H^+ and OH^- permeation through voltage-gated proton channels has been considered mainly a technical question, bordering on sophistry, but was recently reawakened by the discovery of anion-selective hH_V1 mutants that in addition have substantial permeability to H^+/OH^- (362). Several neutralizing mutations of Asp^{112} resulted in loss of proton-specific conduction and gain of substantial anion permeability. Ionic

strength reduction indicated a strong preference for anions. For a 90% reduction in ionic strength, V_{rev} would shift +58 mV for a perfectly anion-selective channel. For all mutants studied, the shift was less. Traditionally, such deviations are interpreted to mean that while the channel is preferentially permeable to anions, it conducts some cations as well (23). However, the lack of discernable change in V_{rev} when the main external cation TMA^+ was replaced with either smaller (Na^+ or K^+) or larger (TEA^+ or N -methyl- D -glucamine $^+$) cations argues against significant cation permeability (362). V_{rev} in these mutants changed in the “right” direction when pH was varied, but less than in the WT channel, so they evidently conducted anions and H^+/OH^- . Both observations could be explained by postulating that the mutant channels have significant permeability to either H^+ or OH^- or both. But which is permeant? The Goldman-Hodgkin-Katz equation (184, 216, 221) can be viewed as setting the rules for competition among possibly permeant ions for domination of V_{rev} , each ion trying to push V_{rev} toward its own Nernst potential

$$V_{\text{rev}} = \frac{RT}{F} \log \frac{P_{\text{Cl}^-}[\text{Cl}^-]_i + P_{\text{CH}_3\text{SO}_3^-}[\text{CH}_3\text{SO}_3^-]_i + P_{\text{OH}^-}[\text{OH}^-]_i + P_{\text{TMA}^+}[\text{TMA}^+]_o + P_{\text{H}^+}[\text{H}^+]_o}{P_{\text{Cl}^-}[\text{Cl}^-]_o + P_{\text{CH}_3\text{SO}_3^-}[\text{CH}_3\text{SO}_3^-]_o + P_{\text{OH}^-}[\text{OH}^-]_o + P_{\text{TMA}^+}[\text{TMA}^+]_i + P_{\text{H}^+}[\text{H}^+]_i} \quad (2)$$

Here we see the difficulty in separating permeation of H^+ and OH^- . The usual approach to determining selectivity is to vary the concentrations of ions and measure V_{rev} , but changing pH changes both E_{H} and E_{OH} simultaneously and identically.

One approach is to compare the shift of V_{rev} when sucrose is introduced at pH_o 5.5 or 7.0. If OH^- is permeant, changes in $[\text{OH}^-]$ should have greater impact on V_{rev} (eq. 2) at pH_o 7.0, where $[\text{OH}^-]$ is 32 times larger (and $[\text{H}^+]$ is 32 times smaller) than at pH_o 5.5. This argument also works from the opposite perspective: in a situation where there is greater relative effect of OH^- , V_{rev} will be changed less by sucrose substitution, because $[\text{OH}^-]$ will remain constant as other anions are diluted. Consistent with this hypothesis, the shift of V_{rev} produced by 9:1 dilution with isotonic sucrose was smaller (and therefore the relative effect of OH^- was larger) at pH_o 7.0 than at pH_o 5.5 for all mutants tested (except for D112K) (362). Another strategy is to force H^+ and OH^- to compete in the presence of a third permeant species, such as Cl^- . Sucrose dilution effects should be larger in Cl^- than in CH_3SO_3^- solutions, because Cl^- is more permeant than CH_3SO_3^- . This prediction was also borne out for all anion-selective mutants except D112N where the shifts were similar. Finally, substituting Cl^- for CH_3SO_3^- should shift V_{rev} more at pH_o 5.5 than at pH_o 7.0. This prediction, too, was borne out in all six anion-selective mutants. Thus the data all point to a high OH^- permeability of the mutants.

In a single-file channel, outward H^+ flux and inward OH^- flux both likely occur by a Grotthuss mechanism, or “prototropic transfer” (289). H^+ moves in water by hopping from H_3O^+ to H_2O , whereas OH^- conduction occurs when OH^- extracts a proton from a nearby H_2O . The latter process involves proton transfer between neutral and negatively charged species, and thus seems more reasonable for an anion-selective channel. The implication of this conclusion is that D112x mutant channels are essentially completely anion selective, conducting OH^- in addition to more conventional anions. Thus H_V1 is a single amino acid away from being an anion channel.

A useful generality is that proton transfer through water is most likely mediated by traditional Grotthuss proton hopping when the pK_a of donor and acceptor are both acidic ($\text{pK}_a < 7$), but occurs by proton “hole” (i.e., OH^-) migration when the $\text{pK}_a > 7$ (421). The proton hole concept simply reiterates that OH^- permeation occurs by protons hopping between neutral waters and OH^- , rather than by bodily diffusion of the OH^- anion; the conductivity of OH^- in water is sufficiently high (422) that it clearly reflects a more efficient process than hydrodynamic diffusion (87, 90, 141, 228, 289). Applying this principle to hH_V1 , we see that the central role of Asp^{112} in proton selectivity of (WT) hH_V1 channels also favors H^+ rather than OH^- permeation, because its pK_a is likely quite low.

D. Voltage-Dependent Gating

1. Does S4 in H_V1 move the way it does in K_V and Na_V channels?

In most voltage-gated Na^+ or K^+ channels the S4 TM segment has a run of positively charged residues (Arg or Lys) at every third position. Mutations that replace some of these residues with neutral amino acids result in gating with weaker voltage sensitivity, implicating the four outermost Arg residues as crucial to voltage sensing (4, 299, 304, 397, 400, 448, 474). These results suggest that the charged residues contribute to voltage sensing, but do not directly prove that they move in response to voltage. Some mutations of uncharged amino acids have similar effects (306, 321, 460).

Overwhelming evidence that the charged residues in the S4 segment move across the membrane during gating has been provided by Cys scanning studies. In this approach, individual amino acids are mutated to Cys, and the resulting molecule is treated with membrane-impermeant MTS (methane thiosulfonate) reagents. These reagents can be applied from either side of the membrane to reveal which residues are accessible to external or internal solutions, and during test pulses or at negative voltages to evaluate accessibility of open or closed channels, respectively. Any modification of the current is taken as an indication that the site is accessible. These studies indicate movement of S4 during gating, by virtue of state-dependent changes in accessibility in both Na^+ and K^+ channel VSDs (16, 278, 529, 531, 536). Structural studies are also consistent with substantial S4 movement during gating (244, 245, 305). Lanthanide-based resonance energy transfer (LRET) confirms S4 movement during gating, but also indicates that rotation and tilt contribute to the accessibility changes (64).

Rather than requiring that these charged groups move all the way across the membrane, strong voltage dependence is accomplished in part by the existence of aqueous crevices that focus the electric field across a narrow isthmus. The most dramatic demonstration of this phenomenon was the series of Arg→His mutants generated by Starace, Bezanilla, and Stefani (469–471) and described earlier (see sect. VC2). They mutated each of the four outermost Arg residues (R1-R4) in the *Shaker* K^+ channel VSD and found that each mutant transported H^+ across the membrane. The R1H mutant conducted H^+ current at negative voltages; the R4H mutant conducted H^+ current at positive voltages; and at intermediate voltages the R2H and R3H mutants were H^+ carriers. Two important conclusions can be drawn: 1) the S4 segment moves outward during channel opening (relative to the rest of the molecule and/or the electric field), and 2) in the R1H and R4H mutants the His residue was accessible to both internal and external solutions simultaneously. Therefore, when a charged group passes the constriction, it has effectively crossed most of the membrane electrical field. There is some voltage drop across

the aqueous access pores, depending on their dimensions (189), but the electrical field is nonetheless highly concentrated.

We now ask to what extent S4 in H_V1 behaves the way it does in other voltage-gated ion channels. Molecular dynamics simulations based on homology models that predict H_V1 structure by mapping its sequence onto the crystal structures of the VSD of K^+ channels tend to agree that the general picture of an hourglass of water molecules that narrows to a central constriction applies also to H_V1 (170, 267, 415, 521). A closer look produces signs of some significant differences from the K^+ channel VSD. First of all, the H_V1 S4 helix has only three Arg residues that align with R1-R3 or R2-R4 or R3-K5 of K^+ channels, depending on who does the alignment (9, 106, 170, 185, 330, 415, 428, 432, 462, 521); other alignments are also plausible. The contribution of the three S4 Arg residues to gating charge is best determined from the limiting slope of the g_H -V relationship plotted semi-logarithmically (10, 454, 455). Estimates of the gating charge range from 5.4–8.0 e_0 for native proton currents (r H_V1) (107, 108), to 4.1 e_0 for m H_V1 (172), and 6.0 for expressed h H_V1 (185, 355). The effective gating charge in *Shaker* K^+ (4, 235, 383, 440, 448) and Na^+ channels (217) is 12–14 e_0 , about twice as large, consistent with four subunits that must undergo a conformational change before the channel opens, compared with two for H_V1 (see sect. VD2). The Larsson group reported that each of the three Arg residues in Ci H_V1 contributes measurably to voltage sensing (186). On one hand, this result is not surprising, in view of the analogous function of the outermost four Arg residues in the S4 segment of voltage-gated K^+ channels. On the other hand, the extent to which S4 of H_V1 moves outward during channel opening was called into question by a study in which the m H_V1 channel was truncated at the C-terminal end as far into S4 as between the second and third Arg residues, and this mutant still exhibited voltage-gating, Zn^{2+} sensitivity, and H^+ selectivity (428). It is difficult to reconcile this result with the view that S4 moves as far in H_V1 during channel opening as it apparently does in K^+ channels.

Three studies have examined accessibility of S4 residues in H_V1 , two using Cys scanning. Sakata et al. (428) combined cysteine scanning with glycosylation (“PEGylation-protection” assay, described in Ref. 308) and found that the S4 segment of m H_V1 is inaccessible to a maleimide reagent between Gly¹⁹⁵ and Arg²⁰⁴ (murine numbering, corresponding with Gly²⁰⁰ and Arg²⁰⁸ in h H_V1), with partial accessibility on either side of this: from Glu¹⁹² to Lys¹⁹⁴ and Val²⁰⁵ (428), as illustrated in **FIGURE 12**. This appears to indicate a long stretch of 10–14 buried residues. Gonzalez and et al. (185) evaluated accessibility of S4 residues in Ci H_V1 using Cys scanning combined with functional measurements. Their studies identified residues with external access preferentially in open channels including A246C,



FIGURE 12. Accessibility of S4 residues in open and closed H_v1 channels. Cys scanning with MTS reagents was done in CiH_v1 (185). Residues in CiH_v1 that were externally accessible preferentially when the channel was open (i.e., measured at positive voltage) are orange; residues that were internally accessible preferentially when the channel was closed (i.e., measured at negative voltage) are green; residues not accessible in either state are red. Yellow shading indicates state-dependent accessibility; gray complete inaccessibility. Minimum stretches that are inaccessible in closed or open states deduced from the CiH_v1 MTS data are indicated by arrows. For mH_v1, presumably in the closed state, PEGylation assays indicated residues with full accessibility (blue), partial accessibility (brown), and inaccessibility (red), with shading indicated partial (gray) or complete (dark gray) inaccessibility (428). For hH_v1, Zn²⁺ inhibition of currents produced by Arg→His mutants indicated external accessibility (orange) and internal accessibility (blue) of open channels (361).

I248C, and V252C (corresponding to E197, L199, and I203 in hH_v1), completely inaccessible residues L256C and V259 (L206 and V209 in hH_v1), and residues with internal access preferentially in the closed state I262C and N264C (I212 and N214 in hH_v1). This study therefore indicates a small region that includes the middle S4 Arg residue that is inaccessible in all states (shaded dark gray in **FIGURE 12**). The stretch of residues that are inaccessible changes in closed and open states (arrows in **FIGURE 12**); in the closed state, inaccessibility spans A246 to V259 (E196 to V209 in hH_v1), while in the open state inaccessibility includes L256 to N264 (L206 to N214 in hH_v1). State-dependent accessibility confirms that S4 moves outward during H_v1 channel opening. The perfect agreement of the mH_v1 inaccessible region with that deduced for CiH_v1 in the closed state suggests that the channel was closed in the former measurements. In summary, both Cys scanning studies reported a band of inaccessibility roughly a dozen residues wide (185, 428).

Roughly similar accessibility was deduced in Cys scanning studies of voltage-gated Na⁺ and K⁺ channels. If we focus on the basic S4 residues, two Arg are inaccessible from either side in closed and open states for H_v1 (**FIGURE 12**). For K⁺ channels, one Arg is buried in closed and four in open states (16, 278). For Na⁺ channels, only the outermost Arg is buried in closed and none in open states: R3 is externally accessible, while R4 is internally accessible (529), although R4 and R5 have reduced accessibility (530). Four caveats with all such accessibility studies are as follows: 1) the Cys-reactive molecule used as an accessibility probe is much larger than a proton or ordinary ion, and is therefore prone to underestimating aqueous accessibility from the vantage point of a hydronium ion or a proton; 2) the presumption is that the mutation does not affect the global structure of the protein; 3) intermediate gating states may

have different accessibility; and 4) more specifically, one must assume that the most stable open and closed configurations of the mutant channel correspond with those occurring in the WT channel. Nevertheless, a quite different and less invasive approach that eschewed the use of mutations confirms this general picture. By measuring the reduction of measured gating charge at low ionic strength, Islas and Sigworth (234) concluded that the solvent-inaccessible septum was 3–7 Å in length.

According to MD simulations of H_v1, there is a narrow central region, perhaps 5–10 Å long, filled with immobile water molecules (415, 521). This ice jam would presumably prevent access of MTS reagents, and possibly even monovalent ions, but not protons, as is obvious from the empirical fact that protons permeate H_v1 channels! That Cl⁻ and even CH₃SO₃⁻ can permeate D112x mutants (362) may indicate that these mutations melt the ice or alter the open state. For example, if Asp¹¹² normally faces a cationic charge, electrostatic attraction would tend to narrow the pore, but in D112x mutants the pore might relax to a wider diameter. MD simulations support this intuition (361).

Not surprisingly, using a proton (or more accurately, a hydronium ion, H₃O⁺), as a probe, rather than MTS reagents, produces a more generous degree of accessibility than does Cys scanning. The Arg→His mutations of the K_v VSD were consistent with a single residue exposed to both external and internal solutions simultaneously, both in open and closed states (469–471). A slightly different picture emerged from studies of hH_v1 in which each of the S4 Arg residues was mutated to His (361). In contrast to the hyperpolarization-activated inward H⁺ current in Shaker VSD (470), there was no hint of inward H⁺ current in the closed state of hH_v1 with the R205H mutation. Accessibility was also evaluated by Zn²⁺ effects on the Arg→His mutants. Both R1 (Arg²⁰⁵) and R2 (Arg²⁰⁸) were accessible to the external solution, whereas R3 (Arg²¹¹) was accessible to the internal solution, even in the open state. MD simulations supported the external accessibility of R1 and R2 in the open state. Keeping in mind the caveats listed above, these results (**FIGURE 12**) do not support the idea of immobile waters filling a long stretch of the hH_v1 pore. In addition, they do not support a large excursion of S4 during channel opening. If we assume that R1 resides in the charge transfer center in closed hH_v1 channels, then at most, R1 and R2 may cross the constriction or gating pore during opening, with R3 interacting with Phe¹⁵⁰ in the open state.

How far does S4 move in K⁺ channels? Accessibility studies provide evidence for fairly large S4 movements (478). MacKinnon and colleagues proposed that the charged residues in S4 of the *Shaker* K⁺ channel VSD move through a “gating charge transfer center” (486), with an upper boundary corresponding to Phe¹⁵⁰ in hH_v1 (cf. **FIGURE 5**). This Phe is highly conserved, not only in K⁺ and Na⁺ chan-

nel VSDs, but also in H_V1 , and in fact in all classes of VSD containing molecules (462); it thus makes an excellent reference point. [The only other universally conserved residues are Asp¹⁷⁴ (hH_V1) = Asp³¹⁶ in *Shaker* and Arg²⁰⁸ = Arg³⁷¹ in *Shaker*.] A recent study by Papazian's group revealed that the first Arg in S4 (R1) resides in the charge transfer center in closed channels, and the fifth (K5) is there in the open state (300). A systematic study using Cys scanning of S4 in *Shaker* to form Cd²⁺ bridges revealed at least a 12 Å displacement of S4, with 4 Arg moving past the F290 hydrophobic seal (212). Similarly, in the Na⁺ channel VSD, at least three S4 Arg residues appear to move completely across the hydrophobic seal region (533). If S4 in hH_V1 moves as indicated by His scanning (361), with R1 at the charge transfer center in closed and R3 there in open channels, this would constitute only half the movement that occurs in the K⁺ channel VSD. In summary, existing evidence, which admittedly is somewhat sparse for H_V1 , suggests that S4 movement in H_V1 is less extensive, probably roughly half that of S4 in K⁺ channels. This difference may reflect the smaller number of charged residues in S4 in H_V1 than in Na⁺ and K⁺ channels. In the open state, Na⁺ and K⁺ channels are stabilized by external and internal charge networks (239, 305, 396, 478). If gating required all three Arg in S4 of hH_V1 to move past Phe¹⁵⁰, none would be left inside. Our model shows that the open channel is stabilized by robust charge clusters in both external and internal regions, precisely because Arg²¹¹ remains in the internal cluster (361).

After focusing on minutia of putative S4 movement in H_V1 , we should step back and recall two important differences. First, in other channels, S4 movement is linked to a conformational change in the S5-S6 helices that results in pore opening (FIGURE 3). In H_V1 , S5 and S6 are absent altogether, and although S4 movement presumably results in channel opening, we do not know what "open" means for H_V1 . The recent proposal that S4 is rigidly connected to the C-terminal domain, the coiled-coil interaction of pairs of which mediates cooperative gating of the H_V1 dimer (172), raises questions about how similar S4 movement needs to be or could be to that in other channels. The second major distinction is that gating in H_V1 is strongly regulated by ΔpH (see sect. VE), and thus, S4 movement itself must be regulated by ΔpH in a way that does not occur (at least not to the same extent) in other channels. Alternatively, after both protomers have undergone an activating conformational change, a concerted gating step must take place, which is regulated by ΔpH and is required for channel opening.

2. Interactive gating in the dimer

Gating refers to the tendency of ion channels to behave as though they exist in distinct open or closed states. The physical mechanisms that produce conducting and nonconducting states can be envisioned in various ways,

most simply as physical occlusion of the pathway, at least for ordinary ion channels. Proton pathways may be gated by subtler mechanisms. For example, proton uptake into cytochrome *c* oxidase of *Rhodobacter sphaeroides* may be regulated by conformational adjustments in the side chain of Asn¹³⁹ that allow or disallow formation of a water wire (213). Such a proton pathway was disrupted entirely by the substitution of the hydrophobic Val residue at this position. A "water-gated" mechanism was proposed for cytochrome *c* oxidase, in which redox-dependent electric field-induced orientation of water chains switches proton conduction between two pathways at appropriate times in the pump cycle (518), although this idea was later challenged (532). At present, the gating mechanism (i.e., the distinction between conducting and nonconducting states) of hH_V1 is unknown.

Like voltage-gated K⁺ channels, proton channels are strongly voltage sensitive and open with depolarization. The current turns on with a sigmoid time course, reminiscent of Na⁺ or K⁺ channels (FIGURE 13, A versus B). Proton channels even exhibit the "Cole-Moore effect" (86), which means that holding the membrane at more negative potentials increases the sigmoidicity of current turn-on during a depolarizing pulse (113). The sigmoidal activation time course suggests that despite the fact that both protomers in the dimeric proton channel have their own conduction pathway, both must undergo an opening transition before either can conduct (185, 360).

In species in which it is a dimer, including human, mouse, and *Ciona intestinalis* (259, 286, 359, 360, 497), the proton channel can be forced to express as a monomer by truncating the C terminus, both N and C termini, or by replacing the C terminus with the C terminus of Ci-VSP (cf. FIGURE 3), which is believed to exist as a monomer (260). Because each monomer has its own conduction pathway, this provides a rare opportunity to observe the gating of each monomer separately. There are several intriguing differences in the behavior of monomeric and dimeric (WT) channels. FIGURE 13A illustrates that dimeric WT hH_V1 channels activate sigmoidally, whereas when the channel is expressed as a monomer, activation is exponential (FIGURE 13B). It is noteworthy that the monomeric construct activates substantially faster than does the dimer for both mH_V1 (259) and hH_V1 (359, 360, 497) (FIGURE 13, A versus B); evidently opening is a more cumbersome process in the dimer. The g_{H^+} -V relationship is less steep with a slightly more positive midpoint in monomeric than dimeric constructs (359, 497).

Several types of evidence support the idea that the two protomers interact during gating in Ci H_V1 (185) and hH_V1 (359, 360, 498). Based on studies with dimers assembled from various combinations of mutations, Tombola et al. (498) proposed that the protomers gate individually, but

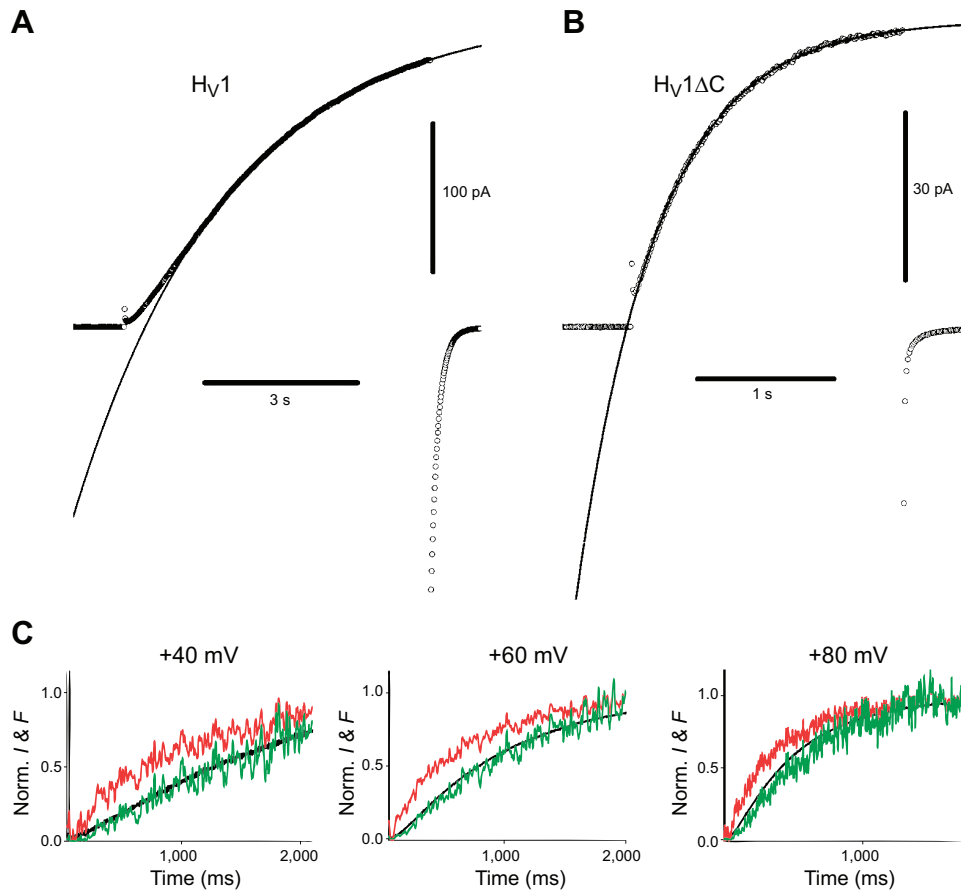


FIGURE 13. Dimeric (WT) hH_v1 proton currents activate sigmoidally (A), whereas monomeric channels activate more rapidly and exponentially (B). [From Musset et al. (360).] C: the fluorescence signal from a tag on S4 of CiH_v1 (red) reports movement of S4 during depolarization to the indicated voltages and changes faster and earlier than the current turns on (black line), which exhibits sigmoid activation kinetics. The S4 signal squared (green) mimics the current. [From Gonzalez et al. (185), with permission from The Nature Publishing Group.]

when one opens, strong positive cooperativity increases the probability that the second will follow suit. On the other hand, the E153C mutation was found to shift the $g_{\text{H}}-V$ relationship by -50 mV, but tandem dimers of one E153C protomer and one WT protomer resulted in a $g_{\text{H}}-V$ relationship essentially in the WT position, indicating that the protomer least likely to open determines when either will conduct (498). Further support for the idea that neither channel can open until both have undergone an opening transition is shown in **FIGURE 13C**. Gonzalez et al. (185) introduced a fluorophore in the S4 segment and observed changes in fluorescence during channel opening (**FIGURE 13C**). The fluorescence change (red trace) was slightly faster and had an exponential time course, whereas the simultaneously recorded H⁺ current (black) time course was sigmoid and lagged slightly. Raising the fluorescence signal to the power of 2 (green) roughly matched the time course of the current, as would be predicted for a Hodgkin-Huxley-type n^2 gating mechanism (220). These results are nicely explained if both subunits (monomers) must undergo a conformational change before either one can conduct. Gating appears slightly more complex than an n^2 gating mechanism in native pro-

ton channels, because no single fixed exponent reproduced proton current kinetics at all voltages, at least in rat alveolar epithelial cells where the optimal exponent ranged 1.1–2.0 (74) or in neutrophils where currents were fitted by exponents 1.5–2.0 (111). The relatively brief delay and slow, nearly exponential rising phase of proton currents is consistent with each monomer undergoing a conformational change, followed by a concerted opening step (222, 360).

The effective gating charge estimated from the limiting slope of the $g_{\text{H}}-V$ relationship (10, 455) is $\sim 6 e_0$ (electronic charges) for native rat proton channels (107, 108), for hH_v1 expressed in HEK-293 cells (355), and for CiH_v1 expressed in *Xenopus* oocytes (185), or $\sim 4 e_0$ for mH_v1 expressed in HEK-293 cells (172). In comparison, the gating charge for Na⁺ or K⁺ channels is 12–14 e_0 (4, 217, 235, 383, 440, 448). That the monomeric channel has only half the effective gating charge of the WT dimeric channel, 3 e_0 for CiH_v1 (185) or 2 e_0 for mH_v1 (172), strongly supports the idea that both protomers must open before either can conduct. If the protomers in the dimer opened and closed

independently, the dimer would have the same gating charge as the monomer.

Cooperative gating of other voltage-gated ion channels is understandable. They have multiple VSDs each of which undergoes conformational changes that are relayed mechanically to a single centrally located conduction pathway. Precisely how cooperative gating might occur in a dimer with two conduction pathways is not obvious. Tombola et al. (498) made the intriguing observation that E153C mutation produced a -50 mV shift of the g_H - V relationship, but that this shift did not occur in the C-truncated monomeric channel. They concluded that Glu¹⁵³ might be involved in coupling between monomers in the native dimeric channel. More recently, the C terminus was proposed to mediate cooperative gating (172). The interactions that comprise cooperative gating in H_V1 remain incompletely understood.

E. Δ pH-Dependent Gating

Like voltage-gated K^+ channels, proton channels are strongly voltage sensitive. Unlike most other channels, however, the voltage activation curve is extremely sensitive to the permeant ion concentration, i.e., the pH on either side of the membrane. A systematic study of rH_V1 in rat

alveolar epithelial cells by Cherny et al. (74) revealed that the g_H - V relationship shifts 40 mV/unit change in Δ pH, regardless of whether pH_o or pH_i is changed. This relationship can be summarized in various ways. A convenient equation is (74)

$$V_{\text{threshold}} = 20 - 40 \Delta\text{pH mV} \quad (3)$$

where $V_{\text{threshold}}$ is the “threshold” voltage at which distinct proton current is first observed. Because this formulation assumes that pH control is perfect, which is never true in practice, a tighter correlation can be obtained by (107)

$$V_{\text{threshold}} = 0.76V_{\text{rev}} + 18 \text{ mV} \quad (4)$$

where V_{rev} is the measured reversal potential. A slight variant of this relationship, illustrated in **FIGURE 14** (blue line), described all native proton currents reported up to 2003, including 15 cell types (104). All of these proton channels shared identical Δ pH dependence. This property is a hallmark of voltage-gated proton channels and a key to their function.

Despite the universal applicability of Δ pH-dependent gating, certain qualifications to Eq. 4 should be noted. First, $V_{\text{threshold}}$ is an arbitrary parameter, because g_H is a continuous function of voltage. Second, $V_{\text{threshold}}$ may be more positive than the predicted value if solutions contain con-

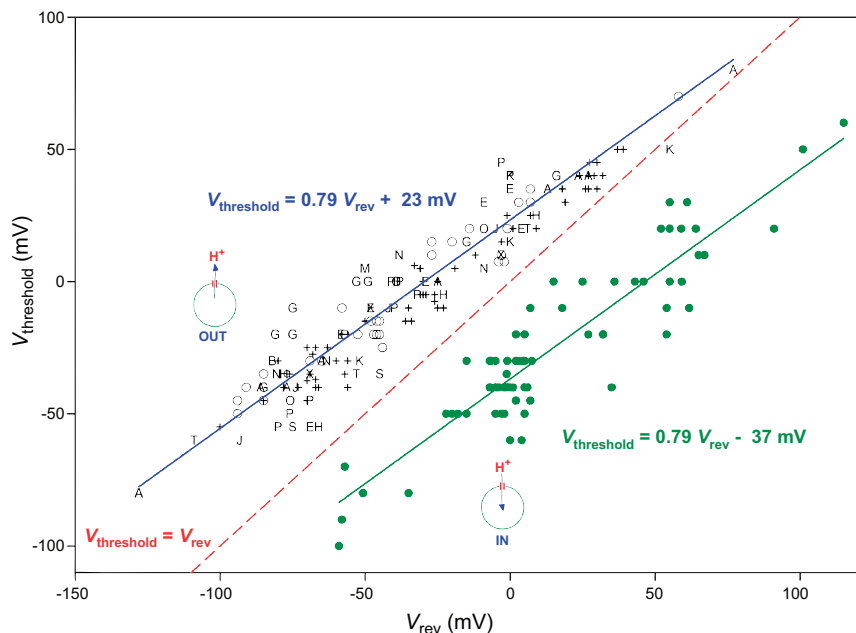


FIGURE 14. All proton channels share Δ pH-dependent gating. When $V_{\text{threshold}}$ is determined along with V_{rev} over a range of pH gradients, the result falls on a line defined by Eqs. 4 and 5 (text). Combined data from 15 different cell types were described by the blue line [Eq. 5, using values given in **TABLE 3**]. The red dashed line shows equality between V_{rev} and $V_{\text{threshold}}$, a data point that falls above this line means that when the channel opens, only outward current is possible. These channels open only when the electrochemical gradient is outward, when opening will result in acid extrusion from the cell. Data from the dinoflagellate, *K. veneficum*, have an identical slope, but are offset by 60 mV to more negative values. As a result, this channel opens and conducts inward H^+ current over a wide voltage range, and consequently must serve quite different functions. [Redrawn and combined from DeCoursey (104) and Smith et al. (462).]

taminant polyvalent metal cations (74). Most labs routinely include EGTA (along with excess Ca^{2+} , if one is concerned about this cation) as a precaution. Finally, several situations are known in which the relationship in Eq. 4 does not apply. We will therefore generalize Eq. 4 to encompass all known situations

$$V_{\text{threshold}} = \text{slope} \times V_{\text{rev}} + \text{offset} \quad (5)$$

It is significant that thus far, the slope appears to be constant, and only the offset varies. Ramsey et al. (415) generated and evaluated 30 different hH_V1 mutant channels and found that the offset varied widely (by >200 mV), but the slope never deviated far from 40 mV/unit pH (in terms of Eq. 3), with the minor exceptions of the N-terminal truncation (28 mV) and R211A (53 mV). The constancy of the slope likely reflects the importance of the ΔpH dependence of gating to the function of all voltage-gated proton channels. Such a critical function is evidently guarded by a robust mechanism to ensure failure avoidance.

TABLE 3 summarizes several situations in which offset differs from Eq. 4. A naturally occurring alteration in hH_V1 offset was first identified in the enhanced gating mode (see sect. VIII D) in human eosinophils (19). “Activation” of proton channels shifts offset in professional phagocytes by −40 mV compared with channels in unstimulated cells (115, 117, 354). When hH_V1 or mH_V1 is expressed heterologously in HEK-293 or COS-7 cells, $V_{\text{threshold}}$ tends to be somewhat more negative than in native proton currents (233, 355, 415, 416), for reasons that remain obscure. The naturally occurring human mutation M91T shifts $V_{\text{threshold}}$ positively by ~30 mV, decreasing the likelihood of channel opening (233). A recent reevaluation of published data from mollusks produced different slopes for pH_i and pH_o

(323), which might indicate a modified mechanism. Finally, kH_V1 in a dinoflagellate (*Karlodinium veneficum*) has a radically different offset, activating at voltages 60 mV more negative than all other proton channels (462). The effect of this aberrant offset is to produce a substantial voltage region in which inward H⁺ currents are activated. The stark contrast of this behavior with H_V1 in all other species led to the proposal that the fundamental functions of proton channels in dinoflagellates were different than in other species, in which the fundamental function deduced from design details is acid extrusion from cells. The proton channel in dinoflagellates is well suited to signaling functions and mediating action potentials (462) (see sect. VIA).

V. S. Markin devised a simple model to account for the ΔpH dependence of proton channel gating (74). This model postulated titratable groups that sensed pH_o and pH_i and specified rules that govern the accessibility of these sites. The expectation of this model is that if the pH sensing sites could be identified and mutated, the “Rule of Forty” (the 40 mV shift per unit change in ΔpH) should presumably no longer apply. Ramsey et al. (415) tested this prediction by mutating dozens of titratable residues in the hH_V1 molecule, and with two exceptions (see above), all mutants still obeyed the Rule of Forty. Either multiple sites are involved, or a fundamentally different mechanism must exist. Ramsey et al. (415) proposed that “protonated waters in the central crevice electrostatically interact with S4 arginine residues,” thereby communicating local pH to the voltage-sensing mechanism. The mechanism of pH sensing, despite its central importance to all known functions of the channel, remains mysterious.

Table 3. The ΔpH dependence of voltage-gated proton channels in various situations

Cell Type	Slope	Offset, mV	Reference Nos.
Rat alveolar epithelium	0.76	+18	107
Native proton current (15 cell types)	0.79	+23	104
Phagocyte (enhanced gating mode)	Approximately 0.63	Approximately −22	104
WT hH _V 1 in HEK-293	0.82	+13	416
WT hH _V 1 in COS-7 or HEK-293	0.66–0.73	−9 to −11	355
WT hH _V 1 in HEK-293	—	+7	415
WT hH _V 1 in COS-7 cells	0.78	+2.1	233
M91T hH _V 1 in COS-7 cells	0.81	+34	233
<i>Karlodinium veneficum</i> , kH _V 1	0.79	−37	462
Mollusc (pH _o)	1.35	+60	323
Mollusc (pH _i)	0.5	+8	323

The relationship between $V_{\text{threshold}}$ and V_{rev} in each case was fitted by linear regression, and the fitted values of slope and offset are defined in Eq. 5: $V_{\text{threshold}} = \text{slope} \times V_{\text{rev}} + \text{offset}$. The parameter values for enhanced gating mode are from a limited data set and should be considered approximate. Values for rat alveolar epithelium are a subset of “native proton current.” The final entries are from a reevaluation of data originally published in 1984 in *Lymnaea stagnalis* (53) and 1986 in *Helix pomatia* (130), which resulted in different slopes for changes in pH_i and pH_o (323).

F. Pharmacology: Inhibition by Zn^{2+}

Most ion channels can be inhibited by a variety of organic and inorganic substances, and many are exquisitely sensitive to specific peptides such as venoms and toxins that evolved specifically for that purpose. In contrast, there are almost no organic inhibitors of proton channels. Several weak bases give the illusion of inhibiting proton channels by permeating the membrane in neutral form, and depleting intracellular protons (104, 113, 318, 325). Several antidepressants (imipramine, amitriptyline, desipramine, and fluoxetine; IC_{50} 2.1–5.8 μM) and dextromethorphan (IC_{50} 51.7 μM) were reported recently to inhibit proton currents in the BV2 microglial cell line (465, 466). There was no change in V_{rev} or shift of the g_H - V relationship, arguing against an indirect effect due to pH changes by these weak bases. Application at various pH indicated that the intracellular charged form was active. Because the IC_{50} values were determined at pH_o 7.3, pH_i 5.5, the active drug form would be concentrated at the active site in the cell ~ 63 -fold by the pH gradient (370).

The classical H_V1 inhibitor is the zinc ion, which is active in its divalent form, Zn^{2+} (71). Thomas and Meech (492) found that several polyvalent metal cations (Zn^{2+} , Cd^{2+} , Cu^{2+} , La^{3+} , and Co^{2+}) inhibited proton current, and Martyn Mahaut-Smith (314) showed that Zn^{2+} was 80-fold more effective inhibiting H^+ currents than Ca^{2+} currents in *Helix* neurons. This observation was important because at that time, many scientists (including this author) harbored suspicions that proton channels per se did not exist and that proton currents were conducted through other ion channels. Demonstrating inhibition by Zn^{2+} , and to a lesser extent Cd^{2+} , became de rigueur in any characterization of proton currents in a new cell type. With the relentless discovery of proton channels in new species, especially those evolutionarily remote from humans, mammals, or even vertebrates, it was inevitable that Zn^{2+} -insensitive proton channels would crop up, and indeed they have. CiH_V1 in the humble sea squirt, *Ciona intestinalis*, is 27 times less sensitive than mH_V1 in the mouse (432). Even weaker Zn^{2+} sensitivity is exhibited by two unicellular marine species, *Emiliana huxleyi* (489) and *Karlodinium veneficum* (S. M. E. Smith, B. Musset, D. Morgan, V. V. Cherny, A. R. Place, J. W. Hastings, and T. E. DeCoursey, unpublished observations). This situation should not be a cause for alarm, unless of course, one is characterizing putative proton currents in a human cell type. After all, Zn^{2+} does not fit into a crucial constriction and sterically occlude the conduction pathway like a toxin, but simply binds at a relatively exposed location. The inhibitory effects in hH_V1 are almost completely eliminated by mutating two His residues, His¹⁴⁰ and His¹⁹³ (360, 416), and thus it is not surprising that species whose proton channel protein lacks one or both of these His might be insensitive.

The inhibition of mammalian proton currents by Zn^{2+} has provided a wealth of information about the channel. Like divalent metal cation effects on virtually all voltage-gated ion channels (146, 182, 216), Zn^{2+} slows activation (channel opening) and shifts the g_H - V relationship positively, at least in mammalian H_V1 . To a first approximation, these effects can be viewed as reflecting electrostatic effects of the metal cation on the voltage sensor, as proposed by Frankenhaeuser and Hodgkin (169) at the suggestion of Andrew F. Huxley. The membrane potential is sensed as being more negative than its actual value, and consequently, more depolarization is required to open the channel. Although reality is more complicated (146), this mechanism helps organize one's thinking on the general effects of metals on gating. Metal cations also tend to reduce the maximum conductance ($g_{H,max}$) possibly by neutralizing negative charges at the membrane or protein surface and consequently lowering the local cation concentration (180, 215). It seems clear that Zn^{2+} binds specifically to the channel, because it has a distinct additional slowing effect on activation not shared by Cd^{2+} . The slowing of τ_{act} by Cd^{2+} in rat rH_V1 (71), but not in *Lymnaea stagnalis* LsH_V1 (53), can be fully accounted for by assuming that all kinetic parameters are shifted along the voltage axis by the same amount as the g_H - V relationship. In contrast, after this "correction," Zn^{2+} still produces slowing in rH_V1 (71). The relative potency of Cd^{2+} is 30 times less than Zn^{2+} for shifting the g_H - V relationship, but >100 times weaker for slowing τ_{act} (71). The relative potency of several polyvalent metal cations on mammalian cells or snail neurons, derived from data from several sources is (98): $Zn^{2+} \approx Cu^{2+} \approx La^{3+} > Ni^{2+} > Cd^{2+} > Co^{2+} > Mn^{2+} > Ba^{2+}, Ca^{2+}, Mg^{2+} = 0$.

A different sequence may apply to other species. In fact, kH_V1 is more sensitive to La^{3+} , Cu^{2+} , and Ni^{2+} than to Zn^{2+} , but none of these is very potent (D. Morgan, B. Musset, S. M. E. Smith, V. V. Cherny, A. R. Place, J. W. Hastings, and T. E. DeCoursey, unpublished observations).

The effects of Zn^{2+} on mammalian H_V1 are extraordinarily sensitive to pH_o (71), as illustrated in **FIGURE 15**. For example, reducing pH_o from 6 to 5 decreases the apparent potency of Zn^{2+} for slowing activation by 100-fold, and that for shifting the g_H - V relationship by 230-fold (71). Viewed as competition between H^+ and Zn^{2+} for a binding site, and considering several possible types of competitive interaction led to the conclusion that the data were described well by postulating a site comprising 2–3 titratable groups with pK_a 6.2–6.6, most likely histidine (71). When the human gene was identified (416), two His were indeed identified that were exposed to the external solution and which together accounted for most of the Zn^{2+} sensitivity. A complication arose when Susan M. E. Smith produced a homology model of the hH_V1 molecule. The two His residues, His¹⁴⁰ and His¹⁹³, were too far apart to coordinate Zn^{2+} between them. When the channel was found to as-

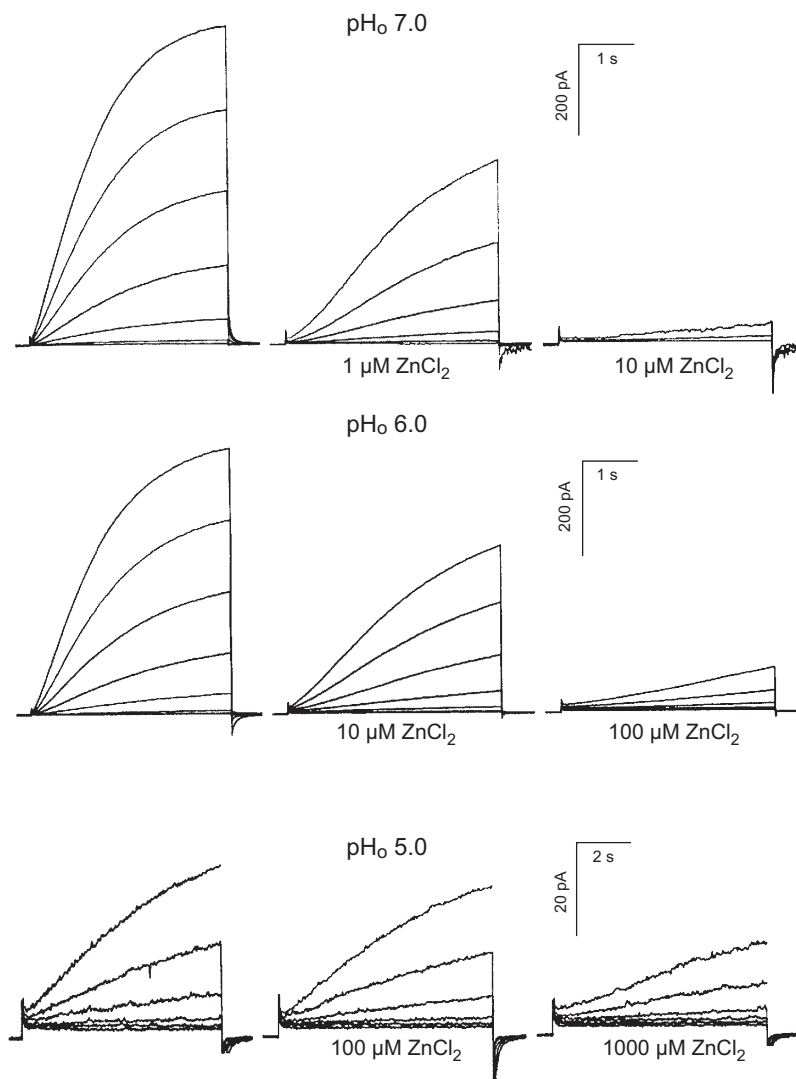


FIGURE 15. Strong pH_o dependence of the inhibitory effects of Zn^{2+} reflects competition for an external binding site. Each row shows currents in a rat alveolar epithelial cell during three identical voltage-clamp families, with pulses applied in 10-mV increments, in the absence or presence of Zn^{2+} . The two main effects, the slowing of activation and the shift of the $g_{\text{H}}\text{-}V$ relationship, both require dramatically higher $[\text{Zn}^{2+}]$ at low pH_o . [From Cherny and DeCoursey (71).]

semble as a dimer (259, 286, 497), a possible solution to this contradiction presented itself. Perhaps Zn^{2+} binds with high affinity at the interface between monomers. If this were the case, then Zn^{2+} effects should be weaker in the monomer. Forcing hH_v1 to exist in monomeric form by truncating the C terminus confirmed this prediction (360). A series of constructs was then generated (FIGURE 16). Profound slowing of activation is seen in the WT channel and the WT tandem dimer. Removing either His from each monomer weakened Zn^{2+} effects, and mutating both abolished the slowing effect altogether. The most surprising result was that a construct with His¹⁴⁰ and His¹⁹³ both present on one monomer, but absent from the other (WT-H140A/H193A tandem dimer), exhibited no slowing. Taken together, these results support the hypothesis that Zn^{2+} slows proton channel opening by binding at the interface between monomers (360).

VI. PHYSIOLOGICAL ROLES: DIVERSE SPECIES

A. Dinoflagellates: A Proton Channel Triggers the Bioluminescent Flash!

The existence of voltage-gated proton channels was first proposed in 1972 by Margaret Fogel and J. Woodland Hastings, who hypothesized that depolarization-activated proton channels triggered the flash in bioluminescent dinoflagellates (161). Numerous dinoflagellates emit light flashes when they are mechanically disturbed (379), for example, by a boat or swimmer, or simply waves crashing on the beach or against pier pilings. Among proposed functions of the flash are disrupting predators by startling, confusing, or blinding them temporarily (50–52, 343), illumi-

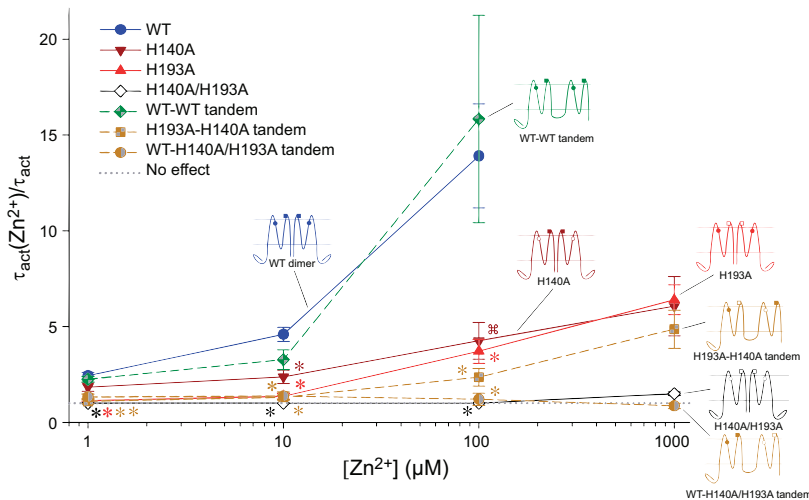


FIGURE 16. Evidence that Zn^{2+} binds with high affinity at the interface between the two monomers in the dimeric human proton channel. The Zn^{2+} dependence of the slowing of channel opening (τ_{act}) by Zn^{2+} is plotted for WT hH_v1 and six related constructs in which one or both of the key His residues, His¹⁴⁰ and His¹⁹³, were replaced with Ala, including three tandem dimers. *Inset* cartoons show His as solid, Ala as open, with circles for position 140 and squares for position 193. Slowing occurs only when at least one His is present in each monomer. [From Musset et al. (360).]

nating nonluminescent prey as a diversionary tactic (160, 327), and the closely related “burglar alarm theory,” attracting secondary predators on the principle that the enemy of my enemy is my friend (1, 48, 343). The mechanism of transduction of the stimulus, shear stress (280, 315), into an action potential is unclear, but seems to involve calcium signaling (508). The presence of small organelles that produced flashes, visible due to the transparency of the *Noctiluca* organism, was described as early as 1850 by A. de Quatrefages (95, 201). Roger Eckert and colleagues explored the phenomenon of an apparently “inverted” action potential (66, 218) that triggered bioluminescent flashes in *Noctiluca miliaris*, since renamed *N. scintillans*, and illuminated the relevant anatomical structures involved. Eckert showed that the action potential was inverted because the recording microelectrode was typically inserted into the large central floatation vacuole, rather than into the extremely thin ($\sim 0.1 \mu m$) surrounding layer of cytoplasm (135, 136), and thus the configuration was the equivalent of extracellular recording of an action potential in a nerve or muscle cell (133, 134). He showed that the flashes originated in tiny evaginations of cytoplasm (FIGURE 17) whose membrane was continuous with the tonoplast, the membrane enclosing the large central vacuole (132). A single *Noctiluca* specimen contains $\sim 50,000$ of these “microsources,” mostly $< 1 \mu m$ in diameter, each one emitting $\sim 100,000$ photons per flash (135).

The Hastings lab isolated microsources from another bioluminescent species, *Gonyaulax polyedra* (126) (now called *Lingulodinium polyedrum*), and christened them “scintillons” (163, 204). These organelles contain almost exclusively three molecules: luciferin, luciferase, and luciferin binding protein (39, 161, 162, 202, 203, 266, 438). Protons

trigger the flash by two distinct mechanisms. Luciferase is inactive at high pH but becomes active at low pH (266, 438). In addition, luciferin binding protein releases luciferin (the substrate for luciferase) at low pH (39, 162, 266, 438). The scintillon is surrounded by vacuolar sap, which has very low pH of 3.5–4.5 (374, 380). If proton-selective channels were opened in the scintillon membrane by the invasion of an action potential from the tonoplast, this enormous chemical gradient would ensure rapid proton flux into the scintillon where the flash would be activated (161). The recent identification of a voltage-gated proton channel gene in the nonbioluminescent dinoflagellate *Karlodinium veneficum* (462) confirms that the H_v1 family tree extends to dinoflagellates, and strongly supports this hypothetical mechanism.

1. A proton action potential?

A related but distinct function for H_v1 in bioluminescent dinoflagellates has also been proposed, namely, mediating the action potential that triggers the flash (104, 373, 380, 462). A membrane permeability increase occurs during the action potential (136), as occurs in nerve (85). The action potential height was found by Nawata and Sibaoka (373) to be insensitive to the vacuolar concentration of all ions except H⁺, indicating that H⁺ flux mediates the action potential. To this author’s knowledge, a proton-mediated action potential is unique to dinoflagellates. A non-voltage-gated proton channel triggers an action potential in sour taste cells (67), but in this case, external acid influx directly triggers an action potential that is itself mediated by voltage-gated Na⁺ channels. Triggering an action potential simply requires sufficient inward current to depolarize the membrane to the threshold for activating the channel that mediates the action potential. To mediate an action potential, a

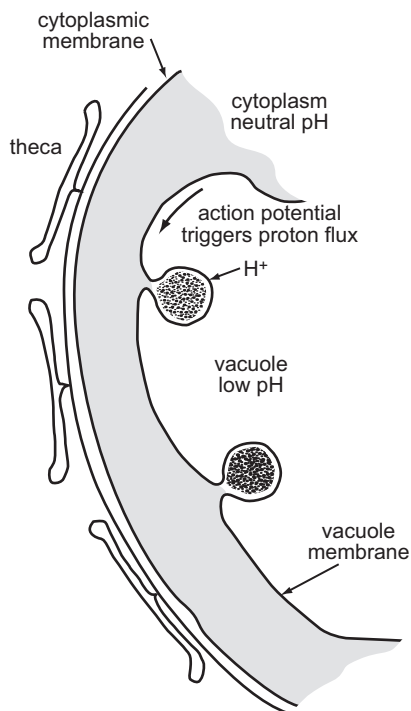


FIGURE 17. Proton channels trigger a light flash in bioluminescent dinoflagellates in response to mechanical stimulation. An action potential travels along the tonoplast, the membrane surrounding the large central flotation vacuole, and invades the scintillon, a small organelle that contains high concentrations of luciferin, luciferase, and luciferin binding protein. The depolarization opens voltage-gated proton channels in the scintillon membrane. The resulting proton influx from the vacuole (at pH 3.5–4.5; Refs. 374, 380) directly triggers the flash both by activating luciferase and by causing LBP to release luciferin, the substrate for luciferase. A proton channel with properties like those in kH_V1 (FIGURES 18 AND 19) could also mediate the action potential. [From Hastings (202).]

channel must exhibit a “negative slope conductance” region in its current-voltage characteristic (237). This simply means that the channel opens with depolarization, but does so negative to its reversal potential.

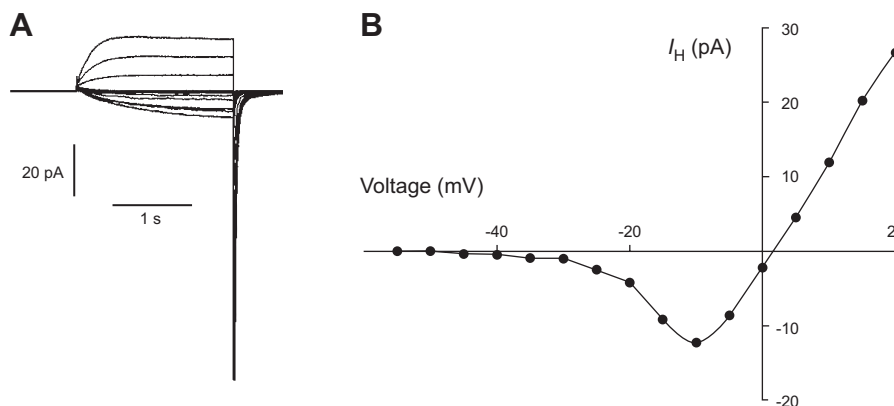


FIGURE 18. The proton channel kH_V1 , from the dinoflagellate *Karlodinium veneficum*, exhibits inward proton currents. **A:** during depolarizing pulses in 5-mV increments from $V_{hold} = -60$ mV through +15 mV at symmetrical pH 7.0, there are inward currents over a wide voltage range. **B:** the current-voltage curve resembles that of voltage-gated Na^+ or Ca^{2+} channels, which are also capable of mediating action potentials. [From Smith et al. (462).]

The properties of the proton channel (kH_V1) identified in the dinoflagellate *Karlodinium veneficum* proved to be unique (462). **FIGURE 18** shows that the kH_V1 channel displays precisely the behavior required to mediate action potentials in dinoflagellates (462)! Like voltage-gated Na^+ or Ca^{2+} channels, $V_{threshold}$ is well negative to the reversal potential, resulting in a substantial voltage range over which the channel conducts inward current. Inward H^+ flux (like inward Na^+ or Ca^{2+} flux) causes depolarization, which activates more voltage-activated channels, resulting in a regenerative response, namely, an action potential. A g_H -mediated action potential in a bioluminescent species like *Noctiluca* could mediate proton flux from the vacuole at pH 3.5 into the scintillon, directly initiating the light flash (**FIGURE 17**). In most respects, kH_V1 behaves like other voltage-gated proton channels, sharing the universal property of ΔpH -dependent gating (**FIGURE 19**), but it differs from all others identified to date in having a $V_{threshold}$ that is 60 mV more negative (**FIGURE 14**). This is precisely the property necessary to perform both proposed functions in bioluminescent dinoflagellates. Because the orientation of the channel would equate vacuole contents with extracellular space (136), the ΔpH dependence of any other H_V1 would only allow outward current (i.e., from cytoplasm into the vacuole). However, triggering the flash requires H^+ flux from vacuole into scintillon, which requires the channel to open negative to E_H . Any other proton channel would simply fail to open (**FIGURE 14**). Similarly, mediating the action potential requires proton influx from vacuole into the cytoplasm. To date, this elegant mechanism remains unproven, because as yet H_V1 has not been confirmed in a bioluminescent species. That the one known dinoflagellate proton channel, kH_V1 , has uniquely ideal properties to carry out these functions provides hope that the final bit of evidence will soon be found.

2. Functions in nonbioluminescent species

Evidence suggests that proton channels trigger tentacle flexion in *Noctiluca* (387). Functions in nonbioluminescent

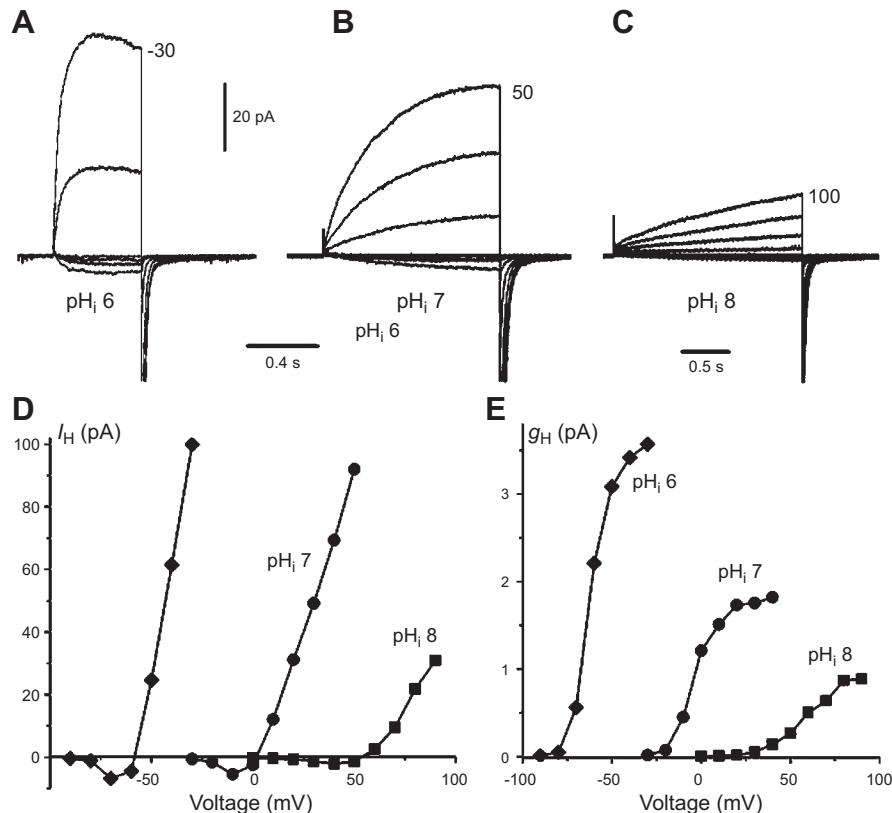


FIGURE 19. Proton channels from the dinoflagellate *Karlodinium veneficum* differ from all known H_V1 in producing distinct inward currents, but share ΔpH-dependent gating. Because the g_H - V relationship is shifted ~60 mV more negative than in other species at any given ΔpH, $V_{\text{threshold}}$ occurs well negative to E_{H^+} . A–C show families of proton currents in an inside-out patch at pH_o 7.0 and at the indicated pH_i. Pulses were applied in 10 mV increments with the most positive voltage labeled. The corresponding current-voltage relationships (D) resemble those for voltage-gated Na⁺ channels, especially at low pH_i. The g_H - V relationship is (E) shifted by changes in pH_i, as in other proton channels. [From Smith et al. (462).]

species are mainly speculative in nature: trichocyst extrusion, prey capture, or digestion (462).

B. Coccolithophores: Proton Channels Facilitate Calcification

Voltage-gated proton channels have been identified in two species of marine phytoplankton, the coccolithophores *Coccolithus pelagicus* ssp *braarudii* and *Emiliania huxleyi* (489). Coccolithophores evolved 250 million years ago, making CpH_V1 and EhH_V1 early examples of the H_V1 family (489). Coccolithophores are major producers of biogenic calcite. They produce calcite, CaCO₃, in intracellular compartments and secrete the resulting coccoliths to the cell surface, forming a coccosphere. The conversion of HCO₃[−] to CaCO₃ impacts the global carbon cycle. The production of calcite occurs by the following pathway (FIGURE 20): Ca²⁺ + HCO₃[−] → CaCO₃ + H⁺.

This reaction produces intracellular protons continuously. These protons must be removed to allow sustained calcification. Inhibition of CpH_V1 with Zn²⁺ led to an immediate

decrease in pH_i, indicating that the g_H is constitutively active and contributes to pH_i regulation. This contrasts with unperturbed mammalian cells, in which the resting membrane potential is usually negative to $V_{\text{threshold}}$ and proton channels are closed. However, this may be a false distinction, because when Ca²⁺ was removed from the seawater, precluding calcification, addition of Zn²⁺ no longer resulted in acidification. In other words, under normal conditions coccolithophores never rest! The importance of pH_i homeostasis during calcification was demonstrated by lowering pH_i for 10 min either by a decrease in pH_o or by an NH₄⁺ pulse. Both interventions decreased the calcification rate by nearly 70%, and the rate remained depressed for ~2 h after removal of the insult (489).

The coccolithophore H⁺ conductance mediates rapid H⁺ efflux and may play an important role in pH homeostasis in calcifying cells. The process requires efficient H⁺ efflux pathways in coccolithophores to sustain intracellular calcification. Proton channels have almost unlimited capacity to extrude H⁺ at no direct metabolic cost to the cell (113) and therefore provide an excellent mechanism for acid extru-

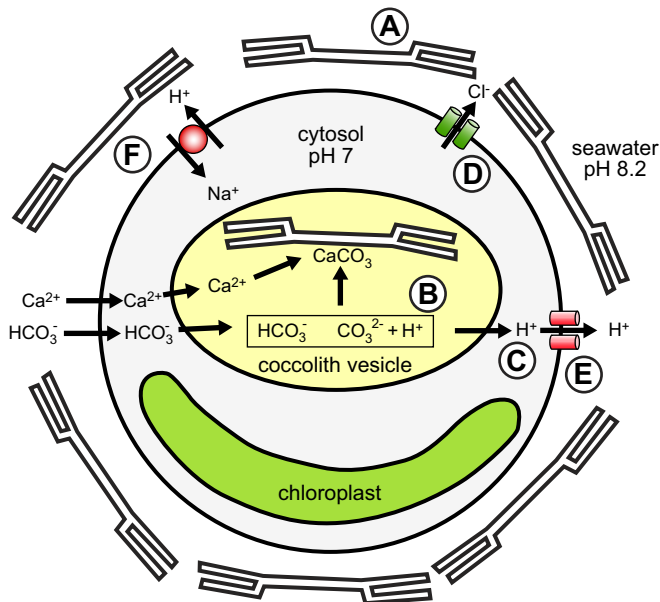


FIGURE 20. Role of proton channels in calcification and pH homeostasis in coccolithophores. Mature coccoliths arranged on the extracellular surface surround the cell to form a coccosphere (A). Coccolith formation occurs within an intracellular Golgi-derived coccolith vesicle (B). Calcium carbonate (CaCO_3) precipitation requires the production of carbonate (CO_3^{2-}) from bicarbonate (HCO_3^-) and results in net production of H^+ . H^+ must be rapidly removed from the coccolith vesicle to maintain a pH conducive to CaCO_3 precipitation. Once in the cytosol (C), some H^+ may be utilized by photosynthesis in the production of CO_2 from HCO_3^- (see text); however, H^+ efflux provides an efficient mechanism to prevent cytosolic acidosis, which inhibits calcification (489). Patch-clamp studies indicate that Cl^- and H^+ are the dominant transmembrane conductances in coccolithophores (487, 489). At normal seawater pH 8.2, pH_i of 7.0–7.2 and membrane potential approximately -60 mV maintained by a Cl^- inward rectifier (D) (487), a drop in pH_i or membrane depolarization or both would activate plasma membrane H^+ channels (E), providing an extremely efficient and rapid mechanism for maintaining constant intracellular pH. [From Taylor et al. (489).]

sion. Some of the H^+ produced may be combined with HCO_3^- to produce CO_2 , the substrate for the main carbon fixing enzyme, ribulose biphosphate carboxylase (RuBISCO) (313). Carbon-concentrating mechanisms exist in many aquatic plants and algae (419), because in spite of the best efforts of pyrophiliac humans, ambient CO_2 in marine systems can be suboptimal for photosynthesis (392). Despite this potential use of the H^+ produced by calcification in photosynthesis, the latter process has been shown to be independent of the former (290). Ocean acidification could impact the ability of coccolithophores to produce calcite by inhibiting the activity of proton channels, due to the ΔpH dependence of gating. Since the last glacial maximum (i.e., Ice Age), CO_2 levels in Antarctic ice have increased from 190 to 280 ppm (a 47% increase), while coccolith mass at low latitudes has declined from 13.6 to 7.5 μg (a 45% decrease) (26). The ΔpH dependence of $\text{H}_\text{V}1$ gating can maintain acid extrusion under a wide range of conditions, but the achievable pH_i is limited by pH_o .

C. Snail Neurons: Acid Extrusion During Trains of Action Potentials

The proton channels in snail neurons are the fastest to open and close. They would be capable of opening during an action potential, and this is the context of their proposed function. Action potentials in snail neurons are conducted by Ca^{2+} channels, and the Ca^{2+} influx is subsequently compensated by $\text{Ca}^{2+}/\text{H}^+$ exchange (6, 324) at the expense of local acidification inside the membrane (53, 325). Proton channels that open during action potentials would help alleviate this acid load. Later studies using confocal imaging of fluorescent pH sensing dyes have confirmed several aspects of this proposal (395, 445). Depolarization produces Ca^{2+} influx resulting in $\text{Ca}^{2+}/\text{H}^+$ exchange, which produces an acid load that can be extruded by proton channels. In addition, proton flux across the plasma membrane can produce substantial pH gradients within individual neuronal cells (395).

D. Proton Channels in Amphibian Eggs

After snail neurons, the second cell type in which voltage-gated proton channels were identified and characterized by voltage-clamp was the *Ambystoma* (salamander) oocyte (22). Proton current decreased and pH_i increased suggestively during oocyte maturation (25), leading to the idea that $\text{H}_\text{V}1$ contributes to alkalinization during maturation. A similar proposal was made for the role of $\text{H}_\text{V}1$ in *Rana esculenta* oocytes (232). It is well established that *Xenopus laevis* oocytes alkalinize during maturation and that the mechanism reflects acid efflux (82). Acidification delays maturation and oocytes can be induced to mature by exogenously induced alkalinization; however, preventing alkalinization did not prevent maturation (285). Intriguingly, proton channels were recently proposed to play a role in alkalinization of human sperm (below), indicating a general role in fecundity. $\text{H}_\text{V}1$ was also proposed to facilitate Ca^{2+} release from inositol triphosphate-sensitive stores in *Rana esculenta* oocytes (231).

VII. ROLES IN MAMMALIAN AND HUMAN CELLS

A. General Functions: Acid Extrusion, Volume Regulation, and Setting Membrane Potential

In the absence of a more specific function, the ΔpH and voltage dependence of proton channel gating ensure that a probable function in any cell (excepting dinoflagellates) is extrusion of excess acid. The design is perfect for the relief of metabolic acid, while incurring no immediate energetic cost to the cell. In rat hippocampal neurons, anoxia or ischemia produces intracellular acidification that is alleviated in part by $\text{H}_\text{V}1$ (127, 451). Proton channels have been shown to contribute to acid

extrusion after acid loading in human neutrophils (122, 368), human basophils (358), murine mast cells (270), murine microglia (525), rat microglia (342), rat alveolar epithelial cells (350), rat hippocampal neurons (70, 127, 451), and rabbit osteoclasts (384, 385), not to mention coccolithophores (489) and snail neurons (492).

Involvement of voltage-gated proton channels in cell volume regulation has been proposed in rat microglia (342) and bovine chondrocytes (429).

Under conditions that preclude other conductances, the proton channel can help set the resting membrane potential of cells. This phenomenon has been demonstrated in solutions lacking permeant ions in human cardiac fibroblasts (144) and in activated human eosinophils (19). Because human eosinophils lack any K^+ conductance active at potentials positive to -60 mV (154), during the respiratory burst, when the membrane is depolarized drastically by NADPH oxidase (see below), it is likely that even in physiological solutions hH_V1 contributes significantly to setting the membrane potential.

B. pH_o Regulation in Airway Epithelium

The first mammalian cells in which voltage-gated proton currents were identified were rat type II alveolar epithelial cells in primary culture (99). Their proton currents are large, stable, and reproducible, and consequently many of the biophysical properties of proton channels were determined in these cells. Beyond the general function of acid extrusion (350), a specific function in promoting CO_2 elimination by the lung via facilitated diffusion was hypothesized, in which dissociation of CO_2 ($+H_2O$) into H^+ and HCO_3^- increased net CO_2 flux by increasing the concentration of diffusing species across the alveolar epithelial apical membrane (100). It is well known that carbonic anhydrase facilitates CO_2 diffusion (177, 191, 192, 426) and does so specifically in intact lung (138, 149, 206, 257, 258, 298, 479, 485). However, hH_V1 -mediated H^+ flux is unlikely to be a quantitatively significant contributor to this process under normal conditions because of the absence of carbonic anhydrase in the apical subphase liquid (100, 138, 139, 480).

Proton currents are also present in airway epithelial cells (that line the proximal airways comprising the conductive zone), including human bronchial epithelium in primary culture, and several airway epithelial cell lines (80, 156, 158). The general function is acid secretion, but the details of this process are still evolving (FIGURE 21). The fluid lining both the airways and the alveolar surface is maintained at low pH (40, 157, 238, 272, 377, 381). Histamine and ATP stimulate apical acid secretion that is inhibitable by Zn^{2+} (158). Identification of several Duox isoforms in airway epithelial cells raised the possibility that proton channels might facilitate reactive oxygen species (ROS) production

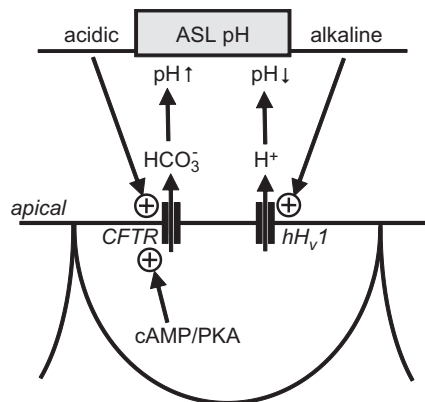


FIGURE 21. Regulation of the pH of airway surface liquid (ASL) by the combined reciprocal efforts of hH_V1 and CFTR. The anion transporter CFTR extrudes HCO_3^- passively, alkalizing the ASL. This increased pH_o opens proton channels, which passively extrude H^+ , restoring the ASL pH to its normal value. [From Fischer (156), with permission from Wiley.]

(166), analogous to their role in phagocytes (see sect. VIII). However, in contrast to phagocytes, airway epithelial cells have relatively constant membrane potential and pH as well as abundant conductances that dwarf the small g_H in these cells (156). Furthermore, Duox activity is much smaller than that of NADPH oxidase in phagocytes (444). These considerations indicate that proton channels in airway epithelia, despite being voltage gated, are not primarily activated by membrane depolarization under physiological conditions. This leaves ΔpH as the factor that must activate proton channels. In further contrast to the phagocyte paradigm, the main contributor to activation by ΔpH is increased pH_o , rather than decreased pH_i (233). Of the three potential acid-secreting transporters, hH_V1 , Na^+/H^+ antiport, and a V-type H^+ -ATPase, basal H^+ secretion against the gradient is likely accomplished by a V-type H^+ -ATPase, whereas proton channels take over when the apical surface fluid becomes alkaline (156, 233). The main culprit responsible for fluid alkalization is CFTR, which extrudes HCO_3^- passively (157, 409). Horst Fischer (156) has proposed that CFTR and hH_V1 form a passive feedback system to control the pH of airway surface liquid, illustrated in FIGURE 21. The proton channel contributes at least half of total acid secretion by human sinonasal mucosa from both normal and asthmatic subjects, but the contribution was less and mucosal pH was lower in asthmatic subjects with chronic rhinosinusitis (80). In summary, the primary function of hH_V1 in airway epithelium appears to be acidifying excessively alkaline airway surface liquid, and not regulating pH_i (156).

C. Histamine Release by Basophils

Basophils and eosinophils are closely related developmentally, but their functions are quite different. In stark contrast to the eosinophil, which has the highest NADPH oxi-

dase activity of any human cell, triple that of neutrophils (97, 115, 273, 405, 527, 528, 535), basophils have no detectable NADPH oxidase activity (92) and do not kill pathogens. Nevertheless, both cells have large proton currents (76, 441). Basophils, like mast cells, secrete histamine in response to allergen binding to allergen-specific IgE. Stimulation of basophils with IgE antibody resulted in enhanced gating of proton channels, usually after a delay of one to several minutes (358). As in phagocytes stimulated with “physiological” agonists, the anti-IgE response was variable, usually smaller than the response to phorbol 12-myristate 13-acetate (PMA), and occurred in only a fraction of cells. Basophils that did not respond to anti-IgE still responded to subsequent PMA stimulation. The anti-IgE response was reversed by the PKC inhibitor GFX (GF109203X). The enhanced gating of proton channels in basophils is thus most likely regulated by PKC, as in phagocytes. Intriguingly, the enhanced gating produced by PMA was weaker in basophils than in phagocytes. As discussed below (see sect. VIII D), this observation supports the idea that fully enhanced gating requires the participation of NADPH oxidase, which basophils lack.

The purpose of proton channel activation in basophils may be to extrude acid generated during the process of histamine secretion. Histamine release stimulated by anti-IgE or PMA was inhibited by Zn^{2+} , with half-maximal inhibition at 20–90 μM . Confocal imaging with the pH sensing fluorescent dye SNARF-1 revealed that basophils acidify after anti-IgE stimulation. The acidification was increased and prolonged in the presence of Zn^{2+} ; thus excessively low pH_i may inhibit histamine release by basophils. A second, more speculative function is charge compensation. Several lines of evidence indicate a requirement for Ca^{2+} influx for a maximal response to physiological agonists like anti-IgE (311, 378, 514) and eosinophil granule major basic protein (312), which may occur via CRAC channels. Outward H^+ flux mediated by hH_V1 would compensate for electrogenic Ca^{2+} influx, thereby maintaining a driving force for Ca^{2+} entry.

D. B Lymphocytes: Proton Channels Participate in B Cell Receptor Signaling

Tom Schilling and Claudia Eder (436) identified voltage-gated proton currents in human B and T lymphocytes, and in the lymphocytic Jurkat cell line. Proton currents were large in human B cells and Jurkat cells, but 100 times smaller (only a few picoamperes per cell) in T lymphocytes, paralleling the ability of these cells to produce ROS. More specific evidence of a role in B cells was provided by identification of the *Hvcn1* gene in a proteomic screen of membrane proteins in B cell lymphoma cells (42). The H_V1 protein was expressed highly in peripheral B lymphocytes but was below the limit of resolution of the technique in T cells (61). Expression was downregulated in proliferating B cells

in the germinal center (61), suggesting a role in early stages of B-cell activation. Indeed, B-cell activation was found to be impaired in knockout (KO) mice (61).

The hH_V1 protein was found to be associated with the B cell receptor (BCR) complex and to colocalize with the receptor upon stimulation. The signaling functions of proton channels in B cells (FIGURE 22) appear to be related to its involvement in ROS production, which is impaired in KO mice (61). The signaling pathways are complex: ROS inhibits protein tyrosine phosphatases (e.g., SHP-1), which inhibits spleen tyrosine kinase (Syk) by dephosphorylation (131), which further regulates other pathways including PI3 kinase (29, 271) and protein kinase Akt (168). The main role of proton channels in B cells thus appears to be modulation of signaling pathways.

On the other end, overexpression of H_V1 in immature B cell lines, which normally do not express it, inhibited cell cycle progression, although the mechanism remains to be identified (475).

E. Proton Channels in Capacitation and Motility of Sperm: The Zn^{2+} Theory

Voltage-gated proton channels with properties similar to those in other human cells are highly expressed in human, but not mouse, spermatozoa (303). An intriguing proposal provides a role for proton channels in the capacitation of sperm, a maturation process that takes place upon arrival in the female reproductive tract, and is prerequisite for fertilization. According to the zinc theory, low pH_i keeps sperm quiescent until they enter the female. Proton channels are prevented from opening by a high concentration of ambient zinc, which is present in higher total concentration in seminal fluid than any other human tissue (320), estimated at 2.2 mM (427). An increase in pH_i stimulates metabolic activity and motility (13) and is associated with an increase in proton permeability (12). Cytoplasmic alkalization occurs both by exposure to more alkaline environment and by removal of Zn^{2+} , which is complexed by proteins in the oviduct and is eventually absorbed (194). Removal of Zn^{2+} allows the proton channels to open and extrude acid, because pH_i is low and pH_o is high already. In turn, the increase in pH_i activates several pH-sensitive processes, including motility, metabolism, and hyperactivation (303).

Two other factors may contribute to proton channel activation in sperm. Anandamide, an endocannabinoid that is present in both male and female reproductive tracts (443), enhances the gating of hH_V1 in sperm (303) much like arachidonic acid does in human neutrophils or eosinophils (73, 111, 187, 335, 441). At similar concentrations of 1–10 μM , both increase H^+ current and shift the g_H-V relationship toward more negative voltages. However, physiological levels of anandamide in human male and female repro-

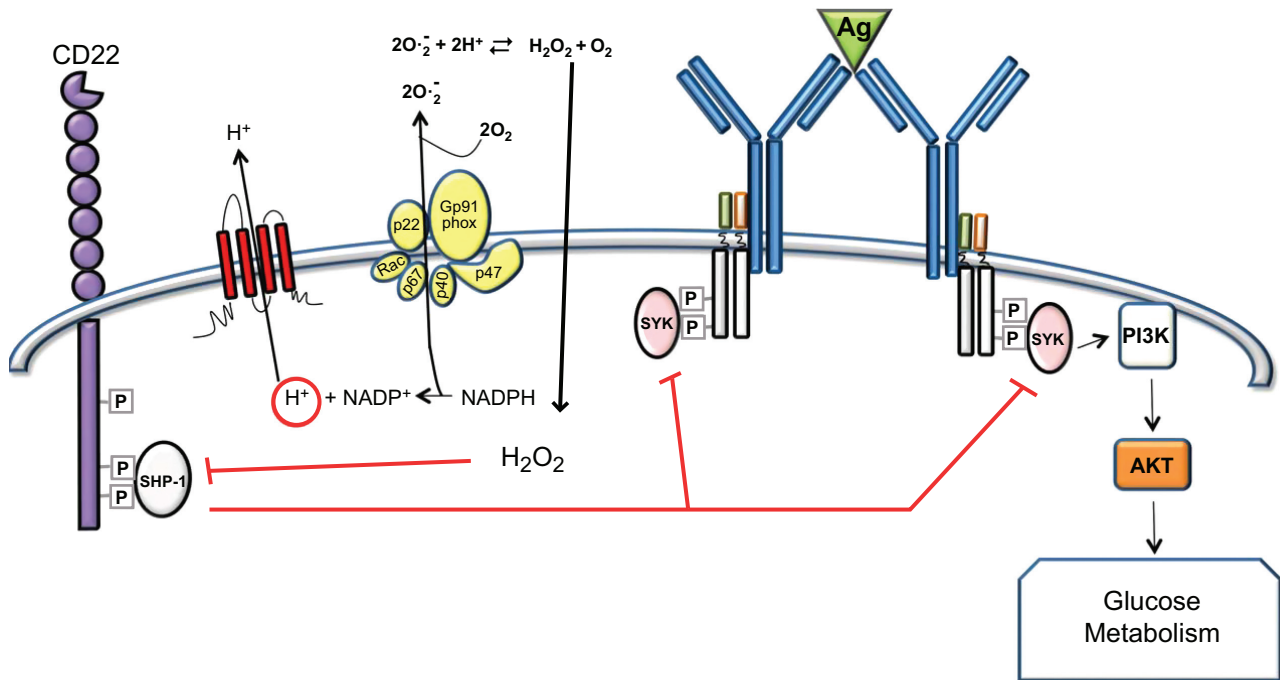


FIGURE 22. Involvement of hH_v1 in B lymphocyte signaling pathways. Antigen binding to the BCR results in phosphorylation of internal signaling molecules, with negative feedback from CD22. BCR stimulation results in NADPH oxidase activation, producing H₂O₂ that diffuses back into the cell where it inhibits SHP-1, thereby relieving inhibition of BCR signaling by the latter. See References 61 and 62 for more detailed descriptions. [From Capasso et al. (62), with permission from Elsevier.]

ductive tracts (443) are three orders of magnitude lower than those that affect proton channel gating, casting doubt on the physiological relevance of this effect. The second factor is enhanced gating of hH_v1 that was observed in capacitated compared with noncapacitated sperm (303). The enhancement of gating appears qualitatively similar to, but weaker than, that observed in phagocytes (see below), but the true effect may well have been underestimated, because measurements were done in whole cell rather than perforated-patch configuration. Enhanced gating of hH_v1 in phagocytes occurs only in perforated-patch studies, because the signaling pathway apparently requires diffusible second messengers (117, 337). The mechanism of enhancement of hH_v1 in sperm is unknown and may or may not share this property. In general, the enhancement of gating means that proton channels will be activated more readily, and presumably this will enhance their function.

Because mouse sperm lack proton channels (303), their proposed role in fertility cannot be evaluated in KO mice. Suggestively, median levels of *Hvcn1* mRNA were 18-fold lower than normal in a sample of 8 teratozoospermic human subjects, i.e., subjects with male infertility (407).

Another role for H_v1 has been described in human spermatozoa, where NOX5 is the main source of superoxide (356) (**FIGURE 23**). In these cells, enhanced gating of H_v1 proton currents correlates with sperm capacitation and hypermotility (303). Interestingly, Zn²⁺ significantly decreases superoxide production in human spermatozoa, and H_v1 was

shown to coimmunoprecipitate with NOX5 (356). Evidence of a functional interaction between hH_v1 and NOX5 came from studies using K562 cells that overexpress NOX5. In these cells that express hH_v1 endogenously, Zn²⁺ or expression of H_v1-specific siRNA reduces NOX5 superoxide-generating activity. However, overexpression of NOX5 did not alter hH_v1 activity. These results suggest that as observed in many cells for NOX2, H_v1 is required in sperm for optimal NOX5 activity.

F. Do Proton Channels Cause Breast Cancer?

Like all good things, in the wrong hands, even proton channels may do harm. A recent study raised the specter of breast tumor cells exploiting proton channels to facilitate metastasis. Levels of hH_v1 mRNA were highest in a highly metastatic cell line MB-231, but very low in a weakly metastatic line MCF7 (512). The correlation was imperfect, however, because a different poorly metastatic line, MB-468, had the second highest hH_v1 mRNA levels of six lines tested. Nevertheless, downregulation of hH_v1 by siRNA reduced invasion and migration indexes preferentially of highly metastatic cells (512). Finally, in siRNA treated cells, pH_i was significantly lowered, indicating a contribution of hH_v1 to resting pH_i, something not seen in normal cells (334). A remarkably similar picture was found for H⁺-ATPase in a previous study (447); levels of expression and activities were highest in metastatic human breast cancer

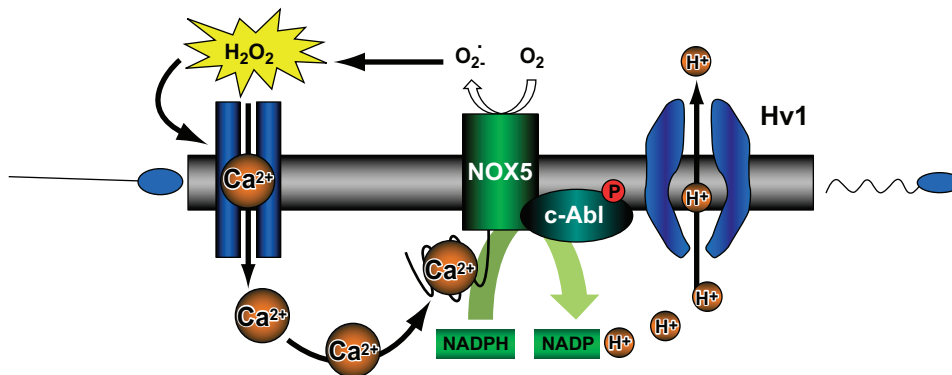


FIGURE 23. The motility of human spermatozoa requires functional interaction between NOX5 and hHv1. H₂O₂ induces calcium influx and the activation of c-Abl through tyrosine phosphorylation, both of which contribute to NOX5 activation. The generation of superoxide anion results in production of protons in the cytoplasm, which are extruded via the proton channel to maintain the optimal pH for NOX5 activity. Inhibition of this pathway abrogates the stimulatory effect of H₂O₂ on spermatozoa motility (356). [From Musset et al. (356), with permission from The American Society for Biochemistry and Molecular Biology.]

cell lines but low in nonmetastatic lines, and inhibition of H⁺-ATPase by bafilomycin inhibited migration of metastatic, but not of nonmetastatic cells. It seems clear that pHi homeostasis is altered in metastatic breast cancer cell lines, but cause and effect need clarification.

A follow-up study by this group provides strong support for the apparent correlation between hHv1 expression and the severity of breast cancer in a clinical study of human subjects (513). When hHv1 expression was divided into “high” and “low” categories, there was a significant correlation between high hHv1 expression and tumor size, tumor classification, and clinical stage. Furthermore, high hHv1 expression correlated with a poor clinical prognosis. At a minimum, hHv1 seems to be a marker for breast cancer. The possibility of targeting hHv1 to control the growth and invasiveness of breast cancer certainly merits further study.

G. Artificial Joints Need Proton Channels

Wear and corrosion products of articulating orthopedic implants are serious complications of joint replacement. In addition to particulate debris, soluble debris includes metal ions such as Co²⁺ and Ni²⁺ which become concentrated in blood and other fluids (199). Daou et al. (91) found that Co²⁺, at concentrations that due to metal leakage from the prosthesis were measured in tissues from patients with metal-on-metal total hip arthroplasty, inhibited bacterial killing, presumably via its inhibitory effect on phagocyte proton channels. In vitro studies with human neutrophils revealed inhibition of bacterial killing by 1–100 μM Co²⁺ (91). In this study, bacterial killing was inhibited by 100 μM Zn²⁺ almost as effectively as by DPI, which directly inhibits NADPH oxidase. Because the biological response to metal debris involves complex signaling and interactions between several other cells, such as macrophages and osteoclasts (56, 249) that have abundant proton channels (250,

340, 369, 384, 515), further exploration of this problem is needed.

H. Too Much of a Good Thing

The facilitation of ROS production by phagocytes is generally considered beneficial, because ROS are crucial to killing pathogens. There are situations, however, in which ROS production may be excessive and deleterious. A prime example is in microglia, which produce ROS in response to brain injury, ischemia, inflammation, or β-amyloid protein found in the brain in Alzheimer’s disease (137). ROS production by microglia may also contribute to the pathology of degenerative neurological diseases (137). Evidence implicating microglial hHv1 in ROS-induced brain damage during stroke has appeared recently (525) and is described below (see sect. IXC).

Cells that use ROS for signaling present a vast range of new opportunities. Numerous tissues express Nox isoforms, and although proton channels have not been shown to participate in all cases, the necessity of tightly regulated ROS production is universally evident (276). B lymphocytes produce ROS for signaling purposes, and the observation that hHv1 inhibition attenuates ROS without abolishing it (61) could be exploited to manage autoimmune diseases characterized by hyperreactive B cells, such as systemic lupus erythematosus or rheumatoid arthritis (62).

VIII. ROLES IN INNATE IMMUNITY

The most thoroughly studied function of proton channels is in the innate immune system. The proton channel in neutrophils, eosinophils, macrophages, and other leukocytes functions in close association with the NADPH oxidase complex (Nox2), which in turn generates ROS that are

crucial to killing bacterial and other microbes (27, 104, 255, 371, 413, 520). In the late 1980s, Lydia Henderson, Brian Chappell and Owen Jones published a series of landmark papers (208–210) that established the foundation for all subsequent studies. Their most important observations were as follows.

The NADPH oxidase enzyme complex is electrogenic.

Electrogenic H^+ efflux was observed to occur when the NADPH oxidase complex was active.

This H^+ efflux was thought to compensate electrically for the electron flux, balancing charge and preventing large voltage changes.

The molecule responsible for this H^+ efflux was proposed to be a voltage-gated proton channel.

The interactions between proton channels and NADPH oxidase are summarized in **FIGURE 24**. NADPH oxidase is formed from six main components that are not all physically associated with each other in resting cells (83). Activation by pathogens, chemotactic peptides, phagocytosis, phorbol esters, arachidonic acid, and other stimuli results in assembly of the enzyme complex, which is generally assumed to be active once it is fully assembled (118). Activation occurs by many complex pathways, most of which converge on phosphorylation of the oxidase components by protein kinase C (27, 118, 190, 372, 412). The assembled NADPH oxidase complex produces superoxide anion ($O_2^{\cdot-}$), which is released into the phagosome or the extracellular space if the complex assembles on the plasma membrane. The activity of the oxidase is electrogenic (120, 209, 442) because electrons are translocated from intracellular NADPH across the membrane, via a redox chain comprising FAD and then sequentially two hemes (37, 89, 101). The activity of this enzyme can be detected directly as an

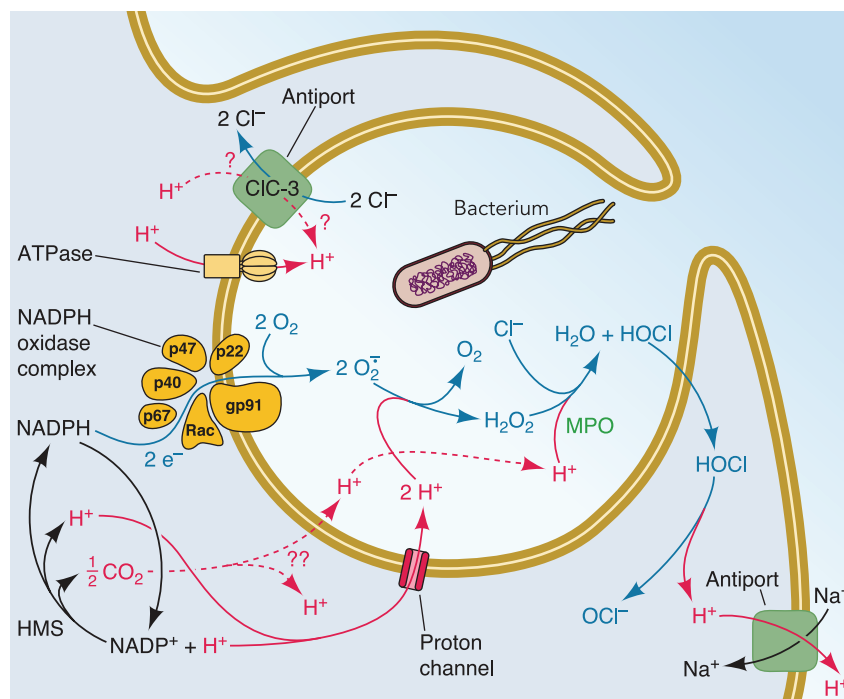


FIGURE 24. Molecules and transporters that participate in charge compensation and pH regulation during the respiratory burst. A phagocyte is shown engulfing a bacterium into a nascent phagosome, which will close and become an intracellular compartment. NADPH oxidase assembles preferentially in the phagosomal membrane in neutrophils (44, 246, 389) and begins to function before the phagocytic cup has sealed (297). The oxidase assembles mainly at the plasma membrane in eosinophils (273), macrophages (246), and neutrophils that are stimulated with soluble agonists (41, 390). NADPH oxidase activity drives the entire system. Electrons from intracellular NADPH are translocated across the membrane to reduce O_2 to superoxide anion ($O_2^{\cdot-}$) in the phagosome or extracellular space. This electrogenic process (209) can be measured directly as electron current (117, 120, 442). Each electron removed from the cell leaves behind approximately one proton. Thus NADPH oxidase activity tends to depolarize the membrane, decrease pH_i , and increase pH_o or $pH_{\text{phagosome}}$. CIC-3 is shown moving H^+ into the phagosome in exchange for Cl^- , as might occur at depolarized potentials that exist during the respiratory burst (275). In endosomes lacking NADPH oxidase, CIC-3 is thought to operate in the reverse direction, removing H^+ and injecting Cl^- into the interior to compensate for electrogenic H^+ -ATPase activity (240). HOCl is membrane permeant (506) and reacts rapidly with cytoplasmic contents such as taurine (322) or glutathione (519). As a result, HOCl effectively shuttles protons out of the phagosome (334). Despite the arrows, the protons in any compartment are equivalent. [From DeCoursey (105).]

electron current in voltage-clamped cells (442). The electron current is sensitive to membrane potential, and large depolarization inhibits enzyme activity, with complete inhibition occurring at +200 mV (120).

A. Consequences of NADPH Oxidase Activity

The main consequences to the immune cell of NADPH oxidase activity are membrane depolarization and cytoplasmic H^+ generation. The rapid production of ROS is often called the “respiratory burst” because there is an enormous increase in O_2 consumption (18). Strictly speaking, this term is a misnomer because almost all the O_2 consumed is simply substrate that is converted into $O_2^{\cdot-}$ and thus metabolic inhibitors have little effect (236, 433). The magnitude of NADPH oxidase activity in neutrophils and eosinophils is truly prodigious. The calculated rate of depolarization is ~ 1.1 V/s in human neutrophils, based on electron current measured at room temperature, and in human eosinophils at 37°C is 1.1 kV/min (104). Clearly, the cell membrane would rapidly rupture due to dielectric breakdown in the absence of effective charge compensation. In principle, electron current could be balanced by cation efflux or anion influx, either one of which would have osmotic consequences. As electrons leave the cell, protons left behind will lower pH_i , and when the oxidase is in the phagosome membrane, the phagosomal pH will tend to increase. The overall reaction is as follows (14): $NADPH + 2 O_2 \rightarrow NADP^+ + 2 O_2^{\cdot-} + H^+$, which leaves behind a proton in the cytoplasm, as $O_2^{\cdot-}$ is released into the phagosome. Another cytoplasmic proton is produced when NADPH is regenerated from $NADP^+$; to be fastidious, half of a CO_2 molecule is also produced. In effect, each electron translocated by NADPH oxidase leaves one proton behind, tending to lower pH_i . Inside the phagosome, $O_2^{\cdot-}$ rapidly and spontaneously dismutates to form H_2O_2 (174): $2 O_2^{\cdot-} + 2H^+ \rightarrow H_2O_2 + O_2$.

This reaction consumes protons and therefore tends to increase phagosomal pH. The production of HOCl from H_2O_2 is catalyzed by myeloperoxidase and also consumes protons (174): $H_2O_2 + H^+ + Cl^- \rightarrow HOCl + H_2O$.

In deciding which transporters should be involved in dealing with the consequences of oxidase activity, the cell must keep in mind that the main point of all of this is to generate large quantities of ROS. To produce $O_2^{\cdot-}$ (15), H_2O_2 (424, 425), and HOCl (256) requires large amounts of the key ingredients: H^+ , O_2 , and Cl^- in the phagosome. Despite evidence that several types of Cl^- channels are present in phagosomes (197, 332, 393), any Cl^- that is squandered compensating charge is no longer available for synthesis of HOCl, which is an important product of roughly half or more of the $O_2^{\cdot-}$ generated (68, 164, 243, 490, 516). A final consideration is that the sheer magnitude of charge compensation required is such that the osmotic consequences of flux of the ion selected for the job must be kept in mind.

Voltage-gated proton channels are ideally suited to preserving homeostasis in the face of all four of the consequences of NADPH oxidase activity. H^+ efflux balances charge, prevents large excursions of pH_i or $pH_{phagosome}$, and minimizes volume changes (by virtue of the fact that most of the molecules that are formed are membrane permeant), and H^+ is a required substrate for H_2O_2 and HOCl production in the phagosome. The fraction of charge that is compensated by voltage-gated proton channels in human neutrophil phagosomes was estimated to be $\geq 95\%$ (351).

B. Charge Compensation

The evidence that proton currents compensate electrically for NADPH oxidase activity is substantial. The proton current inhibitor Zn^{2+} reduces NADPH oxidase activity substantially in numerous studies (34, 81, 91, 120, 122, 145, 154, 208, 210, 251, 307, 353, 356, 388, 414, 417, 435, 458, 468, 491, 525, 534). This effect is not on the oxidase itself, because electron currents are unaffected by millimolar Zn^{2+} (120, 403, 442). In addition, in H_V1 knockout mice, ROS production was attenuated, but not abolished (61, 145, 391, 417, 525). Finally, when H_V1 levels are reduced by siRNA, ROS production is diminished (356). This kind of evidence shows that proton channels are involved, but does not establish that the mechanism of this involvement is charge compensation. However, several other results point clearly at charge compensation as the mechanism. Thus inhibition of proton channels results in greater plasma membrane depolarization during the respiratory burst (19, 20, 125, 145, 209, 274, 414). The depolarization is also exacerbated in H_V1 KO mice (145), and in phagosome membranes of human neutrophils in the presence of Zn^{2+} (339). Finally, in the presence of Zn^{2+} , in H_V1 KO mouse neutrophils, or in siRNA-treated PLB-985 cells, part of the defect in ROS production by NADPH oxidase can be restored by introduction of a protonophore (120, 145, 210) or ionophore (404). These results establish unequivocally that proton channels participate significantly in charge compensation.

C. pH Homeostasis

There is also strong evidence that proton channels regulate pH during the respiratory burst, and that if this function were compromised, pH_i would drop to levels that would inhibit NADPH oxidase. Early studies showed that under conditions where Na^+/H^+ antiport was prevented, Zn^{2+} resulted in additional acidification of activated neutrophils (84, 122, 208). As illustrated in **FIGURE 25**, Deri Morgan monitored pH_i in individual human neutrophils during phagocytosis of opsonized zymosan particles, using confocal fluorescence imaging

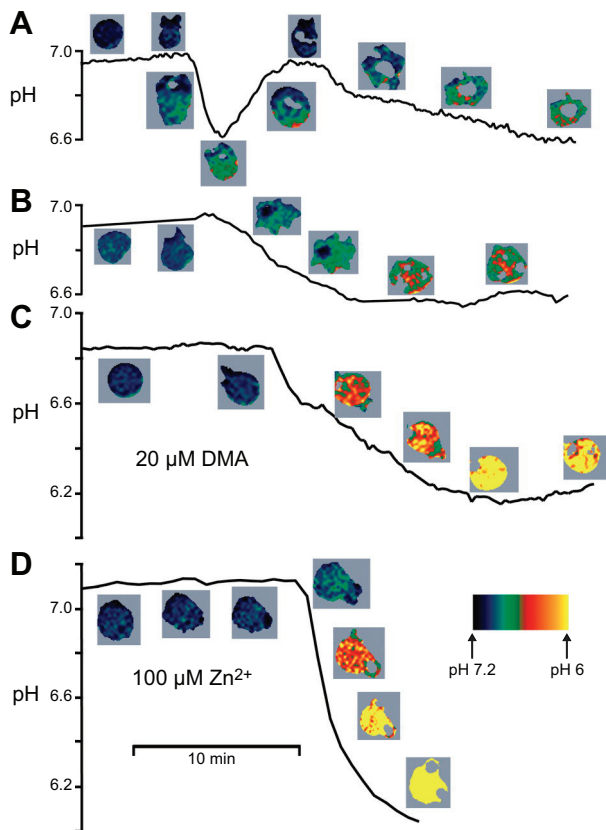


FIGURE 25. Intracellular pH (pH_i) during phagocytosis in four human neutrophils, imaged with SNARF-1 using the SEER approach (281). Pseudocolor images of the cells are positioned near the pH_i record at the corresponding time. When the opsonized zymosan particle is engulfed, there is a rapid spike of acidification, followed in most (A), but not all cells (B) by rapid recovery. The Na^+/H^+ antiport inhibitor dimethylamiloride (DMA) consistently prevented recovery (C) as did the proton channel inhibitor Zn^{2+} (D). The relative impact on pH_i was $H_V1 > Na^+/H^+$ antiport $> H^+$ -ATPase. [From Morgan et al. (334).]

(334). Cells exhibited a rapid spike of acidification that occurred simultaneously with the initial phagocytotic event. The initial rate of acidification doubled when proton current was inhibited by Zn^{2+} or in H_V1 KO mouse cells. In contrast, inhibition of H^+ -ATPase or Na^+/H^+ antiport had no effect on the initial rate; hence, the proton channel is the first transporter to respond. Na^+/H^+ antiport became active later, with a minor and belated contribution from H^+ -ATPase (84, 334). When proton channels were inhibited by Zn^{2+} or in H_V1 KO mice, the extent of acidification was severe enough to inhibit NADPH oxidase by 50% after 2 min and 80% after 10 min (334), based on the effect of pH_i on NADPH oxidase activity measured directly as electron current (336).

D. Enhanced Gating of H_V1 Maximizes the Efficiency of the Respiratory Burst

The properties of proton currents in certain cells and species are altered dramatically in the “enhanced gating mode”

(FIGURE 26). In most phagocytes and related cells, proton channels in enhanced gating mode open two to five times faster and close three to six times more slowly, the maximum conductance is increased two- to fourfold, and the g_H-V relationship is shifted by -30 to -40 mV (354). Enhanced gating has been observed in human neutrophils (117), eosinophils (19, 73, 115), basophils (358), monocytes (353), PLB-985 cells (116), K562 cells (356), and sperm (303), and in murine osteoclasts (340), neutrophils (145), granulocytes (335), and dendritic cells (482). Enhanced gating can be detected under some conditions in whole cell configuration (19, 303, 482), but is preferentially studied in perforated-patch configuration. A wide variety of agents stimulates enhanced gating. In phagocytes and related cells, anything that activates NADPH oxidase also produces enhanced gating of proton currents, with agonists including PMA, arachidonic acid, oleic acid, chemotactic peptides like formyl-methionyl-leucyl-phenylalanine (fMLF), leukotriene B_4 (LTB_4), interleukin-5 (IL-5), IgE, lipopolysaccharide (LPS), and simple adherence to glass (20, 73, 115–117, 335, 340, 358, 482). **FIGURE 27** illustrates the PMA response of a human eosinophil that includes enhanced gating of proton currents as well as activation of electron current, which reflects the electrogenic translocation of electrons across the membrane by NADPH oxidase. The most potent and effective activator in several systems is PMA, which directly activates protein kinase C (PKC). Other, more physiological agonists often produce a smaller and more variable response, and some cells that fail to respond, for example, a fraction of mouse neutrophils stimulated with fMLF or human basophils stimulated with anti-IgE, subsequently exhibit a full response to PMA (335, 358). Most of the other agonists also activate PKC. The induction of enhanced gating can be prevented by pretreatment with PKC inhibitors (21, 335, 340, 482), and even after enhanced gating is established, it can be partially or

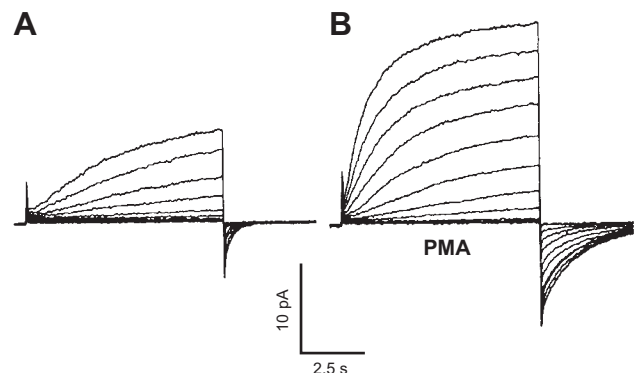


FIGURE 26. Proton currents in a human neutrophil in perforated-patch configuration at rest (A) and in the enhanced gating mode (B). Identical families of depolarizing pulses were applied to -20 through $+80$ mV in 10 -mV increments from a holding potential of -40 mV, at symmetrical pH 7.0. After stimulation by PMA, proton currents activate faster and deactivate more slowly, the maximum conductance is increased, and the voltage at which channels first open, $V_{threshold}$ is shifted by -40 mV. [From DeCoursey et al. (117).]

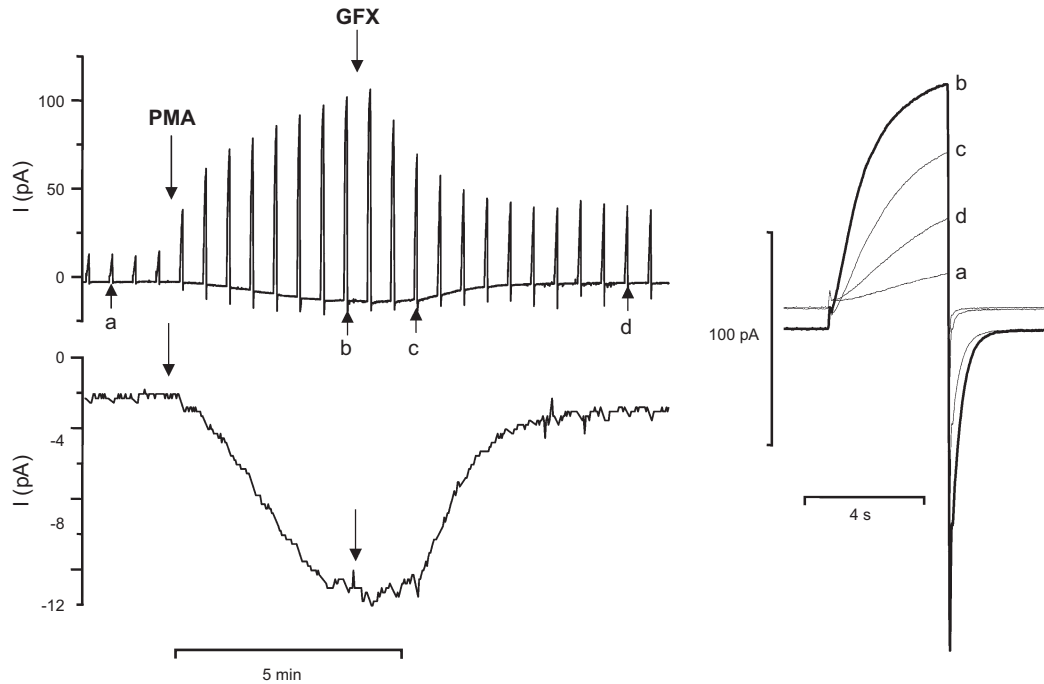


FIGURE 27. Regulation of enhanced gating of the proton channel, as well as NADPH oxidase activity, by PKC-dependent phosphorylation. *Top left:* proton currents during test pulses to +60 mV applied every 30 s from a holding potential of -60 mV. Examples of currents at an expanded time base are superimposed (*right*) with lowercase letters identifying the time of the pulse. At the arrows, the PKC activator PMA or the PKC inhibitor GFX (GF109203X) were added. *Bottom left:* the current at -60 mV at high gain (with pulses blanked) shows inward electron current that reflects NADPH oxidase activity. [From Morgan et al. (335).]

entirely reversed by PKC inhibitors (335, 352, 356, 358), as illustrated in **FIGURE 27**. These results indicate that most, if not all, of enhanced gating is mediated by PKC. A study of two candidate PKC phosphorylation sites in the intracellular N terminus of hH_V1 identified one, Thr²⁹, that appeared to be responsible for enhanced gating (352). Mutation of the other site did not prevent enhanced gating.

The mechanism by which phosphorylation of Thr²⁹ in the N terminus of hH_V1 produces enhanced gating is completely unknown. The pronounced modulation of gating might reflect an influence of the N terminus on S4 movement during channel opening, or destabilization of the closed state. A quite different type of mechanism could be envisioned, in which the phosphate concentrates protons locally near a group that senses pH_i. Most of the enhanced gating behaviors resemble those produced by a decrease in pH_i of ~1 unit. Especially intriguing is the increase in $g_{H,max}$ which in principle might reflect an increase in the maximum open probability of the channel (P_{open}) or in the single-channel conductance (or both), assuming that the number of channels remains constant. Noise measurements reveal that P_{open} during large depolarizations limits to 0.95 at pH_i 5.5, decreasing to 0.75 at pH_i 6.5 (75). Despite the fact that P_{open} was not determined at physiological pH_i in this study, it is still difficult to imagine that increasing P_{open} could, by itself, produce the 1.9- to 3.9-fold increase in $g_{H,max}$ that has been observed in various cells (354). Therefore, some increase in the single-channel conductance is likely, which might occur if protons were concentrated near the con-

duction pathway. This line of reasoning leads to the impression that Thr²⁹ is located near both a pH_i sensor and the conduction pathway.

Intuitively, the enhanced gating mode would appear to increase the activity of proton channels, because all four changes are in the direction to increase proton currents at any given membrane potential. Ricardo Murphy (351) modeled enhanced gating quantitatively using parameters that were all measured directly in human neutrophils and eosinophils. In the context of the respiratory burst, in which a major function of proton current is to compensate electrically for the electron flux that occurs during NADPH oxidase activity, enhanced gating resulted in proton currents fully compensating for the electron current at substantially more negative potentials than in the same system if proton channels are assumed to retain resting properties. With enhanced gating, less depolarization is required to activate enough proton channels, and because depolarization per se inhibits NADPH oxidase activity (120, 403), the overall efficiency of the oxidase was improved by 18%. If the proton channel were prevented from engaging in enhanced gating, enough channels would open eventually, but at the expense of more excessive depolarization, and consequently, ROS production would be compromised (351).

Not all cells with proton currents exhibit enhanced gating. Under perforated-patch conditions identical to those producing enhanced gating in other cells, native proton currents in rat

alveolar epithelial cells (117), and hH_{V1} expressed in HEK-293 or COS-7 cells, do not respond to PMA. The failure to respond may reflect an absence of the correct PKC isoform. More intriguing are cells that display a distinctly abbreviated form of enhanced gating. The examples identified thus far indicate a strong correlation between the capacity of the stimulated cell to produce ROS via NADPH oxidase and the degree of enhanced gating (354). Full-blown enhanced gating occurs in human neutrophils, eosinophils, and monocytes (19, 115, 116, 353, 354), all of which produce large amounts of ROS. Related cells that lack the complete enzymatic machinery to produce ROS, such as human basophils (92) or neutrophils from humans afflicted with CGD, exhibit a reduced response (116, 358). Cells with finite but low levels of ROS production also have a reduced response (352, 356). Cells with the attenuated enhanced gating phenotype exhibit almost no slowing of deactivation (τ_{tail}), and the $g_{\text{H}}-V$ relationship shifts negatively by only 10–20 mV rather than 40 mV. One possible explanation is that a product of NADPH oxidase activity, such as intracellular H^+ , may modulate H^+ channel gating; however, other possibilities exist and the explanation remains mysterious (354).

IX. MANIFESTATIONS IN THE KO MOUSE MODEL

It should be emphasized that proton current has not been detected in any of the several tissues examined so far in KO mice, including neutrophils (145, 391), granulocytes (334, 417), B lymphocytes (61), monocytes, alveolar epithelial cells (105), and microglia (525). Because the properties of proton currents in different tissues appear to differ fairly substantially (98), this result is important support for the idea that only one gene exists in any given species. Obviously, this conclusion applies most directly to the single species in which *Hvcn1* has been knocked out, *Mus musculus*.

As with many single gene knockouts, the *Hvcn1* knockout mouse does not exhibit dramatic defects. Decreased lifespan or increased morbidity has not been reported. Certainly, life is possible without voltage-gated proton channels, but is it worth living? Several more subtle manifestations indicate that the quality of life does indeed suffer without proton channels (see Note Added in Proof).

A. Defective ROS Production by NADPH Oxidase

The first defect to be identified in *Hvcn1* KO mice was attenuated ROS production by leukocytes. In all studies, NADPH oxidase activity was reduced, but not abolished. ROS production by neutrophils was reduced by 65–75% (417), 30% (391), or 74% (145), in B lymphocytes by 65% (61), and in microglia by ~50% (525). Several observations

support the idea that the NADPH oxidase complex is normal and intact in *Hvcn1* KO mice. Direct evidence is that NADPH oxidase-generated electron currents, stimulated by PMA, were identical in WT and KO mouse granulocytes (145, 334). In a cell-free assay, NADPH oxidase activity was normal in KO granulocytes (417), consistent with the absence of proton channels reducing ROS production by preventing charge compensation, allowing excessive pH_i decreases or both. Addition of the nonselective cation channel gramicidin to KO neutrophils restored ROS production, also implicating charge compensation as the key mechanism (145). Similarly, the nonselective ionophore amphotericin enhanced ROS production after siRNA knockdown of H_{V1} (404). Stimulation of phagocytes from KO mice produces abnormal pH_i decreases that resemble the effects of Zn^{2+} in WT cells (145, 334).

The incomplete elimination of ROS production when H_{V1} function or expression is abolished makes hH_{V1} an attractive target for pharmaceutical intervention. If the goal is to suppress ROS production with the intent of altering signaling pathways, for example, in B cells (62), then the residual ROS production in phagocytes would still be adequate to prevent infections, because there is a safety factor built into this process. Examination of subjects with hereditary abnormalities of NADPH oxidase that reduce activity without abolishing it (“variant” forms of chronic granulomatous disease) reveals that a substantial fraction of ROS production by neutrophils can be eliminated without seriously compromising host defense. Carriers who have ~50% normal and 50% dysfunctional neutrophils are relatively free from infections, but present with skin lesions (128); however, subjects with >90% loss of ROS production usually present with severe disease symptoms (46, 128, 293, 423, 446, 453, 461).

B. Defective Bacterial Killing

NADPH oxidase activity in neutrophils is thought to facilitate killing of bacteria (15, 247, 255, 371, 413). Ramsey et al. (417) observed a significant reduction of killing of *S. aureus* by bone marrow cells from mH_{V1} KO mice. No difference in phagocytosis was detected, suggesting that the defect in killing was due to attenuated ROS production (417).

C. H_{V1} Exacerbates Brain Damage in Ischemic Stroke

ROS production is not always beneficial. Nox2-dependent ROS production by microglia was lower in *Hvcn1* KO mice than in normal mice, and this deficiency was demonstrably protective against brain damage from ischemic stroke (525). *Hvcn1* KO mice subjected to middle cerebral artery occlusion for 24 h had smaller infarct volume and better

neurological scores than WT mice. Neuronal death in the area surrounding the infarcts was greater in WT than in KO mice. In vitro oxygen-glucose deprivation in microglia-neuron cocultures produced greater neuronal death in WT than in KO cells, and this was prevented by inhibiting NADPH oxidase, supporting the above mechanism (525).

D. Defective Ca^{2+} Influx Due to Depolarization Impairs Migration

Ca^{2+} signaling is especially important in neutrophil migration, which was found to be defective in neutrophils from $\text{H}_{\text{V}}1$ KO mice that were stimulated with a chemotactic peptide. NADPH oxidase is electrogenic and tends to depolarize the membrane. Increased depolarization after PMA stimulation was observed in KO neutrophils (145). Ca^{2+} influx through store-operated Ca^{2+} channels, which occurs when formyl peptide receptors are activated (e.g., by chemotactic peptides), was attenuated in KO neutrophils, reflecting the loss of driving force for Ca^{2+} entry (145). The importance of maintaining a large negative membrane potential to provide a driving force for Ca^{2+} entry via store-operated Ca^{2+} channels has been observed in several cell types (55, 176, 224, 294, 382), although this task is usually assigned to K^+ rather than H^+ channels. This defect was restored by ionomycin (in $5 \mu\text{M}$ Ca^{2+}), confirming that the mechanism involved Ca^{2+} signaling.

E. Defective BCR-Mediated Signaling in B Lymphocytes

A variety of manifestations related to B lymphocyte function and development have been detected in KO mice. As mentioned, ROS production was lower in *Hvcn1* KO mouse B cells, by 70% for PMA stimulation or by 60% for the more physiological stimulant F(ab')₂ anti-IgM (61). Inhibition of SHP-1, which is required for the initiation of BCR signaling cascades, was impaired, resulting in reduced activation of the tyrosine kinase Syk. Activation of Akt was severely impaired, with the result that metabolic activity and proliferation were attenuated. In vivo, this resulted in defective isotope class-switch responses.

X. HUMAN MUTATIONS

One naturally occurring mutation of the human proton channel has been discovered. Fischer's group cloned the human proton channel gene from airway epithelium, in part to confirm that proton channels in this tissue were coded for by the same gene responsible for proton currents in phagocytes and other tissues. In one of two clones, they serendipitously discovered a mutation that changed a single amino acid, producing the M91T mutant channel (233). Heterologous expression of the mutant gene revealed abnormal function of the resulting channel protein. As shown in **FIGURE 28**, the M91T channel

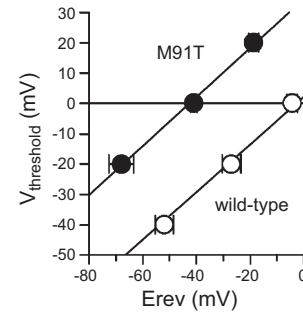


FIGURE 28. The naturally occurring hH_v1 mutation M91T shifts $V_{\text{threshold}}$ of the expressed channel by ~ 30 mV to more positive voltages. The slopes of the fitted lines, as defined by Eq. 5, are the same, but the offset voltage is +2 mV for WT, and +34 mV for M91T. The mutant channel requires a larger ΔpH to open. [From Iovannisci et al. (233).]

activates at voltages ~ 30 mV more positive than normal. Because airway epithelial cells that express this channel have fairly stable membrane potentials, but experience a wide range of pH, the mutant channel can be better described as requiring 0.5 units higher pH_o to activate than WT. Unfortunately, no information regarding the consequences of this mutation in other tissues exists.

XI. FUTURE DIRECTIONS

The rapidly expanding field of proton channel research is still in relative infancy in most respects. Although genes have been identified and confirmed in eight species, orthologous genes in dozens of species have yet to be studied. As the number of species increases, greater diversity of structures as well as functions seems inevitable. Already, surprising new properties of H_v1 in unicellular species have shattered previously valid generalizations about proton channel properties (activation of only outward current, Zn^{2+} sensitivity, and assembly as a dimer). Knowledge of the amino acid sequence has enabled structure-function studies; however, in many areas, progress has raised more questions than have been convincingly answered. Parallels as well as differences between H_v1 and other classes of VSD-containing molecules (other voltage gated ion channels, VSPs, and c15orf27) will doubtless enlighten these fields synergistically in ways that can scarcely be imagined. Finally, a deluge of recent studies illuminating profound involvement of hH_v1 in diverse areas of human health has created exciting prospects for targeting proton channels.

NOTE ADDED IN PROOF

A recent study describes symptoms of autoimmune disease (splenomegaly and nephritis) in *Hvcn1* KO mice (Sasaki M, Tojo A, Okochi Y, Miyawaki N, Kamimura D, Yamaguchi A, Murakami M, Okamura Y. Autoimmune disorder phenotypes in *Hvcn1* gene deficient mice. *Biochem J*. Online before print.)

ACKNOWLEDGMENTS

I appreciate helpful comments, critiques, and original figures by Colin Brownlee, Melania Capasso, Vladimir V. Cherny, William F. DeGrado, Robert H. Fillingame, Horst Fischer, Amina El Jamali, Ehud Y. Isacoff, H. Peter Larsson, Emily Liman, Polina V. Lishko, John F. Nagle, Yasushi Okamura, David N. Silverman, Susan M. E. Smith, Alison R. Taylor, Francesco Tombola, and Glen Wheeler.

Address for reprint requests and other correspondence: T. E. DeCoursey, Dept. of Molecular Biophysics and Physiology, Rush University Medical Center HOS-036, 1750 West Harrison, Chicago, IL 60612 (e-mail: tdecours@rush.edu).

GRANTS

This work was supported in part by National Institute of General Medical Sciences Grant R01-GM087507 and National Science Foundation Grant MCB-0943362. The content is solely the responsibility of the author and does not necessarily represent the views of the National Institute of General Medical Sciences or the National Institutes of Health.

DISCLOSURES

No conflicts of interest, financial or otherwise, are declared by the author.

REFERENCES

1. Abrahams MV, Townsend LD. Bioluminescence in dinoflagellates: a test of the burglar alarm hypothesis. *Ecology* 74: 258–260, 1993.
2. Acharya R, Carnevale V, Fiorin G, Levine BG, Polishchuk AL, Balannik V, Samish I, Lamb RA, Pinto LH, DeGrado WF, Klein ML. Structure and mechanism of proton transport through the transmembrane tetrameric M2 protein bundle of the influenza A virus. *Proc Natl Acad Sci USA* 107: 15075–15080, 2010.
3. Adl SM, Simpson AG, Farmer MA, Andersen RA, Anderson OR, Barta JR, Bowser SS, Brugerolle G, Fensome RA, Fredericq S, James TY, Karpov S, Kugrens P, Krug J, Lane CE, Lewis LA, Lodge J, Lynn DH, Mann DG, McCourt RM, Mendoza L, Moestrup O, Mozley-Standridge SE, Nerad TA, Shearer CA, Smirnov AV, Spiegel FW, Taylor MF. The new higher level classification of eukaryotes with emphasis on the taxonomy of protists. *J Eukaryot Microbiol* 52: 399–451, 2005.
4. Aggarwal SK, MacKinnon R. Contribution of the S4 segment to gating charge in the Shaker K⁺ channel. *Neuron* 16: 1169–1177, 1996.
5. Agmon N. The Grotthuss mechanism. *Chem Phys Lett* 244: 456–462, 1995.
6. Ahmed Z, Connor JA. Intracellular pH changes induced by calcium influx during electrical activity in molluscan neurons. *J Gen Physiol* 75: 403–426, 1980.
7. Akeson M, Deamer DW. Proton conductance by the gramicidin water wire. Model for proton conductance in the F₁F₀ ATPases? *Biophys J* 60: 101–109, 1991.
8. Al Khazaaly S, Beilby MJ. Zinc ions block H⁺/OH⁻ channels in *Chara australis*. *Plant Cell Environ* 2012.
9. Alabi AA, Bahamonde MI, Jung HJ, Kim JI, Swartz KJ. Portability of paddle motif function and pharmacology in voltage sensors. *Nature* 450: 370–375, 2007.
10. Almers W. Gating currents and charge movements in excitable membranes. *Rev Physiol Biochem Pharmacol* 82: 96–190, 1978.

11. An H, Tu C, Duda D, Montanez-Clemente I, Math K, Laipis PJ, McKenna R, Silverman DN. Chemical rescue in catalysis by human carbonic anhydrases II and III. *Biochemistry* 41: 3235–3242, 2002.
12. Babcock DF, Pfeiffer DR. Independent elevation of cytosolic [Ca²⁺] and pH of mammalian sperm by voltage-dependent and pH-sensitive mechanisms. *J Biol Chem* 262: 15041–15047, 1987.
13. Babcock DF, Rufo GA Jr, Lardy HA. Potassium-dependent increases in cytosolic pH stimulate metabolism and motility of mammalian sperm. *Proc Natl Acad Sci USA* 80: 1327–1331, 1983.
14. Babior BM, Curnutte JT, McMurrich BJ. The particulate superoxide-forming system from human neutrophils. Properties of the system and further evidence supporting its participation in the respiratory burst. *J Clin Invest* 58: 989–996, 1976.
15. Babior BM, Kipnes RS, Curnutte JT. Biological defense mechanisms. The production by leukocytes of superoxide, a potential bactericidal agent. *J Clin Invest* 52: 741–744, 1973.
16. Baker OS, Larsson HP, Mannuzzo LM, Isacoff EY. Three transmembrane conformations and sequence-dependent displacement of the S4 domain in shaker K⁺ channel gating. *Neuron* 20: 1283–1294, 1998.
17. Baldauf SL. The deep roots of eukaryotes. *Science* 300: 1703–1706, 2003.
18. Baldrige CW, Gerard RW. The extra respiration of phagocytosis. *Am J Physiol* 103: 235–236, 1932.
19. Bánfi B, Schrenzel J, Nüsse O, Lew DP, Ligeti E, Krause KH, Demaurex N. A novel H⁺ conductance in eosinophils: unique characteristics and absence in chronic granulomatous disease. *J Exp Med* 190: 183–194, 1999.
20. Bankers-Fulbright JL, Gleich GJ, Kephart GM, Kita H, O'Grady SM. Regulation of eosinophil membrane depolarization during NADPH oxidase activation. *J Cell Sci* 116: 3221–3226, 2003.
21. Bankers-Fulbright JL, Kita H, Gleich GJ, O'Grady SM. Regulation of human eosinophil NADPH oxidase activity: a central role for PKC δ . *J Cell Physiol* 189: 306–315, 2001.
22. Barish ME, Baud C. A voltage-gated hydrogen ion current in the oocyte membrane of the axolotl, *Ambystoma*. *J Physiol* 352: 243–263, 1984.
23. Barry PH. The reliability of relative anion-cation permeabilities deduced from reversal (dilution) potential measurements in ion channel studies. *Cell Biochem Biophys* 46: 143–154, 2006.
24. Barry PH, Lynch JW. Liquid junction potentials and small cell effects in patch-clamp analysis. *J Membr Biol* 121: 101–117, 1991.
25. Baud C, Barish ME. Changes in membrane hydrogen and sodium conductances during progesterone-induced maturation of *Ambystoma* oocytes. *Dev Biol* 105: 423–434, 1984.
26. Beaufort L, Probert I, de Garidel-Thoron T, Bendif EM, Ruiz-Pino D, Metz N, Goyet C, Buchet N, Coupel P, Grelaud M, Rost B, Rickaby RE, de Vargas C. Sensitivity of coccolithophores to carbonate chemistry and ocean acidification. *Nature* 476: 80–83, 2011.
27. Bedard K, Krause KH. The NOX family of ROS-generating NADPH oxidases: physiology and pathophysiology. *Physiol Rev* 87: 245–313, 2007.
28. Beitz E, Wu B, Holm LM, Schultz JE, Zeuthen T. Point mutations in the aromatic/arginine region in aquaporin 1 allow passage of urea, glycerol, ammonia, and protons. *Proc Natl Acad Sci USA* 103: 269–274, 2006.
29. Beitz LO, Fruman DA, Kurosaki T, Cantley LC, Scharenberg AM. SYK is upstream of phosphoinositide 3-kinase in B cell receptor signaling. *J Biol Chem* 274: 32662–32666, 1999.
30. Berger TK, Isacoff EY. The pore of the voltage-gated proton channel. *Neuron* 72: 991–1000, 2011.
31. Bernal JD, Fowler RH. A theory of water and ionic solution, with particular reference to hydrogen and hydroxyl ions. *J Chem Phys* 1: 515–548, 1933.
32. Berndt A, Prigge M, Gradmann D, Hegemann P. Two open states with progressive proton selectivities in the branched channelrhodopsin-2 photocycle. *Biophys J* 98: 753–761, 2010.

33. Bernheim L, Krause RM, Baroffio A, Hamann M, Kaelin A, Bader CR. A voltage-dependent proton current in cultured human skeletal muscle myotubes. *J Physiol* 470: 313–333, 1993.
34. Beswick PH, Brannen PC, Hurles SS. The effects of smoking and zinc on the oxidative reactions of human neutrophils. *J Clin Lab Immunol* 21: 71–75, 1986.
35. Bezanilla F. The voltage sensor in voltage-dependent ion channels. *Physiol Rev* 80: 555–592, 2000.
36. Bianchi L, Díez-Sampedro A. A single amino acid change converts the sugar sensor SGLT3 into a sugar transporter. *PLoS One* 5: e10241, 2010.
37. Biberstine-Kinkade KJ, DeLeo FR, Epstein RI, LeRoy BA, Nauseef WM, Dinauer MC. Heme-ligating histidines in flavocytochrome b_{558} : identification of specific histidines in gp91^{phox}. *J Biol Chem* 276: 31105–31112, 2001.
38. Blaustein RO, Finkelstein A. A hydroxide ion carrier in planar phospholipid bilayer membranes: $(C_6F_5)_2Hg$ (dipentafluorophenylmercury). *Biochim Biophys Acta* 946: 221–226, 1988.
39. Bode VC, Desa R, Hastings JW. Daily rhythm of luciferin activity in *Gonyaulax polyedra*. *Science* 141: 913–915, 1963.
40. Bodem CR, Lampton LM, Miller DP, Tarka EF, Everett ED. Endobronchial pH. Relevance of aminoglycoside activity in gram-negative bacillary pneumonia. *Am Rev Respir Dis* 127: 39–41, 1983.
41. Borregaard N, Heiple JM, Simons ER, Clark RA. Subcellular localization of the *b*-cytochrome component of the human neutrophil microbicidal oxidase: translocation during activation. *J Cell Biol* 97: 52–61, 1983.
42. Boyd RS, Jukes-Jones R, Walewska R, Brown D, Dyer MJ, Cain K. Protein profiling of plasma membranes defines aberrant signaling pathways in mantle cell lymphoma. *Mol Cell Proteomics* 8: 1501–1515, 2009.
43. Brewer ML, Schmitt UW, Voth GA. The formation and dynamics of proton wires in channel environments. *Biophys J* 80: 1691–1702, 2001.
44. Briggs RT, Drath DB, Karnovsky ML, Karnovsky MJ. Localization of NADH oxidase on the surface of human polymorphonuclear leukocytes by a new cytochemical method. *J Cell Biol* 67: 566–586, 1975.
45. Brzezinski P, Gennis RB. Cytochrome *c* oxidase: exciting progress and remaining mysteries. *J Bioenerg Biomembr* 40: 521–531, 2008.
46. Bu-Ghanim HN, Segal AW, Keep NH, Casimir CM. Molecular analysis in three cases of X91⁻ variant chronic granulomatous disease. *Blood* 86: 3575–3582, 1995.
47. Buch-Pedersen MJ, Pedersen BP, Veierskov B, Nissen P, Palmgren MG. Protons and how they are transported by proton pumps. *Pflügers Arch* 457: 573–579, 2009.
48. Burkenroad MD. A possible function of bioluminescence. *J Mar Res* 5: 161–164, 1943.
49. Burki F, Shalchian-Tabrizi K, Minge M, Skjæveland A, Nikolaev SI, Jakobsen KS, Pawlowski J. Phylogenomics reshuffles the eukaryotic supergroups. *PLoS One* 2: e790, 2007.
50. Buskey EJ, Mills L, Swift E. The effects of dinoflagellate bioluminescence on the swimming behavior of a marine copepod. *Limnol Oceanogr* 28: 575–579, 1983.
51. Buskey EJ, Swift E. Behavioral responses of oceanic zooplankton to simulated bioluminescence. *Biol Bull* 168: 263–275, 1985.
52. Buskey EJ, Swift E. Behavioral responses of the coastal copepod *Acartia hudsonica* (Pinhey) to simulated dinoflagellate bioluminescence. *J Exp Marine Biol Ecol* 72: 43–58, 1983.
53. Byerly L, Meech R, Moody W Jr. Rapidly activating hydrogen ion currents in perfused neurones of the snail, *Lymnaea stagnalis*. *J Physiol* 351: 199–216, 1984.
54. Byerly L, Suen Y. Characterization of proton currents in neurones of the snail, *Lymnaea stagnalis*. *J Physiol* 413: 75–89, 1989.
55. Cahalan MD, Chandy KG. The functional network of ion channels in T lymphocytes. *Immunol Rev* 231: 59–87, 2009.
56. Caicedo MS, Desai R, McAllister K, Reddy A, Jacobs JJ, Hallab NJ. Soluble and particulate Co-Cr-Mo alloy implant metals activate the inflammasome danger signaling pathway in human macrophages: a novel mechanism for implant debris reactivity. *J Orthop Res* 27: 847–854, 2009.
57. Campos FV, Chanda B, Roux B, Bezanilla F. Two atomic constraints unambiguously position the S4 segment relative to S1 and S2 segments in the closed state of Shaker K channel. *Proc Natl Acad Sci USA* 104: 7904–7909, 2007.
58. Cao Y, Li M, Mager S, Lester HA. Amino acid residues that control pH modulation of transport-associated current in mammalian serotonin transporters. *J Neurosci* 18: 7739–7749, 1998.
59. Cao Z, Peng Y, Yan T, Li S, Li A, Voth GA. Mechanism of fast proton transport along one-dimensional water chains confined in carbon nanotubes. *J Am Chem Soc* 132: 11395–11397, 2010.
60. Capasso M. Proton channels in non-phagocytic cells of the immune system. *Wiley Interdiscip Rev: Membr Trans Signal*. In press.
61. Capasso M, Bhamrah MK, Henley T, Boyd RS, Langlais C, Cain K, Dinsdale D, Pulford K, Khan M, Musset B, Cherny VV, Morgan D, Gascoyne RD, Vigorito E, DeCoursey TE, MacLennan IM, Dyer MS. HVCN1 modulates BCR signal strength via regulation of BCR-dependent generation of reactive oxygen species. *Nat Immunol* 11: 265–272, 2010.
62. Capasso MS, DeCoursey TE, Dyer MJ. pH regulation and beyond: unanticipated functions for the voltage-gated proton channel, HVCN1. *Trends Cell Biol* 21: 20–28, 2011.
63. Carland JE, Moorhouse AJ, Barry PH, Johnston GA, Chebib M. Charged residues at the 2' position of human GABAC rho 1 receptors invert ion selectivity and influence open state probability. *J Biol Chem* 279: 54153–54160, 2004.
64. Cha A, Snyder GE, Selvin PR, Bezanilla F. Atomic scale movement of the voltage-sensing region in a potassium channel measured via spectroscopy. *Nature* 402: 809–813, 1999.
65. Chanda B, Bezanilla F. A common pathway for charge transport through voltage-sensing domains. *Neuron* 57: 345–351, 2008.
66. Chang JJ. Electrophysiological studies of a non-luminescent form of the dinoflagellate *Noctiluca miliaris*. *J Cell Comp Physiol* 56: 33–42, 1960.
67. Chang RB, Waters H, Liman ER. A proton current drives action potentials in genetically identified sour taste cells. *Proc Natl Acad Sci USA* 107: 22320–22325, 2010.
68. Chapman AL, Hampton MB, Senthilmohan R, Winterbourn CC, Kettle AJ. Chlorination of bacterial and neutrophil proteins during phagocytosis and killing of *Staphylococcus aureus*. *J Biol Chem* 277: 9757–9762, 2002.
69. Chen X, Gründer S. Permeating protons contribute to tachyphylaxis of the acid-sensing ion channel (ASIC) 1a. *J Physiol* 579: 657–670, 2007.
70. Cheng YM, Kelly T, Church J. Potential contribution of a voltage-activated proton conductance to acid extrusion from rat hippocampal neurons. *Neuroscience* 151: 1084–1098, 2008.
71. Cherny VV, DeCoursey TE. pH-dependent inhibition of voltage-gated H⁺ currents in rat alveolar epithelial cells by Zn²⁺ and other divalent cations. *J Gen Physiol* 114: 819–838, 1999.
72. Cherny VV, Henderson LM, DeCoursey TE. Proton and chloride currents in Chinese hamster ovary cells. *Membr Cell Biol* 11: 337–347, 1997.
73. Cherny VV, Henderson LM, Xu W, Thomas LL, DeCoursey TE. Activation of NADPH oxidase-related proton and electron currents in human eosinophils by arachidonic acid. *J Physiol* 535: 783–794, 2001.
74. Cherny VV, Markin VS, DeCoursey TE. The voltage-activated hydrogen ion conductance in rat alveolar epithelial cells is determined by the pH gradient. *J Gen Physiol* 105: 861–896, 1995.
75. Cherny VV, Murphy R, Sokolov V, Levis RA, DeCoursey TE. Properties of single voltage-gated proton channels in human eosinophils estimated by noise analysis and by direct measurement. *J Gen Physiol* 121: 615–628, 2003.
76. Cherny VV, Thomas LL, DeCoursey TE. Voltage-gated proton currents in human basophils. *Biologicheskie Membrany* 18: 458–465, 2001.
77. Chernyshev A, Cukierman S. Thermodynamic view of activation energies of proton transfer in various gramicidin A channels. *Biophys J* 82: 182–192, 2002.

78. Chernyshev A, Pomès R, Cukierman S. Kinetic isotope effects of proton transfer in aqueous and methanol containing solutions, and in gramicidin A channels. *Biophys Chem* 103: 179–190, 2003.
79. Chizhnikov IV, Geraghty FM, Ogden DC, Hayhurst A, Antoniou M, Hay AJ. Selective proton permeability and pH regulation of the influenza virus M2 channel expressed in mouse erythroleukaemia cells. *J Physiol* 494: 329–336, 1996.
80. Cho DY, Hajjehaseemi M, Hwang PH, Illek B, Fischer H. Proton secretion in freshly excised sinonasal mucosa from asthma and sinusitis patients. *Am J Rhinol Allergy* 23: e10–e13, 2009.
81. Chvapil M, Stankova L, Bernhard DS, Weldy PL, Carlson EC, Campbell JB. Effect of zinc on peritoneal macrophages in vitro. *Infect Immun* 16: 367–373, 1977.
82. Cicirelli MF, Robinson KR, Smith LD. Internal pH of *Xenopus* oocytes: a study of the mechanism and role of pH changes during meiotic maturation. *Dev Biol* 100: 133–146, 1983.
83. Clark RA, Leidal KG, Pearson DW, Nauseef WM. NADPH oxidase of human neutrophils. Subcellular localization and characterization of an arachidonate-activatable superoxide-generating system. *J Biol Chem* 262: 4065–4074, 1987.
84. Coakley RJ, Taggart C, McElvaney NG, O'Neill SJ. Cytosolic pH and the inflammatory microenvironment modulate cell death in human neutrophils after phagocytosis. *Blood* 100: 3383–3391, 2002.
85. Cole KS, Curtis HJ. Electric impedance of the squid giant axon during activity. *J Gen Physiol* 22: 649–670, 1939.
86. Cole KS, Moore JW. Potassium ion current in the squid giant axon: dynamic characteristic. *Biophys J* 1: 1–14, 1960.
87. Conway BE, Bockris JOM, Linton H. Proton conductance and the existence of the H_3O^+ ion. *J Chem Phys* 24: 834–850, 1956.
88. Crooks GE, Hon G, Chandonia JM, Brenner SE. WebLogo: a sequence logo generator. *Genome Res* 14: 1188–1190, 2004.
89. Cross AR, Rae J, Curnutte JT. Cytochrome b_{245} of the neutrophil superoxide-generating system contains two nonidentical hemes. Potentiometric studies of a mutant form of gp91^{phox}. *J Biol Chem* 270: 17075–17077, 1995.
90. Danneel H. Notiz über Ionengeschwindigkeiten *Zeitschrift für Elektrochemie und angewandte physikalische Chemie* 11: 249–252, 1905.
91. Daou S, El Chemaly A, Christofilopoulos P, Bernard L, Hoffmeyer P, Demaurex N. The potential role of cobalt ions released from metal prosthesis on the inhibition of Hv1 proton channels and the decrease in *Staphylococcus epidermidis* killing by human neutrophils. *Biomaterials* 32: 1769–1777, 2011.
92. De Boer M, Roos D. Metabolic comparison between basophils and other leukocytes from human blood. *J Immunol* 136: 3447–3454, 1986.
93. De Grotthuss CJ. Memoir on the decomposition of water and of the bodies that it holds in solution by means of galvanic electricity: 1805. *Biochim Biophys Acta* 1757: 871–875, 2006.
94. De Grotthuss CJT. Mémoire sur la décomposition de l'eau et des corps qu'elle tient en dissolution à l'aide de l'électricité galvanique. *Annales de Chimie* LVIII: 54–74, 1806.
95. De Quatrefages A. Observations sur les noctiluques. *Ann Sci Nat Zool Ser 3* 14: 226–235, 1850.
96. Deamer DW, Nichols JW. Proton flux mechanisms in model and biological membranes. *J Membr Biol* 107: 91–103, 1989.
97. DeChatelet LR, Shirley PS, McPhail LC, Huntley CC, Muss HB, Bass DA. Oxidative metabolism of the human eosinophil. *Blood* 50: 525–535, 1977.
98. DeCoursey TE. Four varieties of voltage-gated proton channels. *Front Biosci* 3: d477–525–d482, 1998.
99. DeCoursey TE. Hydrogen ion currents in rat alveolar epithelial cells. *Biophys J* 60: 1243–1253, 1991.
100. DeCoursey TE. Hypothesis: do voltage-gated H^+ channels in alveolar epithelial cells contribute to CO_2 elimination by the lung? *Am J Physiol Cell Physiol* 278: C1–C10, 2000.
101. DeCoursey TE. Interactions between NADPH oxidase and voltage-gated proton channels: why electron transport depends on proton transport. *FEBS Lett* 555: 57–61, 2003.
102. DeCoursey TE. Voltage-gated proton channels. *Cell Mol Life Sci* 65: 2554–2573, 2008.
103. DeCoursey TE. Voltage-gated proton channels. *Comp Physiol* 2: 1355–1385, 2012.
104. DeCoursey TE. Voltage-gated proton channels and other proton transfer pathways. *Physiol Rev* 83: 475–579, 2003.
105. DeCoursey TE. Voltage-gated proton channels find their dream job managing the respiratory burst in phagocytes. *Physiology* 25: 27–40, 2010.
106. DeCoursey TE. Voltage-gated proton channels: what's next? *J Physiol* 586: 5305–5324, 2008.
107. DeCoursey TE, Cherny VV. Deuterium isotope effects on permeation and gating of proton channels in rat alveolar epithelium. *J Gen Physiol* 109: 415–434, 1997.
108. DeCoursey TE, Cherny VV. Effects of buffer concentration on voltage-gated H^+ currents: does diffusion limit the conductance? *Biophys J* 71: 182–193, 1996.
109. DeCoursey TE, Cherny VV. Na^+H^+ antiport detected through hydrogen ion currents in rat alveolar epithelial cells and human neutrophils. *J Gen Physiol* 103: 755–785, 1994.
110. DeCoursey TE, Cherny VV. Pharmacology of voltage-gated proton channels. *Curr Pharm Des* 13: 2400–2420, 2007.
111. DeCoursey TE, Cherny VV. Potential, pH, and arachidonate gate hydrogen ion currents in human neutrophils. *Biophys J* 65: 1590–1598, 1993.
112. DeCoursey TE, Cherny VV. Temperature dependence of voltage-gated H^+ currents in human neutrophils, rat alveolar epithelial cells, and mammalian phagocytes. *J Gen Physiol* 112: 503–522, 1998.
113. DeCoursey TE, Cherny VV. Voltage-activated hydrogen ion currents. *J Membr Biol* 141: 203–223, 1994.
114. DeCoursey TE, Cherny VV. Voltage-activated proton currents in human THP-1 monocytes. *J Membr Biol* 152: 131–140, 1996.
115. DeCoursey TE, Cherny VV, DeCoursey AG, Xu W, Thomas LL. Interactions between NADPH oxidase-related proton and electron currents in human eosinophils. *J Physiol* 535: 767–781, 2001.
116. DeCoursey TE, Cherny VV, Morgan D, Katz BZ, Dinauer MC. The gp91^{phox} component of NADPH oxidase is not the voltage-gated proton channel in phagocytes, but it helps. *J Biol Chem* 276: 36063–36066, 2001.
117. DeCoursey TE, Cherny VV, Zhou W, Thomas LL. Simultaneous activation of NADPH oxidase-related proton and electron currents in human neutrophils. *Proc Natl Acad Sci USA* 97: 6885–6889, 2000.
118. DeCoursey TE, Ligeti E. Regulation and termination of NADPH oxidase activity. *Cell Mol Life Sci* 62: 2173–2193, 2005.
119. DeCoursey TE, Morgan D, Cherny VV. The gp91^{phox} component of NADPH oxidase is not a voltage-gated proton channel. *J Gen Physiol* 120: 773–779, 2002.
120. DeCoursey TE, Morgan D, Cherny VV. The voltage dependence of NADPH oxidase reveals why phagocytes need proton channels. *Nature* 422: 531–534, 2003.
121. Demaurex N. Functions of proton channels in phagocytes. *Wiley Interdiscip Rev: Membr Transp Signal* 1: 3–15, 2012.
122. Demaurex N, Downey GP, Waddell TK, Grinstein S. Intracellular pH regulation during spreading of human neutrophils. *J Cell Biol* 133: 1391–1402, 1996.
123. Demaurex N, El Chemaly A. Physiological roles of voltage-gated proton channels in leukocytes. *J Physiol* 588: 4659–4665, 2010.
124. Demaurex N, Grinstein S, Jaconi M, Schlegel W, Lew DP, Krause KH. Proton currents in human granulocytes: regulation by membrane potential and intracellular pH. *J Physiol* 466: 329–344, 1993.
125. Demaurex N, Petheö GL. Electron and proton transport by NADPH oxidases. *Philos Trans R Soc Lond B Biol Sci* 360: 2315–2325, 2005.

126. Desa R, Hastings JW, Vatter AE. Luminescent "crystalline" particles: an organized subcellular bioluminescent system. *Science* 141: 1269–1270, 1963.
127. Diarra A, Sheldon C, Brett CL, Baimbridge KG, Church J. Anoxia-evoked intracellular pH and Ca^{2+} concentration changes in cultured postnatal rat hippocampal neurons. *Neuroscience* 93: 1003–1016, 1999.
128. Dinauer MC, Nauseef WM, Newburger PEI. Inherited disorders of oxidative phagocyte killing. In: *The Metabolic and Molecular Bases of Inherited Disease*, edited by C. R. Scriver, A. L. Beaudet, W. S. Sly, D. Valle. New York: McGraw-Hill, 2009, chapt. 189.
129. Dong H, Fillingame RH. Chemical reactivities of cysteine substitutions in subunit a of ATP synthase define residues gating H^+ transport from each side of the membrane. *J Biol Chem* 285: 39811–39818, 2010.
130. Doroshenko PA, Kostyuk PG, Martynyuk AE. Transmembrane outward hydrogen current in intracellularly perfused neurones of the snail *Helix pomatia*. *Gen Physiol Biophys* 5: 337–350, 1986.
131. Dustin LB, Plas DR, Wong J, Hu YT, Soto C, Chan AC, Thomas ML. Expression of dominant-negative src-homology domain 2-containing protein tyrosine phosphatase-1 results in increased Syk tyrosine kinase activity and B cell activation. *J Immunol* 162: 2717–2724, 1999.
132. Eckert R. Excitation and luminescence in *Noctiluca miliaris*. In: *Bioluminescence in Progress*, edited by Johnson FH and Haneda Y. Princeton, NJ: Princeton Univ. Press, 1966, p. 269–300.
133. Eckert RI. Specific nature of triggering events. *Science* 147: 1140–1142, 1965.
134. Eckert R 2nd. Asynchronous flash initiation by a propagated triggering potential. *Science* 147: 1142–1145, 1965.
135. Eckert R, Reynolds GT. The subcellular origin of bioluminescence in *Noctiluca miliaris*. *J Gen Physiol* 50: 1429–1458, 1967.
136. Eckert R, Sibaoka T. The flash-triggering action potential of the luminescent dinoflagellate *Noctiluca*. *J Gen Physiol* 52: 258–282, 1968.
137. Eder C, DeCoursey TE. Voltage-gated proton channels in microglia. *Prog Neurobiol* 64: 277–305, 2001.
138. Effros RM, Mason G, Silverman P. Asymmetric distribution of carbonic anhydrase in the alveolar-capillary barrier. *J Appl Physiol* 51: 190–193, 1981.
139. Effros RM, Olson L, Lin W, Audi S, Hogan G, Shaker R, Hoagland K, Foss B. Resistance of the pulmonary epithelium to movement of buffer ions. *Am J Physiol Lung Cell Mol Physiol* 285: L476–L483, 2003.
140. Eigen M. Proton transfer, acid-base catalysis, and enzymatic hydrolysis. Part I: elementary processes. *Angewandte Chemie International Edition* 3: 1–19, 1964.
141. Eigen M, De Maeyer L. Self-dissociation and protonic charge transport in water and ice. *Proc Roy Soc Lond A* 247: 505–533, 1958.
142. Eisenhauer K, Kuhne J, Ritter E, Berndt A, Wolf S, Freier E, Bartl F, Hegemann P, Gerwert K. In channelrhodopsin-2 Glu-90 is crucial for ion selectivity and is deprotonated during the photocycle. *J Biol Chem* 287: 6904–6911, 2012.
143. El Chemaly A, Demaurex N. Do Hv1 proton channels regulate the ionic and redox homeostasis of phagosomes? *Mol Cell Endocrinol* 353: 82–87, 2012.
144. El Chemaly A, Guinamard R, Demion M, Fares N, Jebara V, Faivre JF, Bois P. A voltage-activated proton current in human cardiac fibroblasts. *Biochem Biophys Res Commun* 340: 512–516, 2006.
145. El Chemaly A, Okochi Y, Sasaki M, Arnaudeau S, Okamura Y, Demaurex N. VSOP/Hv1 proton channels sustain calcium entry, neutrophil migration, and superoxide production by limiting cell depolarization and acidification. *J Exp Med* 207: 129–139, 2010.
146. Elinder F, Århem P. Metal ion effects on ion channel gating. *Q Rev Biophys* 36: 373–427, 2003.
147. Elliott JA, Paddison SJ. Modelling of morphology and proton transport in PFSA membranes. *Phys Chem Chem Phys* 9: 2602–2618, 2007.
148. England JL, Haran G. Role of solvation effects in protein denaturation: from thermodynamics to single molecules and back. *Annu Rev Phys Chem* 62: 257–277, 2011.
149. Enns T, Hill EP. CO_2 diffusing capacity in isolated dog lung lobes and the role of carbonic anhydrase. *J Appl Physiol* 54: 483–490, 1983.
150. Eriksson AE, Jones TA, Liljas A. Refined structure of human carbonic anhydrase II at 2.0 Å resolution. *Proteins* 4: 274–282, 1988.
151. Eriksson AE, Kylsten PM, Jones TA, Liljas A. Crystallographic studies of inhibitor binding sites in human carbonic anhydrase II: a pentacoordinated binding of the SCN^- ion to the zinc at high pH. *Proteins* 4: 283–293, 1988.
152. Fairman WA, Sonders MS, Murdoch GH, Amara SG. Arachidonic acid elicits a substrate-gated proton current associated with the glutamate transporter EAAT4. *Nat Neurosci* 1: 105–113, 1998.
153. Fei YJ, Romero MF, Krause M, Liu JC, Huang W, Ganapathy V, Leibach FH. A novel H^+ -coupled oligopeptide transporter (OPT3) from *Caenorhabditis elegans* with a predominant function as a H^+ channel and an exclusive expression in neurons. *J Biol Chem* 275: 9563–9571, 2000.
154. Femling JK, Cherny VV, Morgan D, Rada B, Davis AP, Czirájk G, Enyedi P, England SK, Moreland JG, Ligeti E, Nauseef WM, DeCoursey TE. The antibacterial activity of human neutrophils and eosinophils requires proton channels but not BK channels. *J Gen Physiol* 127: 659–672, 2006.
155. Fillingame RH, Angevine CM, Dmitriev OY. Mechanics of coupling proton movements to c-ring rotation in ATP synthase. *FEBS Lett* 555: 29–34, 2003.
156. Fischer H. Function of proton channels in lung epithelia. *Wiley Interdiscip Rev: Membr Transp Signal* 1: 247–258, 2011.
157. Fischer H, Widdicombe JH. Mechanisms of acid and base secretion by the airway epithelium. *J Membr Biol* 211: 139–150, 2006.
158. Fischer H, Widdicombe JH, Illek B. Acid secretion and proton conductance in human airway epithelium. *Am J Physiol Cell Physiol* 282: C736–C743, 2002.
159. Fisher Z, Hernandez Prada JA, Tu C, Duda D, Yoshioka C, An H, Govindasamy L, Silverman DN, McKenna R. Structural and kinetic characterization of active-site histidine as a proton shuttle in catalysis by human carbonic anhydrase II. *Biochemistry* 44: 1097–1105, 2005.
160. Fleisher KJ, Case JF. Cephalopod predation facilitated by dinoflagellate luminescence. *Biol Bull* 189: 263–271, 1995.
161. Fogel M, Hastings JW. Bioluminescence: mechanism and mode of control of scintillon activity. *Proc Natl Acad Sci USA* 69: 690–693, 1972.
162. Fogel M, Hastings JW. A substrate-binding protein in the *Gonyaulax* bioluminescence reaction. *Arch Biochem Biophys* 142: 310–321, 1971.
163. Fogel M, Schmitter RE, Hastings JW. On the physical identity of scintillons: bioluminescent particles in *Gonyaulax polyedra*. *J Cell Sci* 11: 305–317, 1972.
164. Foote CS, Goynes TE, Lehrer RI. Assessment of chlorination by human neutrophils. *Nature* 301: 715–716, 1983.
165. Forrest LR, Tieleman DP, Sansom MSP. Defining the transmembrane helix of M2 protein from influenza A by molecular dynamics simulations in a lipid bilayer. *Biophys J* 76: 1886–1896, 1999.
166. Forteza R, Salathe M, Miot F, Forteza R, Conner GE. Regulated hydrogen peroxide production by Duox in human airway epithelial cells. *Am J Respir Cell Mol Biol* 32: 462–469, 2005.
167. Frank RAW, Titman CM, Pratap JV, Luisi BF, Perham RN. A molecular switch and proton wire synchronize the active sites in thiamine enzymes. *Science* 306: 872–876, 2004.
168. Franke TF, Kaplan DR, Cantley LC. PI3K: downstream AKTion blocks apoptosis. *Cell* 88: 435–437, 1997.
169. Frankenhaeuser B, Hodgkin AL. The action of calcium on the electrical properties of squid axons. *J Physiol* 137: 218–244, 1957.
170. Freitas JA, Tobias DJ, White SH. A voltage-sensor water pore. *Biophys J* 91: L90–92, 2006.
171. French RJ, Finol-Urdaneta RK. Open-state stabilization in Kv channels: voltage-sensor relaxation and pore propping by a bound ion. *J Gen Physiol* 140: 463–467, 2012.

172. Fujiwara Y, Kurokawa T, Takeshita K, Kobayashi M, Okochi Y, Nakagawa A, Okamura Y. The cytoplasmic coiled-coil mediates cooperative gating temperature sensitivity in the voltage-gated H⁺ channel Hv1. *Nat Commun* 3: 816, 2012.
173. Fujiwara Y, Kurokawa T, Takeshita K, Nakagawa A, Larsson HP, Okamura Y. Gating of the designed trimeric/tetrameric voltage-gated H⁺ channels. *J Physiol* 591: 627–640, 2013.
174. Gabig TG, Lefker BA, Ossanna PJ, Weiss SJ. Proton stoichiometry associated with human neutrophil respiratory-burst reactions. *J Biol Chem* 259: 13166–13171, 1984.
175. Galzi JL, Devillers-Thiéry A, Hussy N, Bertrand S, Changeux JP, Bertrand D. Mutations in the channel domain of a neuronal nicotinic receptor convert ion selectivity from cationic to anionic. *Nature* 359: 500–505, 1992.
176. Gao YD, Hanley PJ, Rinné S, Zuzarte M, Daut J. Calcium-activated K⁺ channel (K_{Ca}3.1) activity during Ca²⁺ store depletion and store-operated Ca²⁺ entry in human macrophages. *Cell Calcium* 48: 19–27, 2010.
177. Geers C, Gros G. Carbon dioxide transport and carbonic anhydrase in blood and muscle. *Physiol Rev* 80: 681–715, 2000.
178. Ghosh A, Qiu J, DeGrado WF, Hochstrasser RM. Tidal surge in the M2 proton channel, sensed by 2D IR spectroscopy. *Proc Natl Acad Sci USA* 108: 6115–6120, 2011.
179. Gierer A, Wirtz K. Anomale H⁺- und OH⁻-Ionenbeweglichkeit im Wasser. *Annalen Physik* 6: 257–304, 1949.
180. Gilbert DL, Ehrenstein G. Use of a fixed charge model to determine the pK of the negative sites on the external membrane surface. *J Gen Physiol* 55: 822–825, 1970.
181. Gilbertson TA, Avenet P, Kinnamon SC, Roper SD. Proton currents through amiloride-sensitive Na channels in hamster taste cells. Role in acid transduction. *J Gen Physiol* 100: 803–824, 1992.
182. Gilly WF, Armstrong CM. Divalent cations and the activation kinetics of potassium channels in squid giant axons. *J Gen Physiol* 79: 965–996, 1982.
183. Golan A, Bravaya KB, Kudirka R, Kostko O, Leone SR, Krylov AI, Ahmed M. Ionization of dimethyluracil dimers leads to facile proton transfer in the absence of hydrogen bonds. *Nat Chem* 4: 323–329, 2012.
184. Goldman DE. Potential, impedance, and rectification in membranes. *J Gen Physiol* 27: 37–60, 1943.
185. Gonzalez C, Koch HP, Drum BM, Larsson HP. Strong cooperativity between subunits in voltage-gated proton channels. *Nat Struct Mol Biol* 17: 51–56, 2010.
186. Gonzalez C, Rebolledo S, Wang X, Perez M, Larsson HP. Contribution of S4 charges to gating mechanism in Hv channels (Abstract). *Biophys J* 100: 173a, 2011.
187. Gordienko DV, Tare M, Parveen S, Fenech CJ, Robinson C, Bolton TB. Voltage-activated proton current in eosinophils from human blood. *J Physiol* 496: 299–316, 1996.
188. Gosselin-Badaroudine P, Keller DI, Huang H, Pouliot V, Chatelier A, Osswald S, Brink M, Chahine M. A proton leak current through the cardiac sodium channel is linked to mixed arrhythmia and the dilated cardiomyopathy phenotype. *PLoS One* 7: e38331, 2012.
189. Grabe M, Lecar H, Jan YN, Jan LY. A quantitative assessment of models for voltage-dependent gating of ion channels. *Proc Natl Acad Sci USA* 101: 17640–17645, 2004.
190. Groemping Y, Rittinger K. Activation and assembly of the NADPH oxidase: a structural perspective. *Biochem J* 386: 401–416, 2005.
191. Gros G, Moll W. Facilitated diffusion of CO₂ across albumin solutions. *J Gen Physiol* 64: 356–371, 1974.
192. Gros G, Moll W, Hoppe H, Gros H. Proton transport by phosphate diffusion: a mechanism of facilitated CO₂ transfer. *J Gen Physiol* 67: 773–790, 1976.
193. Gu X, Sackin H. Effect of pH on potassium and proton conductance in renal proximal tubule. *Am J Physiol Renal Physiol* 269: F289–F308, 1995.
194. Gunn SA, Gould TC. Role of zinc in fertility and fecundity in the rat. *Am J Physiol* 193: 505–508, 1958.
195. Gunthorpe MJ, Lummis SCR. Conversion of the ion selectivity of the 5-HT_{3A} receptor from cationic to anionic reveals a conserved feature of the ligand-gated ion channel superfamily. *J Biol Chem* 276: 10977–10983, 2001.
196. Gutknecht J. Proton/hydroxide conductance through lipid bilayer membranes. *J Membr Biol* 82: 105–112, 1984.
197. Haggie PM, Verkman AS. Cystic fibrosis transmembrane conductance regulator-independent phagosomal acidification in macrophages. *J Biol Chem* 282: 31422–31428, 2007.
198. Haines TH. Do sterols reduce proton and sodium leaks through lipid bilayers? *Prog Lipid Res* 40: 299–324, 2001.
199. Hallab NJ, Jacobs JJ. Biologic effects of implant debris. *Bull NYU Hosp Jt Dis* 67: 182–188, 2009.
200. Harrington LH, Walker CW, Lesser MP. Stereological analysis of nutritive phagocytes and gametogenic cells during the annual reproductive cycle of the green sea urchin, *Strongylocentrotus droebachiensis*. *Invertebrate Biol* 126: 202–209, 2007.
201. Harvey EB. A physiological study of *Noctiluca*, with special reference to light production, anaesthesia and specific gravity. *Proc Natl Acad Sci USA* 3: 15–16, 1917.
202. Hastings JW. Bioluminescence. In: *Cell Physiology Sourcebook: A Molecular Approach* (3rd ed.), edited by Sperelakis N. San Diego: Academic, 2001, p. 1115–1131.
203. Hastings JW, Sweeney BM. The luminescent reaction in extracts of the marine dinoflagellate, *Gonyaulax polyedra*. *J Cell Physiol* 49: 209–225, 1957.
204. Hastings JW, Vergin M, DeSa R. Scintillons: the biochemistry of dinoflagellate bioluminescence. In: *Bioluminescence in Progress*, edited by Haneda FH. Princeton, NJ: Princeton Univ. Press, 1966, p. 301–329.
205. Hellwig N, Plant TD, Janson W, Schäfer M, Schultz G, Schaefer M. TRPV1 acts as proton channel to induce acidification in nociceptive neurons. *J Biol Chem* 279: 34553–34561, 2004.
206. Heming TA, Geers C, Gros G, Bidani A, Crandall ED. Effects of dextran-bound inhibitors on carbonic anhydrase activity in isolated rat lungs. *J Appl Physiol* 61: 1849–1856, 1986.
207. Henderson LM, Banting G, Chappell JB. The arachidonate-activable, NADPH oxidase-associated H⁺ channel. Evidence that gp91-phox functions as an essential part of the channel. *J Biol Chem* 270: 5909–5916, 1995.
208. Henderson LM, Chappell JB, Jones OTG. Internal pH changes associated with the activity of NADPH oxidase of human neutrophils. Further evidence for the presence of an H⁺ conducting channel. *Biochem J* 251: 563–567, 1988.
209. Henderson LM, Chappell JB, Jones OTG. The superoxide-generating NADPH oxidase of human neutrophils is electrogenic and associated with an H⁺ channel. *Biochem J* 246: 325–329, 1987.
210. Henderson LM, Chappell JB, Jones OTG. Superoxide generation by the electrogenic NADPH oxidase of human neutrophils is limited by the movement of a compensating charge. *Biochem J* 255: 285–290, 1988.
211. Henderson LM, Meech RW. Proton conduction through gp91^{phox}. *J Gen Physiol* 120: 759–765, 2002.
212. Henrion U, Renhorn J, Börjesson SI, Nelson EM, Schwaiger CS, Bjelkmar P, Wallner B, Lindahl E, Elinder F. Tracking a complete voltage-sensor cycle with metal-ion bridges. *Proc Natl Acad Sci USA* 109: 8552–8557, 2012.
213. Henry RM, Yu CH, Roderger T, Pomès R. Functional hydration and conformational gating of proton uptake in cytochrome c oxidase. *J Mol Biol* 387: 1165–1185, 2009.
214. Hicks DB, Liu J, Fujisawa M, Krulwich TA. F₁F₀-ATP synthases of alkaliphilic bacteria: lessons from their adaptations. *Biochim Biophys Acta* 1797: 1362–1377, 2010.
215. Hille B. Charges and potentials at the nerve surface. Divalent ions and pH. *J Gen Physiol* 51: 221–236, 1968.
216. Hille B. *Ion Channels of Excitable Membranes*. Sunderland, MA: Sinauer, 2001.
217. Hirschberg B, Rovner A, Lieberman M, Patlak J. Transfer of twelve charges is needed to open skeletal muscle Na⁺ channels. *J Gen Physiol* 106: 1053–1068, 1995.
218. Hisada M. Membrane resting and action potentials from a protozoan, *Noctiluca scintillans*. *J Cell Comp Physiol* 50: 57–71, 1957.

219. Hladky SB, Haydon DA. Ion transfer across lipid membranes in the presence of gramicidin A. I. Studies of the unit conductance channel. *Biochim Biophys Acta* 274: 294–312, 1972.
220. Hodgkin AL, Huxley AF. A quantitative description of membrane current and its application to conduction and excitation in nerve. *J Physiol* 117: 500–544, 1952.
221. Hodgkin AL, Katz B. The effect of sodium ions on the electrical activity of giant axon of the squid. *J Physiol* 108: 37–77, 1949.
222. Horrigan FT, Cui J, Aldrich RW. Allosteric voltage gating of potassium channels. I. Msls ionic currents in the absence of Ca^{2+} . *J Gen Physiol* 114: 277–304, 1999.
223. Hosler JP, Ferguson-Miller S, Mills DA. Energy transduction: proton transfer through the respiratory complexes. *Annu Rev Biochem* 75: 165–187, 2006.
224. Hoth M. Depletion of intracellular calcium stores activates an outward potassium current in mast and RBL-1 cells that is correlated with CRAC channel activation. *FEBS Lett* 390: 285–288, 1996.
225. Hu F, Luo W, Hong M. Mechanisms of proton conduction and gating in influenza M2 proton channels from solid-state NMR. *Science* 330: 505–508, 2010.
226. Hu F, Schmidt-Rohr K, Hong M. NMR detection of pH-dependent histidine-water proton exchange reveals the conduction mechanism of a transmembrane proton channel. *J Am Chem Soc* 134: 3703–3713, 2012.
227. Hu J, Fu R, Nishimura K, Zhang L, Zhou HX, Busath DD, Vijayvergiya V, Cross TA. Histidines, heart of the hydrogen ion channel from influenza A virus: toward an understanding of conductance and proton selectivity. *Proc Natl Acad Sci USA* 103: 6865–6870, 2006.
228. Hückel E. Theorie der Beweglichkeiten des Wasserstoff- und Hydroxylions in wässriger Lösung. *Z Elektrochemie und angewandte physikalische Chemie* 34: 546–562, 1928.
229. Huggins ML. Hydrogen bridges in ice and liquid water. *J Phys Chem* 40: 723–731, 1936.
230. Huggins ML. The role of hydrogen bonds in conduction by hydrogen and hydroxyl ions. *J Am Chem Soc* 53: 3190–3191, 1931.
231. Humez S, Collin T, Matifat F, Guilbault P, Fournier F. InsP_3 -dependent Ca^{2+} oscillations linked to activation of voltage-dependent H^+ conductance in *Rana esculenta* oocytes. *Cell Signal* 8: 375–379, 1996.
232. Humez S, Fournier F, Guilbault P. A voltage-dependent and pH-sensitive proton current in *Rana esculenta* oocytes. *J Membr Biol* 147: 207–215, 1995.
233. Iovannisci D, Illek B, Fischer H. Function of the HVCN1 proton channel in airway epithelia and a naturally occurring mutation, M91T. *J Gen Physiol* 136: 35–46, 2010.
234. Islas LD, Sigworth FJ. Electrostatics and the gating pore of *Shaker* potassium channels. *J Gen Physiol* 117: 69–89, 2001.
235. Islas LD, Sigworth FJ. Voltage sensitivity and gating charge in *Shaker* and *Shab* family potassium channels. *J Gen Physiol* 114: 723–742, 1999.
236. Iyer GYN, Islam MF, Quastel JH. Biochemical aspects of phagocytosis. *Nature* 192: 535–541, 1961.
237. Jack JJB, Noble D, Tsien RW. Nonlinear properties of excitable membranes. In: *Electric Current Flow in Excitable Cells*. Oxford, UK: Clarendon, 1975, chapt. 8, p. 225–260.
238. Jayaraman S, Song Y, Vetrivel L, Shankar L, Verkman AS. Noninvasive in vivo fluorescence measurement of airway-surface liquid depth, salt concentration, and pH. *J Clin Invest* 107: 317–324, 2001.
239. Jensen MO, Jogini V, Borhani DW, Leffler AE, Dror RO, Shaw DE. Mechanism of voltage gating in potassium channels. *Science* 336: 229–233, 2012.
240. Jentsch TJ. Chloride and the endosomal-lysosomal pathway: emerging roles of CLC chloride transporters. *J Physiol* 578: 633–640, 2007.
241. Jewell DA, Tu CK, Paranawithana SR, Tanhauser SM, LoGrasso PV, Laipis PJ, Silverman DN. Enhancement of the catalytic properties of human carbonic anhydrase III by site-directed mutagenesis. *Biochemistry* 30: 1484–1490, 1991.
242. Jiang J, Li M, Yue L. Potentiation of TRPM7 inward currents by protons. *J Gen Physiol* 126: 137–150, 2005.
243. Jiang Q, Griffin DA, Barofsky DF, Hurst JK. Intraphagosomal chlorination dynamics and yields determined using unique fluorescent bacterial mimics. *Chem Res Toxicol* 10: 1080–1089, 1997.
244. Jiang Y, Lee A, Chen J, Ruta V, Cadene M, Chait BT, MacKinnon R. X-ray structure of a voltage-dependent K^+ channel. *Nature* 423: 33–41, 2003.
245. Jiang Y, Ruta V, Chen J, Lee A, MacKinnon R. The principle of gating charge movement in a voltage-dependent K^+ channel. *Nature* 423: 42–48, 2003.
246. Johansson A, Jesaitis AJ, Lundqvist H, Magnusson KE, Sjölin C, Carlsson A, Dahlgren C. Different subcellular localization of cytochrome *b* and the dormant NADPH-oxidase in neutrophils and macrophages: effect on the production of reactive oxygen species during phagocytosis. *Cell Immunol* 161: 61–71, 1995.
247. Johnston RB Jr, Keele BB Jr, Misra HP, Lehmeier JE, Webb LS, Baehner RL, Rajagopalan KV. The role of superoxide anion generation in phagocytic bactericidal activity: Studies with normal and chronic granulomatous disease leukocytes. *J Clin Invest* 55: 1357–1372, 1975.
248. Jurkat-Rott K, Lehmann-Horn F. Do hyperpolarization-induced proton currents contribute to the pathogenesis of hypokalemic periodic paralysis, a voltage sensor channelopathy? *J Gen Physiol* 130: 1–5, 2007.
249. Kanaji A, Caicedo MS, Virdi AS, Sumner DR, Hallab NJ, Sena K. Co-Cr-Mo alloy particles induce tumor necrosis factor alpha production in MLO-Y4 osteocytes: a role for osteocytes in particle-induced inflammation. *Bone* 45: 528–533, 2009.
250. Kapus A, Romanek R, Qu AY, Rotstein OD, Grinstein S. A pH-sensitive and voltage-dependent proton conductance in the plasma membrane of macrophages. *J Gen Physiol* 102: 729–760, 1993.
251. Kapus A, Szászi K, Ligeti E. Phorbol 12-myristate 13-acetate activates an electrogenic H^+ -conducting pathway in the membrane of neutrophils. *Biochem J* 281: 697–701, 1992.
252. Keramidis A, Moorhouse AJ, Pierce KD, Schofield PR, Barry PH. Cation-selective mutations in the M2 domain of the inhibitory glycine receptor channel reveal determinants of ion-charge selectivity. *J Gen Physiol* 119: 393–410, 2002.
253. Khurana E, Dal Peraro M, DeVane R, Vemparala S, DeGrado WF, Klein ML. Molecular dynamics calculations suggest a conduction mechanism for the M2 proton channel from influenza A virus. *Proc Natl Acad Sci USA* 106: 1069–1074, 2009.
254. Kirichok Y, Lishko PV. Rediscovering sperm ion channels with the patch-clamp technique. *Mol Hum Reprod* 17: 478–499, 2011.
255. Klebanoff SJ. Myeloperoxidase: friend and foe. *J Leukoc Biol* 77: 598–625, 2005.
256. Klebanoff SJ. Oxygen metabolites from phagocytes. In: *Inflammation: Basic Principles and Clinical Correlates* (3rd ed.), edited by Gallin JI and Snyderman R. Philadelphia, PA: Lippincott Williams & Wilkins, 1999, p. 721–768.
257. Klocke RA. Catalysis of CO_2 reactions by lung carbonic anhydrase. *J Appl Physiol* 44: 882–888, 1978.
258. Klocke RA. Equilibrium of CO_2 reactions in the pulmonary capillary. *J Appl Physiol* 48: 972–976, 1980.
259. Koch HP, Kurokawa T, Okochi Y, Sasaki M, Okamura Y, Larsson HP. Multimeric nature of voltage-gated proton channels. *Proc Natl Acad Sci USA* 105: 9111–9116, 2008.
260. Kohout SC, Ulbrich MH, Bell SC, Isacoff EY. Subunit organization and functional transitions in Ci-VSP. *Nat Struct Mol Biol* 15: 106–108, 2008.
261. Kolesnikov SS, Margolskee RF. Extracellular K^+ activates a K^+ - and H^+ -permeable conductance in frog taste receptor cells. *J Physiol* 507: 415–432, 1998.
262. Krah A, Pogoryelov D, Langer JD, Bond PJ, Meier T, Faraldo-Gómez JD. Structural and energetic basis for H^+ versus Na^+ binding selectivity in ATP synthase F_o rotors. *Biochim Biophys Acta* 1797: 763–772, 2010.
263. Krause RM, Bernheim L, Bader CR. Human skeletal muscle has a voltage-gated proton current. *Neuromuscular Disorders* 3: 407–411, 1993.
264. Krauss D, Gillespie D. Sieving experiments and pore diameter: it's not a simple relationship. *Eur Biophys J* 39: 1513–1521, 2010.

265. Kreuer KD, Paddison SJ, Spohr E, Schuster M. Transport in proton conductors for fuel-cell applications: simulations, elementary reactions, and phenomenology. *Chem Rev* 104: 4637–4678, 2004.
266. Krieger N, Hastings JW. Bioluminescence: pH activity profiles of related luciferase fractions. *Science* 161: 586–589, 1968.
267. Kulleperuma K, Smith SME, Holyoake J, Chakrabarti N, Morgan D, Musset B, DeCoursey TE, Cherny VV, Pomès R. A homology modeling-simulation protocol for construction and assessment of H_v1 models. *Biophys J* 102: 266a, 2012.
268. Kumánovics A, Levin G, Blount P. Family ties of gated pores: evolution of the sensor module. *FASEB J* 16: 1623–1629, 2002.
269. Kuno M, Ando H, Morihata H, Sakai H, Mori H, Sawada M, Oiki S. Temperature dependence of proton permeation through a voltage-gated proton channel. *J Gen Physiol* 134: 191–205, 2009.
270. Kuno M, Kawawaki J, Nakamura F. A highly temperature-sensitive proton current in mouse bone marrow-derived mast cells. *J Gen Physiol* 109: 731–740, 1997.
271. Kurosaki T. Molecular mechanisms in B cell antigen receptor signaling. *Curr Opin Immunol* 9: 309–318, 1997.
272. Kyle H, Ward JP, Widdicombe JG. Control of pH of airway surface liquid of the ferret trachea in vitro. *J Appl Physiol* 68: 135–140, 1990.
273. Lacy P, Abdel-Latif D, Steward M, Musat-Marcu S, Man SF, Moqbel R. Divergence of mechanisms regulating respiratory burst in blood and sputum eosinophils and neutrophils from atopic subjects. *J Immunol* 170: 2670–2679, 2003.
274. Laggner H, Philipp K, Goldenberg H. Free zinc inhibits transport of vitamin C in differentiated HL-60 cells during respiratory burst. *Free Radic Biol Med* 40: 436–443, 2006.
275. Lamb FS, Moreland JG, Miller FJ Jr. Electrophysiology of reactive oxygen production in signaling endosomes. *Antioxid Redox Signal* 11: 1335–1347, 2009.
276. Lambeth JD. Nox enzymes, ROS, and chronic disease: an example of antagonistic pleiotropy. *Free Radic Biol Med* 43: 332–347, 2007.
277. Lancaster CRD. The role of electrostatics in proton-conducting membrane protein complexes. *FEBS Lett* 545: 52–60, 2003.
278. Larsson HP, Baker OS, Dhillon DS, Isacoff EY. Transmembrane movement of the Shaker K⁺ channel S4. *Neuron* 16: 387–397, 1996.
279. Latimer WM, Rodebush WH. Polarity and ionization from the standpoint of the Lewis theory of valence. *J Am Chem Soc* 42: 1419–1433, 1920.
280. Latz MI, Bovard M, VanDelinder V, Segre E, Rohr J, Groisman A. Bioluminescent response of individual dinoflagellate cells to hydrodynamic stress measured with millisecond resolution in a microfluidic device. *J Exp Biol* 211: 2865–2875, 2008.
281. Launikonis BS, Zhou J, Royer L, Shannon TR, Brum G, Ríos E. Confocal imaging of [Ca²⁺] in cellular organelles by SEER, shifted excitation and emission ratioing of fluorescence. *J Physiol* 567: 523–543, 2005.
282. Lear JD. Proton conduction through the M2 protein of the influenza A virus: a quantitative, mechanistic analysis of experimental data. *FEBS Lett* 552: 17–22, 2003.
283. Lear JD, Wasserman ZR, DeGrado WF. Synthetic amphiphilic peptide models for protein ion channels. *Science* 240: 1177–1181, 1988.
284. Lecar H, Larsson HP, Grabe M. Electrostatic model of S4 motion in voltage-gated ion channels. *Biophys J* 85: 2854–2864, 2003.
285. Lee SC, Steinhardt RA. pH changes associated with meiotic maturation in oocytes of *Xenopus laevis*. *Dev Biol* 85: 358–369, 1981.
286. Lee SY, Letts JA, Mackinnon R. Dimeric subunit stoichiometry of the human voltage-dependent proton channel Hv1. *Proc Natl Acad Sci USA* 105: 7692–7695, 2008.
287. Lee SY, Letts JA, MacKinnon R. Functional reconstitution of purified human Hv1 H⁺ channels. *J Mol Biol* 387: 1055–1060, 2009.
288. Leiding T, Wang J, Martinsson J, DeGrado WF, Årsköld SP. Proton and cation transport activity of the M2 proton channel from influenza A virus. *Proc Natl Acad Sci USA* 107: 15409–15414, 2010.
289. Lengyel S, Conway BE. Proton solvation and proton transfer in chemical and electrochemical processes. In: *Thermodynamic and Transport Properties of Aqueous and Molten Electrolytes*, edited by Conway BE, Bockris JOM, and Yeager E. New York: Plenum, 1983, p. 339–398.
290. Leonardos N, Read B, Thake B, Young JR. No mechanistic dependence of photosynthesis on calcification in the coccolithophorid *Emiliania huxleyi* (Haptophyta). *J Phycol* 45: 1046–1051, 2009.
291. Levis RA, Rae JL. The use of quartz patch pipettes for low noise single channel recording. *Biophys J* 65: 1666–1677, 1993.
292. Levitt DG, Elias SR, Hautman JM. Number of water molecules coupled to the transport of sodium, potassium and hydrogen ions via gramicidin, nonactin or valinomycin. *Biochim Biophys Acta* 512: 436–451, 1978.
293. Lew PD, Southwick FS, Stossel TP, Whitin JC, Simons E, Cohen HJ. A variant of chronic granulomatous disease: deficient oxidative metabolism due to a low-affinity NADPH oxidase. *N Engl J Med* 305: 1329–1333, 1981.
294. Lewis RS, Cahalan MD. Potassium and calcium channels in lymphocytes. *Annu Rev Immunol* 13: 623–653, 1995.
295. Li H, Chen H, Steinbronn C, Wu B, Beitz E, Zeuthen T, Voth GA. Enhancement of proton conductance by mutations of the selectivity filter of aquaporin-1. *J Mol Biol* 407: 607–620, 2011.
296. Li SJ, Zhao Q, Zhou Q, Unno H, Zhai Y, Sun F. The role and structure of the carboxyl-terminal domain of the human voltage-gated proton channel Hv1. *J Biol Chem* 285: 12047–12054, 2010.
297. Li XJ, Tian W, Stull ND, Grinstein S, Atkinson S, Dinauer MC. A fluorescently tagged C-terminal fragment of p47^{phox} detects NADPH oxidase dynamics during phagocytosis. *Mol Biol Cell* 20: 1520–1532, 2009.
298. Lien YH, Lai LW. Respiratory acidosis in carbonic anhydrase II-deficient mice. *Am J Physiol Lung Cell Mol Physiol* 274: L301–L304, 1998.
299. Liman ER, Hess P, Weaver F, Koren G. Voltage-sensing residues in the S4 region of a mammalian K⁺ channel. *Nature* 353: 752–756, 1991.
300. Lin MC, Hsieh JY, Mock AF, Papazian DM. R1 in the Shaker S4 occupies the gating charge transfer center in the resting state. *J Gen Physiol* 138: 155–163, 2011.
301. Lin TI, Schroeder C. Definitive assignment of proton selectivity and attoampere unitary current to the M2 ion channel protein of influenza A virus. *J Virol* 75: 3647–3656, 2001.
302. Lishko P, Kirichok Y, Ren D, Navarro B, Chung JJ, Clapham DE. The control of male fertility by spermatozoan ion channels. *Annu Rev Physiol* 74: 453–475, 2012.
303. Lishko PV, Botchkina IL, Fedorenko A, Kirichok Y. Acid extrusion from human spermatozoa is mediated by flagellar voltage-gated proton channel. *Cell* 140: 327–337, 2010.
304. Logothetis DE, Movahedi S, Satler C, Lindpaintner K, Nadal-Ginard B. Incremental reductions of positive charge within the S4 region of a voltage-gated K⁺ channel result in corresponding decreases in gating charge. *Neuron* 8: 531–540, 1992.
305. Long SB, Tao X, Campbell EB, MacKinnon R. Atomic structure of a voltage-dependent K⁺ channel in a lipid membrane-like environment. *Nature* 450: 376–382, 2007.
306. Lopez GA, Jan YN, Jan LY. Hydrophobic substitution mutations in the S4 sequence alter voltage-dependent gating in Shaker K⁺ channels. *Neuron* 7: 327–336, 1991.
307. Lowenthal A, Levy R. Essential requirement of cytosolic phospholipase A₂ for activation of the H⁺ channel in phagocyte-like cells. *J Biol Chem* 274: 21603–21608, 1999.
308. Lu J, Deutsch C. Pegylation: a method for assessing topological accessibilities in Kv1.3. *Biochemistry* 40: 13288–13301, 2001.
309. Lucas WJ. Alkaline band formation in *Chara corallina*: due to OH⁻ efflux or H⁺ influx? *Plant Physiol* 63: 248–254, 1979.
310. Ma C, Soto CS, Ohgashi Y, Taylor A, Bournas V, Glawe B, Udo MK, DeGrado WF, Lamb RA, Pinto LH. Identification of the pore-lining residues of the BM2 ion channel protein of influenza B virus. *J Biol Chem* 283: 15921–15931, 2008.

311. MacGlashan DJ Jr, Botana LM. Biphasic Ca^{2+} responses in human basophils. Evidence that the initial transient elevation associated with the mobilization of intracellular calcium is an insufficient signal for degranulation. *J Immunol* 150: 980–991, 1993.
312. MacGlashan DW Jr, Gleich GJ, Thomas LL. Increases in cytosolic Ca^{2+} accompany basophil activation by eosinophil granule major basic protein. *Immunol Lett* 58: 37–42, 1997.
313. Mackinder L, Wheeler G, Schroeder D, Riebesell U, Brownlee C. Molecular mechanisms underlying calcification in coccolithophores. *Geomicrobiol J* 27: 585–595, 2010.
314. Mahaut-Smith MP. The effect of zinc on calcium and hydrogen ion currents in intact snail neurones. *J Exp Biol* 145: 455–464, 1989.
315. Maldonado EM, Latz MI. Shear-stress dependence of dinoflagellate bioluminescence. *Biol Bull* 212: 242–249, 2007.
316. Markovitch O, Chen H, Izvekoy S, Paesani F, Voth GA, Agmon N. Special pair dance and partner selection: elementary steps in proton transport in liquid water. *J Phys Chem B* 112: 9456–9466, 2008.
317. Marx D, Tuckerman ME, Hutter J, Parrinello M. The nature of the hydrated excess proton in water. *Nature* 397: 601–604, 1999.
318. Matsuura T, Mori T, Hasaka M, Kuno M, Kawawaki J, Nishikawa K, Narahashi T, Sawada M, Asada A. Inhibition of voltage-gated proton channels by local anaesthetics in GMI-R1 rat microglia. *J Physiol* 590: 827–844, 2012.
319. Maturana A, Krause KH, Demaurex N. NOX family NADPH oxidases: do they have built-in proton channels? *J Gen Physiol* 120: 781–786, 2002.
320. Mawson CA, Fischer MI. Zinc and carbonic anhydrase in human semen. *Biochem J* 55: 696–700, 1953.
321. McCormack K, Lin L, Sigworth FJ. Substitution of a hydrophobic residue alters the conformational stability of Shaker K^+ channels during gating and assembly. *Biophys J* 65: 1740–1748, 1993.
322. McKenna SM, Davies KJ. The inhibition of bacterial growth by hypochlorous acid. Possible role in the bactericidal activity of phagocytes. *Biochem J* 254: 685–692, 1988.
323. Meech R. A contribution to the history of the proton channel. *Wiley Interdiscip Rev: Membr Trans Signal* 1: 533–537, 2012.
324. Meech RW, Thomas RC. The effect of calcium injection on the intracellular sodium and pH of snail neurones. *J Physiol* 265: 867–879, 1977.
325. Meech RW, Thomas RC. Voltage-dependent intracellular pH in *Helix aspersa* neurones. *J Physiol* 390: 433–452, 1987.
326. Mehrnejad F, Khadem-Maaref M, Ghahremanpour MM, Doustdar F. Mechanisms of amphipathic helical peptide denaturation by guanidinium chloride and urea: a molecular dynamics simulation study. *J Comput Aided Mol Des* 24: 829–841, 2010.
327. Mesinger AF, Case JF. Dinoflagellate luminescence increases susceptibility of zooplankton to teleost predation. *Mar Biol* 112: 207–210, 1992.
328. Miedema H, Felle H, Prins HBA. Effect of high pH on the plasma membrane potential and conductance in *Eloдея densa*. *J Membr Biol* 128: 63–69, 1992.
329. Miller C. Lonely voltage sensor seeks protons for permeation. *Science* 312: 534–535, 2006.
330. Minor DL Jr. A sensitive channel family replete with sense and motion. *Nat Struct Mol Biol* 13: 388–390, 2006.
331. Moffat JC, Vijayvergiya V, Gao PF, Cross TA, Woodbury DJ, Busath DD. Proton transport through influenza A virus M2 protein reconstituted in vesicles. *Biophys J* 94: 434–445, 2008.
332. Moreland JG, Davis AP, Bailey G, Nauseef WM, Lamb FS. Anion channels, including CIC-3, are required for normal neutrophil oxidative function, phagocytosis, and trans-endothelial migration. *J Biol Chem* 281: 12277–12288, 2006.
333. Morgan D, Capasso M, Musset B, Cherny VV, DeCoursey TE. Two isoforms of the human voltage gated proton channel hHv_1 . *Biophys J*. In press.
334. Morgan D, Capasso M, Musset B, Cherny VV, Rios E, Dyer MJS, DeCoursey TE. Voltage-gated proton channels maintain pH in human neutrophils during phagocytosis. *Proc Natl Acad Sci USA* 106: 18022–18027, 2009.
335. Morgan D, Cherny VV, Finnegan A, Bollinger J, Gelb MH, DeCoursey TE. Sustained activation of proton channels and NADPH oxidase in human eosinophils and murine granulocytes requires PKC but not $\text{cPLA}_2\alpha$ activity. *J Physiol* 579: 327–344, 2007.
336. Morgan D, Cherny VV, Murphy R, Katz BZ, DeCoursey TE. The pH dependence of NADPH oxidase in human eosinophils. *J Physiol* 569: 419–431, 2005.
337. Morgan D, Cherny VV, Murphy R, Xu W, Thomas LL, DeCoursey TE. Temperature dependence of NADPH oxidase in human eosinophils. *J Physiol* 550: 447–458, 2003.
338. Morgan D, Cherny VV, Price MO, Dinauer MC, DeCoursey TE. Absence of proton channels in COS-7 cells expressing functional NADPH oxidase components. *J Gen Physiol* 119: 571–580, 2002.
339. Morgan D, DeCoursey TE. Simultaneous measurement of phagosome and plasma membrane potentials in human neutrophils by Di-8-Anepps and SEER. *Biophys J* 96: 55a, 2010.
340. Mori H, Sakai H, Morihata H, Kawawaki J, Amano H, Yamano T, Kuno M. Regulatory mechanisms and physiological relevance of a voltage-gated H^+ channel in murine osteoclasts: phorbol myristate acetate induces cell acidosis and the channel activation. *J Bone Miner Res* 18: 2069–2076, 2003.
341. Morihata H, Kawawaki J, Sakai H, Sawada M, Tsutada T, Kuno M. Temporal fluctuations of voltage-gated proton currents in rat spinal microglia via pH-dependent and -independent mechanisms. *Neurosci Res* 38: 265–271, 2000.
342. Morihata H, Nakamura F, Tsutada T, Kuno M. Potentiation of a voltage-gated proton current in acidosis-induced swelling of rat microglia. *J Neurosci* 20: 7220–7227, 2000.
343. Morin JG. Coastal bioluminescence: patterns and functions. *Bull Mar Sci* 33: 787–817, 1983.
344. Mould JA, Drury JE, Frings SM, Kaupp UB, Pekosz A, Lamb RA, Pinto LH. Permeation and activation of the M_2 ion channel of influenza A virus. *J Biol Chem* 275: 31038–31050, 2000.
345. Mould JA, Paterson RG, Takeda M, Ohigashi Y, Venkataraman P, Lamb RA, Pinto LH. Influenza B virus BM2 protein has ion channel activity that conducts protons across membranes. *Dev Cell* 5: 175–184, 2003.
346. Mozhayeva GN, Naumov AP. The permeability of sodium channels to hydrogen ions in nerve fibres. *Pflügers Arch* 396: 163–173, 1983.
347. Mozhayeva GN, Naumov AP, Negulyaev YA. Interaction of H^+ ions with acid groups in normal sodium channels. *Gen Physiol Biophys* 1: 5–19, 1982.
348. Murata Y, Iwasaki H, Sasaki M, Inaba K, Okamura Y. Phosphoinositide phosphatase activity coupled to an intrinsic voltage sensor. *Nature* 435: 1239–1243, 2005.
349. Murata Y, Okamura Y. Depolarization activates the phosphoinositide phosphatase Ci-VSP , as detected in *Xenopus* oocytes coexpressing sensors of PIP_2 . *J Physiol* 583: 875–889, 2007.
350. Murphy R, Cherny VV, Morgan D, DeCoursey TE. Voltage-gated proton channels help regulate pH_i in rat alveolar epithelium. *Am J Physiol Lung Cell Mol Physiol* 288: L398–L408, 2005.
351. Murphy R, DeCoursey TE. Charge compensation during the phagocyte respiratory burst. *Biochim Biophys Acta* 1757: 996–1011, 2006.
352. Musset B, Capasso M, Cherny VV, Morgan D, Bhamrah M, Dyer MJS, DeCoursey TE. Identification of Thr²⁹ as a critical phosphorylation site that activates the human proton channel *Hvcn1* in leukocytes. *J Biol Chem* 285: 5117–5121, 2010.
353. Musset B, Cherny VV, DeCoursey TE. Strong glucose dependence of electron current in human monocytes. *Am J Physiol Cell Physiol* 302: C286–C295, 2012.
354. Musset B, Cherny VV, Morgan D, DeCoursey TE. The intimate and mysterious relationship between proton channels and NADPH oxidase. *FEBS Lett* 583: 7–12, 2009.
355. Musset B, Cherny VV, Morgan D, Okamura Y, Ramsey IS, Clapham DE, DeCoursey TE. Detailed comparison of expressed and native voltage-gated proton channel currents. *J Physiol* 586: 2477–2486, 2008.
356. Musset B, Clark RA, DeCoursey TE, Petheo GL, Geiszt M, Chen Y, Cornell JE, Eddy CA, Brzyski RG, El Jamal A. NOX5 in human spermatozoa: expression, function and regulation. *J Biol Chem* 287: 9376–9388, 2012.

357. Musset B, DeCoursey TE. Biophysical properties of the voltage-gated proton channel H_{v1} . *Wiley Interdiscip Rev: Membr Trans Signal* 1: 605–620, 2012.
358. Musset B, Morgan D, Cherny VV, MacGlashan DW Jr, Thomas LL, Ríos E, DeCoursey TE. A pH-stabilizing role of voltage-gated proton channels in IgE-mediated activation of human basophils. *Proc Natl Acad Sci USA* 105: 11020–11025, 2008.
359. Musset B, Smith SM, Rajan S, Cherny VV, Morgan D, DeCoursey TE. Oligomerization of the voltage gated proton channel. *Channels* 4: 260–265, 2010.
360. Musset B, Smith SM, Rajan S, Cherny VV, Sujai S, Morgan D, DeCoursey TE. Zinc inhibition of monomeric and dimeric proton channels suggests cooperative gating. *J Physiol* 588: 1435–1449, 2010.
361. Musset B, Smith SME, Kulleperuma K, Morgan D, Holyoake J, Chakrabarti N, Cherny VV, Pomès R, DeCoursey TE. Accessibility of the S4 arginines in the human voltage gated proton channel, H_{v1} . *Biophys J*. In press.
362. Musset B, Smith SME, Rajan S, Morgan D, Cherny VV, DeCoursey TE. Aspartate 112 is the selectivity filter of the human voltage-gated proton channel. *Nature* 480: 273–277, 2011.
363. Myers VB, Haydon DA. Ion transfer across lipid membranes in the presence of gramicidin A. II. The ion selectivity. *Biochim Biophys Acta* 274: 313–322, 1972.
364. Nagel G, Ollig D, Fuhrmann M, Kateriya S, Musti AM, Bamberg E, Hegemann P. Channelrhodopsin-1: a light-gated proton channel in green algae. *Science* 296: 2395–2398, 2002.
365. Nagle JF, Morowitz HJ. Molecular mechanisms for proton transport in membranes. *Proc Natl Acad Sci USA* 75: 298–302, 1978.
366. Nagle JF, Tristram-Nagle S. Hydrogen bonded chain mechanisms for proton conduction and proton pumping. *J Membr Biol* 74: 1–14, 1983.
367. Nair SK, Christianson DW. Unexpected pH-dependent conformation of His-64, the proton shuttle of carbonic anhydrase II. *J Am Chem Soc* 113: 9455–9458, 1991.
368. Nanda A, Gukovskaya A, Tseng J, Grinstein S. Activation of vacuolar-type proton pumps by protein kinase C. Role in neutrophil pH regulation. *J Biol Chem* 267: 22740–22746, 1992.
369. Nanda A, Romanek R, Curmutte JT, Grinstein S. Assessment of the contribution of the cytochrome *b* moiety of the NADPH oxidase to the transmembrane H^+ conductance of leukocytes. *J Biol Chem* 269: 27280–27285, 1994.
370. Narahashi T, Frazier T, Yamada M. The site of action and active form of local anesthetics. I. Theory and pH experiments with tertiary compounds. *J Pharmacol Exp Ther* 171: 32–44, 1970.
371. Nauseef WM. How human neutrophils kill and degrade microbes: an integrated view. *Immunol Rev* 219: 88–102, 2007.
372. Nauseef WM, Volpp BD, McCormick S, Leidal KG, Clark RA. Assembly of the neutrophil respiratory burst oxidase. Protein kinase C promotes cytoskeletal and membrane association of cytosolic oxidase components. *J Biol Chem* 266: 5911–5917, 1991.
373. Nawata T, Sibaoka T. Coupling between action potential and bioluminescence in *Noctiluca*: effects of inorganic ions and pH in vacuolar sap. *J Comp Physiol* 134: 137–149, 1979.
374. Nawata T, Sibaoka T. Ionic composition and pH of the vacuolar sap in marine dinoflagellate *Noctiluca*. *Plant Cell Physiol* 17: 265–272, 1976.
375. Neher E. Correction for liquid junction potentials in patch clamp experiments. *Methods Enzymol* 207: 123–131, 1992.
376. Nelson RD, Kuan G, Saier MH Jr, Montal M. Modular assembly of voltage-gated channel proteins: a sequence analysis and phylogenetic study. *J Mol Microbiol Biotechnol* 1: 281–287, 1999.
377. Ng AW, Bidani A, Heming TA. Innate host defense of the lung: effects of lung-lining fluid pH. *Lung* 182: 297–317, 2004.
378. Nguyen KL, Gillis S, MacGlashan DW Jr. A comparative study of releasing and nonreleasing human basophils: nonreleasing basophils lack an early component of the signal transduction pathway that follows IgE cross-linking. *J Allergy Clin Immunol* 85: 1020–1029, 1990.
379. Nicol JAC. Observations on luminescence in *Noctiluca*. *J Mar Biol Assoc UK* 37: 535–549, 1958.
380. Nicolas MT, Nicolas G, Johnson CH, Bassot JM, Hastings JW. Characterization of the bioluminescent organelles in *Gonyaulax polyedra* (dinoflagellates) after fast-freeze fixation and antiluciferase immunogold staining. *J Cell Biol* 105: 723–735, 1987.
381. Nielson DW, Goerke J, Clements JA. Alveolar subphase pH in the lungs of anesthetized rabbits. *Proc Natl Acad Sci USA* 78: 7119–7123, 1981.
382. Nilius B. Signaltransduction in vascular endothelium: the role of intracellular calcium and ion channels. *Verh K Acad Geneesk Belg* 60: 215–250, 1998.
383. Noceti F, Baldelli P, Wei X, Qin N, Toro L, Birnbaumer L, Stefani E. Effective gating charges per channel in voltage-dependent K^+ and Ca^{2+} channels. *J Gen Physiol* 108: 143–155, 1996.
384. Nordström T, Rotstein OD, Romanek R, Asotra S, Heersche JN, Manolson MF, Brisseau GF, Grinstein S. Regulation of cytoplasmic pH in osteoclasts. Contribution of proton pumps and a proton-selective conductance. *J Biol Chem* 270: 2203–2212, 1995.
385. Nordström T, Shrode LD, Rotstein OD, Romanek R, Goto T, Heersche JN, Manolson MF, Brisseau GF, Grinstein S. Chronic extracellular acidosis induces plasmalemmal vacuolar type H^+ ATPase activity in osteoclasts. *J Biol Chem* 272: 6354–6360, 1997.
386. Numata T, Okada Y. Proton conductivity through the human TRPM7 channel and its molecular determinants. *J Biol Chem* 283: 15097–15103, 2008.
387. Oami K, Maitoh Y. H^+ -dependent contraction of the Triton-extracted tentacle of the dinoflagellate *Noctiluca miliaris*. *J Exp Biol* 145: 1–8, 1989.
388. Ogino K, Izumi Y, Segawa H, Takeyama Y, Ishiyama H, Houbara T, Uda T, Yamashita S. Zinc hydroxide induced respiratory burst in rat neutrophils. *Eur J Pharmacol* 270: 73–78, 1994.
389. Ohno Y, Hirai K, Kanoh T, Uchino H, Ogawa K. Subcellular localization of H_2O_2 production in human neutrophils stimulated with particles and an effect of cytochalasin-B on the cells. *Blood* 60: 253–260, 1982.
390. Ohno YI, Hirai KI, Kanoh T, Uchino H, Ogawa K. Subcellular localization of hydrogen peroxide production in human polymorphonuclear leukocytes stimulated with lectins, phorbol myristate acetate, and digitonin: an electron microscopic study using $CeCl_3$. *Blood* 60: 1195–1202, 1982.
391. Okochi Y, Sasaki M, Iwasaki H, Okamura Y. Voltage-gated proton channel is expressed on phagosomes. *Biochem Biophys Res Commun* 382: 274–279, 2009.
392. Paasche E. A tracer study of the inorganic carbon uptake during coccolith formation and photosynthesis in the coccolithophorid *Coccolithus huxleyi*. *Physiologia Plantarum Suppl* 3: 1–82, 1964.
393. Painter RG, Valentine VG, Lanson NA Jr, Leidal K, Zhang Q, Lombard G, Thompson C, Viswanathan A, Nauseef WM, Wang G, Wang G. CFTR Expression in human neutrophils and the phagolysosomal chlorination defect in cystic fibrosis. *Biochemistry* 45: 10260–10269, 2006.
394. Palmer LG. Ion selectivity of the apical membrane Na channel in the toad urinary bladder. *J Membr Biol* 67: 91–98, 1982.
395. Pantazis A, Keegan P, Postma M, Schwiening CJ. The effect of neuronal morphology and membrane-permeant weak acid and base on the dissipation of depolarization-induced pH gradients in snail neurons. *Pflügers Arch* 452: 175–187, 2006.
396. Papazian DM, Shao XM, Seoh SA, Mock AF, Huang Y, Wainstock DH. Electrostatic interactions of S4 voltage sensor in Shaker K^+ channel. *Neuron* 14: 1293–1301, 1995.
397. Papazian DM, Timpe LC, Jan YN, Jan LY. Alteration of voltage-dependence of Shaker potassium channel by mutations in the S4 sequence. *Nature* 349: 305–310, 1991.
398. Parfrey LW, Barbero E, Lasser E, Dunthorn M, Bhattacharya D, Patterson DJ, Katz LA. Evaluating support for the current classification of eukaryotic diversity. *PLoS Genet* 2: e220, 2006.
399. Pauling L. The hydrogen bond. In: *The Nature of the Chemical Bond and the Structure of Molecules and Crystals: An Introduction to Modern Structural Chemistry*, edited by Pauling L. Ithaca, NY: Cornell Univ. Press, 1939, p. 264–314.

400. Perozo E, Santacruz-Tolozá L, Stefani E, Bezanilla F, Papazian DM. S4 mutations alter gating currents of Shaker K channels. *Biophys J* 66: 345–354, 1994.
401. Petersen MK, Hatt AJ, Voth GA. Orientational dynamics of water in the nafion polymer electrolyte membrane and its relationship to proton transport. *J Phys Chem B* 112: 7754–7761, 2008.
402. Peterson E, Ryser T, Funk S, Inouye D, Sharma M, Qin H, Cross TA, Busath DD. Functional reconstitution of influenza A M2(22–62). *Biochim Biophys Acta* 1808: 516–521, 2011.
403. Petheő GL, Demaurex N. Voltage- and NADPH-dependence of electron currents generated by the phagocytic NADPH oxidase. *Biochem J* 388: 485–491, 2005.
404. Petheő GL, Orient A, Baráth M, Kovács I, Réthi B, Lányi A, Rajki A, Rajnavölgyi E, Geiszt M. Molecular and functional characterization of H_v1 proton channel in human granulocytes. *PLoS One* 5: e14081, 2010.
405. Petreccia DC, Nauseef WM, Clark RA. Respiratory burst of normal human eosinophils. *J Leukoc Biol* 41: 283–288, 1987.
406. Pinto LH, Dieckmann GR, Gandhi CS, Papworth CG, Braman J, Shaughnessy MA, Lear JD, Lamb RA, DeGrado WF. A functionally defined model for the M2 proton channel of influenza A virus suggests a mechanism for its ion selectivity. *Proc Natl Acad Sci USA* 94: 11301–11306, 1997.
407. Platts AE, Dix DJ, Chemes HE, Thompson KE, Goodrich R, Rockett JC, Rawe VY, Quintana S, Diamond MP, Strader LF, Krawetz SA. Success and failure in human spermatogenesis as revealed by teratozoospermic RNAs. *Hum Mol Genet* 16: 763–773, 2007.
408. Polishchuk AL, Lear JD, Ma C, Lamb RA, Pinto LH, DeGrado WF. A pH-dependent conformational ensemble mediates proton transport through the influenza A/M2 protein. *Biochemistry* 49: 10061–10071, 2010.
409. Poulsen JH, Fischer H, Illek B, Machen TE. Bicarbonate conductance and pH regulatory capability of cystic fibrosis transmembrane conductance regulator. *Proc Natl Acad Sci USA* 91: 5340–5344, 1994.
410. Preiss L, Yildiz O, Hicks DB, Krulwich TA, Meier T. A new type of proton coordination in an F₁F_o-ATP synthase rotor ring. *PLoS Biol* 8: e1000443, 2010.
411. Qian M, Tu C, Earnhardt JN, Laipis PJ, Silverman DN. Glutamate and aspartate as proton shuttles in mutants of carbonic anhydrase. *Biochemistry* 36: 15758–15764, 1997.
412. Quinn MT, Gauss KA. Structure and regulation of the neutrophil respiratory burst oxidase: comparison with nonphagocyte oxidases. *J Leukoc Biol* 76: 760–781, 2004.
413. Rada B, Hably C, Meczner A, Timar C, Lakatos G, Enyedi P, Ligeti E. Role of Nox2 in elimination of microorganisms. *Semin Immunopathol* 30: 237–253, 2008.
414. Rada BK, Geiszt M, Káldi K, Timár C, Ligeti E. Dual role of phagocytic NADPH oxidase in bacterial killing. *Blood* 104: 2947–2953, 2004.
415. Ramsey IS, Mokrab Y, Carvacho I, Sands ZA, Sansom MSP, Clapham DE. An aqueous H⁺ permeation pathway in the voltage-gated proton channel H_v1. *Nat Struct Mol Biol* 17: 869–875, 2010.
416. Ramsey IS, Moran MM, Chong JA, Clapham DE. A voltage-gated proton-selective channel lacking the pore domain. *Nature* 440: 1213–1216, 2006.
417. Ramsey IS, Ruchti E, Kaczmarek JS, Clapham DE. H_v1 proton channels are required for high-level NADPH oxidase-dependent superoxide production during the phagocyte respiratory burst. *Proc Natl Acad Sci USA* 106: 7642–7647, 2009.
418. Randa HS, Forrest LR, Voth GA, Sansom MSP. Molecular dynamics of synthetic leucine-serine ion channels in a phospholipid membrane. *Biophys J* 77: 2400–2410, 1999.
419. Raven JA, Giordano M, Beardall J, Maberly SC. Algal and aquatic plant carbon concentrating mechanisms in relation to environmental change. *Photosynth Res* 109: 281–296, 2011.
420. Rebolledo S, Qiu F, Larsson HP. Molecular structure and function of H_v1 channels. *Wiley Interdiscip Rev: Membr Transp Signal* 1: 763–777, 2012.
421. Riccardi D, König P, Prat-Resina X, Yu H, Elstner M, Frauenheim T, Cui Q. “Proton holes” in long-range proton transfer reactions in solution and enzymes: A theoretical analysis. *J Am Chem Soc* 128: 16302–16311, 2006.
422. Robinson RA, Stokes RH. *Electrolyte Solutions*. London: Butterworths, 1959.
423. Roos D, de Boer M, Borregard N, Bjerrum OW, Valerius NH, Seger RA, Mühlebach T, Belohradsky BH, Weening RS. Chronic granulomatous disease with partial deficiency of cytochrome b₅₅₈ and incomplete respiratory burst: variants of the X-linked, cytochrome b₅₅₈-negative form of the disease. *J Leukoc Biol* 51: 164–171, 1992.
424. Root RK, Cohen MS. The microbicidal mechanisms of human neutrophils and eosinophils. *Rev Infect Dis* 3: 565–598, 1981.
425. Root RK, Metcalf JA. H₂O₂ release from human granulocytes during phagocytosis. Relationship to superoxide anion formation and cellular catabolism of H₂O₂: studies with normal and cytochalasin B-treated cells. *J Clin Invest* 60: 1266–1279, 1977.
426. Roughton FJW. Recent work on carbon dioxide transport by the blood. *Physiol Rev* 15: 241–296, 1935.
427. Saaranen M, Suistomaa U, Kantola M, Saarikoski S, Vanha-Perttula T. Lead, magnesium, selenium and zinc in human seminal fluid: comparison with semen parameters and fertility. *Hum Reprod* 2: 475–479, 1987.
428. Sakata S, Kurokawa T, Norholm MH, Takagi M, Okochi Y, von Heijne G, Okamura Y. Functionality of the voltage-gated proton channel truncated in S4. *Proc Natl Acad Sci USA* 107: 2313–2318, 2010.
429. Sánchez JC, Wilkins RJ. Effects of hypotonic shock on intracellular pH in bovine articular chondrocytes. *Comp Biochem Physiol A Mol Integr Physiol* 135: 575–583, 2003.
430. Sandvig K, Olsnes S. Diphtheria toxin-induced channels in Vero cells selective for monovalent cations. *J Biol Chem* 263: 12352–12359, 1988.
431. Sansom MSP, Kerr ID, Smith GR, Son HS. The influenza A virus M2 channel: a molecular modeling and simulation study. *Virology* 233: 163–173, 1997.
432. Sasaki M, Takagi M, Okamura Y. A voltage sensor-domain protein is a voltage-gated proton channel. *Science* 312: 589–592, 2006.
433. Sbarra AJ, Karnovsky ML. The biochemical basis of phagocytosis. I. Metabolic changes during the ingestion of particles by polymorphonuclear leukocytes. *J Biol Chem* 234: 1355–1362, 1959.
434. Scheiner S. *Hydrogen Bonding: A Theoretical Perspective*. New York: Oxford Univ. Press, 1997.
435. Schilling T, Eder C. Stimulus-dependent requirement of ion channels for microglial NADPH oxidase-mediated production of reactive oxygen species. *J Neuroimmunol* 225: 190–194, 2010.
436. Schilling T, Gratopp A, DeCoursey TE, Eder C. Voltage-activated proton currents in human lymphocytes. *J Physiol* 545: 93–105, 2002.
437. Schlegel A, Omar A, Jentsch P, Morell A, Kempf C. Semliki Forest virus envelope proteins function as proton channels. *Biosci Rep* 11: 243–255, 1991.
438. Schmitter RE, Njus D, Sulzman FM, Gooch VD, Hastings JW. Dinoflagellate bioluminescence: a comparative study of in vitro components. *J Cell Physiol* 87: 123–134, 1976.
439. Schneider TD, Stephens RM. Sequence logos: a new way to display consensus sequences. *Nucleic Acids Res* 18: 6097–6100, 1990.
440. Schoppa NE, McCormack K, Tanouye MA, Sigworth FJ. The size of gating charge in wild-type and mutant Shaker potassium channels. *Science* 255: 1712–1715, 1992.
441. Schrenzel J, Lew DP, Krause KH. Proton currents in human eosinophils. *Am J Physiol Cell Physiol* 271: C1861–C1871, 1996.
442. Schrenzel J, Serrander L, Bánfi B, Nüsse O, Fouyouzi R, Lew DP, Demaurex N, Krause KH. Electron currents generated by the human phagocyte NADPH oxidase. *Nature* 392: 734–737, 1998.
443. Schuel H, Burkman LJ. A tale of two cells: endocannabinoid-signaling regulates functions of neurons and sperm. *Biol Reprod* 73: 1078–1086, 2005.
444. Schwarzer C, Machen TE, Illek B, Fischer H. NADPH oxidase-dependent acid production in airway epithelial cells. *J Biol Chem* 279: 36454–36461, 2004.
445. Schwiening CJ, Willoughby D. Depolarization-induced pH microdomains and their relationship to calcium transients in isolated snail neurones. *J Physiol* 538: 371–382, 2002.

446. Seger RA, Tiefenauer L, Matsunaga T, Wildfeuer A, Newburger PE. Chronic granulomatous disease due to granulocytes with abnormal NADPH oxidase activity and deficient cytochrome-b. *Blood* 61: 423–428, 1983.
447. Sennoune SR, Bakunts K, Martínez GM, Chua-Tuan JL, Kebir Y, Attaya MN, Martínez-Zaguilan R. Vacuolar H⁺-ATPase in human breast cancer cells with distinct metastatic potential: distribution and functional activity. *Am J Physiol Cell Physiol* 286: C1443–C1452, 2004.
448. Seoh SA, Sigg D, Papazian DM, Bezanilla F. Voltage-sensing residues in the S2 and S4 segments of the Shaker K⁺ channel. *Neuron* 16: 1159–1167, 1996.
449. Shapiro MS, DeCoursey TE. Permeant ion effects on the gating kinetics of the type L potassium channel in mouse lymphocytes. *J Gen Physiol* 97: 1251–1278, 1991.
450. Sharma M, Yi M, Dong H, Qin H, Peterson E, Busath D, Zhou H, Cross T. Insight into the mechanism of the influenza A proton channel from structure in a lipid bilayer. *Science* 330: 509–512, 2010.
451. Sheldon C, Church J. Intracellular pH response to anoxia in acutely dissociated adult rat hippocampal CA1 neurons. *J Neurophysiol* 87: 2209–2224, 2002.
452. Shepherd LMS, Morrison CA. Simulating proton transport through a simplified model for trans-membrane proteins. *J Phys Chem B* 114: 7047–7055, 2010.
453. Shurin SB, Cohen HJ, Whitin JC, Newburger PE. Impaired granulocyte superoxide production and prolongation of the respiratory burst due to a low-affinity NADPH-dependent oxidase. *Blood* 62: 564–571, 1983.
454. Sigg D, Bezanilla F. Total charge movement per channel. The relation between gating charge displacement and the voltage sensitivity of activation. *J Gen Physiol* 109: 27–39, 1997.
455. Sigworth FJ. Voltage gating of ion channels. *Q Rev Biophys* 27: 1–40, 1994.
456. Silverman D, McKenna R. Solvent-mediated proton transfer in catalysis by carbonic anhydrase. *Acc Chem Res* 40: 669–675, 2007.
457. Silverman DN, Lindskog S. The catalytic mechanism of carbonic anhydrase: implications of a rate-limiting protolysis of water. *Acc Chem Res* 21: 30–36, 1988.
458. Simchowicz L, Foy MA, Cragoe EJ Jr. A role for Na⁺/Ca²⁺ exchange in the generation of superoxide radicals by human neutrophils. *J Biol Chem* 265: 13449–13456, 1990.
459. Slatin SL, Finkelstein A, Kienker PK. Anomalous proton selectivity in a large channel: colicin A. *Biochemistry* 47: 1778–1788, 2008.
460. Smith-Maxwell CJ, Ledwell JL, Aldrich RW. Uncharged S4 residues and cooperativity in voltage-dependent potassium channel activation. *J Gen Physiol* 111: 421–439, 1998.
461. Smith RM, Curnutte JT. Molecular basis of chronic granulomatous disease. *Blood* 77: 673–686, 1991.
462. Smith SME, Morgan D, Musset B, Cherny VV, Place AR, Hastings JW, DeCoursey TE. Voltage-gated proton channel in a dinoflagellate. *Proc Natl Acad Sci USA* 108: 18162–18168, 2011.
463. Smith VJ, Peddie CM. Cell cooperation during host defense in the solitary tunicate *Ciona intestinalis* (L). *Biol Bull* 183: 211–219, 1992.
464. Sokolov S, Scheuer T, Catterall WA. Ion permeation and block of the gating pore in the voltage sensor of Na_v1.4 channels with hypokalemic periodic paralysis mutations. *J Gen Physiol* 136: 225–236, 2010.
465. Song JH, Marszalec W, Kai L, Yeh JZ, Narahashi T. Antidepressants inhibit proton currents and tumor necrosis factor- α production in BV2 microglial cells. *Brain Res* 1435: 15–23, 2012.
466. Song JH, Yeh JZ. Dextromethorphan inhibition of voltage-gated proton currents in BV2 microglial cells. *Neurosci Lett* 516: 94–98, 2012.
467. Soyombo AA, Tjon-Kon-Sang S, Rbaibi Y, Bashllari E, Bisceglia J, Muallem S, Kiselyov K. TRP-ML1 regulates lysosomal pH and acidic lysosomal lipid hydrolytic activity. *J Biol Chem* 281: 7294–7301, 2006.
468. Stankova L, Drach GW, Hicks T, Zukoski CF, Chvapil M. Regulation of some functions of granulocytes by zinc of the prostatic fluid and prostate tissue. *J Lab Clin Med* 88: 640–648, 1976.
469. Starace DM, Bezanilla F. Histidine scanning mutagenesis of basic residues of the S4 segment of the Shaker K⁺ channel. *J Gen Physiol* 117: 469–490, 2001.
470. Starace DM, Bezanilla F. A proton pore in a potassium channel voltage sensor reveals a focused electric field. *Nature* 427: 548–553, 2004.
471. Starace DM, Stefani E, Bezanilla F. Voltage-dependent proton transport by the voltage sensor of the Shaker K⁺ channel. *Neuron* 19: 1319–1327, 1997.
472. Steiner H, Jonsson BH, Lindskog S. The catalytic mechanism of carbonic anhydrase. Hydrogen-isotope effects on the kinetic parameters of the human C isoenzyme. *Eur J Biochem* 59: 253–259, 1975.
473. Struyk AF, Cannon SC. A Na⁺ channel mutation linked to hypokalemic periodic paralysis exposes a proton-selective gating pore. *J Gen Physiol* 130: 11–20, 2007.
474. Stühmer W, Conti F, Suzuki H, Wang XD, Noda M, Yahagi N, Kubo H, Numa S. Structural parts involved in activation and inactivation of the sodium channel. *Nature* 339: 597–603, 1989.
475. Suenaga T, Arase H, Yamasaki S, Kohno M, Yokosuka T, Takeuchi A, Hattori T, Saito T. Cloning of B cell-specific membrane tetraspanning molecule BTS possessing B cell proliferation-inhibitory function. *Eur J Immunol* 37: 3197–3207, 2007.
476. Sutton KA, Jungnickel MK, Jovine L, Florman HM. Evolution of the voltage sensor domain of the voltage-sensitive phosphoinositide phosphatase, VSP/TPTE, suggests a role as a proton channel in eutherian mammals. *Mol Biol Evol* 29: 2147–2155, 2012.
477. Swanson JM, Maupin CM, Chen H, Petersen MK, Xu J, Wu Y, Voth GA. Proton solvation and transport in aqueous and biomolecular systems: insights from computer simulations. *J Phys Chem B* 111: 4300–4314, 2007.
478. Swartz KJ. Sensing voltage across lipid membranes. *Nature* 456: 891–897, 2008.
479. Swenson E. Respiratory and renal roles of carbonic anhydrase in gas exchange and acid-base regulation. In: *The Carbonic Anhydrases: New Horizons*, edited by Chegwid-den W, Carter N, and Edwards Y. Basel: Birkhauser Verlag, 2000, p. 281–341.
480. Swenson ER, Deem S, Kerr ME, Bidani A. Inhibition of aquaporin-mediated CO₂ diffusion and voltage-gated H⁺ channels by zinc does not alter rabbit lung CO₂ and NO excretion. *Clin Sci* 103: 567–575, 2002.
481. Swenson RP Jr, Armstrong CM. K⁺ channels close more slowly in the presence of external K⁺ and Rb⁺. *Nature* 291: 427–429, 1981.
482. Szteyn K, Yang W, Schmid E, Lang F, Shumilina E. Lipopolysaccharide sensitive H⁺ current in dendritic cells. *Am J Physiol Cell Physiol* 303: C204–C212, 2012.
483. Takahashi E, Wraight CA. Small weak acids reactivate proton transfer in reaction centers from *Rhodobacter sphaeroides* mutated at Asp^{L210} and Asp^{M17}. *J Biol Chem* 281: 4413–4422, 2006.
484. Takeda K, Barry PH, Gage PW. Effects of ammonium ions on endplate channels. *J Gen Physiol* 75: 589–613, 1980.
485. Taki K, Kato H, Yoshida I. Elimination of CO₂ in patients with carbonic anhydrase II deficiency, with studies of respiratory function at rest. *Respir Med* 93: 536–539, 1999.
486. Tao X, Lee A, Limapichat W, Dougherty DA, MacKinnon R. A gating charge transfer center in voltage sensors. *Science* 328: 67–73, 2010.
487. Taylor AR, Brownlee C. A novel Cl⁻ inward-rectifying current in the plasma membrane of the calcifying marine phytoplankton *Coccolithus pelagicus*. *Plant Physiol* 131: 1391–1400, 2003.
488. Taylor AR, Brownlee C, Wheeler GL. Proton channels in algae: reasons to be excited. *Trends Plant Sci* 17: 675–684, 2012.
489. Taylor AR, Chrachri A, Wheeler G, Goddard H, Brownlee C. A voltage-gated H⁺ channel underlying pH homeostasis in calcifying coccolithophores. *PLoS Biol* 9: e1001085, 2011.
490. Thomas EL, Grisham MB, Jefferson MM. Myeloperoxidase-dependent effect of amines on functions of isolated neutrophils. *J Clin Invest* 72: 441–454, 1983.
491. Thomas MP, Chartrand K, Reynolds A, Vitvitsky V, Banerjee R, Gendelman HE. Ion channel blockade attenuates aggregated alpha synuclein induction of microglial reactive oxygen species: relevance for the pathogenesis of Parkinson's disease. *J Neurochem* 100: 503–519, 2007.

492. Thomas RC, Meech RW. Hydrogen ion currents and intracellular pH in depolarized voltage-clamped snail neurones. *Nature* 299: 826–828, 1982.
493. Tiwari-Woodruff SK, Schulteis CT, Mock AF, Papazian DM. Electrostatic interactions between transmembrane segments mediate folding of Shaker K⁺ channel subunits. *Biophys J* 72: 1489–1500, 1997.
494. Tombola F, Pathak MM, Isacoff EY. How far will you go to sense voltage? *Neuron* 48: 719–725, 2005.
495. Tombola F, Pathak MM, Isacoff EY. Voltage-sensing arginines in a potassium channel permeate and occlude cation-selective pores. *Neuron* 45: 379–388, 2005.
496. Tombola F, Ulbrich MH, Isacoff EY. Architecture and gating of Hv1 proton channels. *J Physiol* 587: 5325–5329, 2009.
497. Tombola F, Ulbrich MH, Isacoff EY. The voltage-gated proton channel Hv1 has two pores, each controlled by one voltage sensor. *Neuron* 58: 546–556, 2008.
498. Tombola F, Ulbrich MH, Kohout SC, Isacoff EY. The opening of the two pores of the Hv1 voltage-gated proton channel is tuned by cooperativity. *Nat Struct Mol Biol* 17: 44–50, 2010.
499. Tu CK, Silverman DN, Forsman C, Jonsson BH, Lindskog S. Role of histidine 64 in the catalytic mechanism of human carbonic anhydrase II studied with a site-specific mutant. *Biochemistry* 28: 7913–7918, 1989.
500. Turekian KK. *Oceans*. Englewood Cliffs, NJ: Prentice-Hall, 1968.
501. Unal ES, Zhao R, Chang MH, Fiser A, Romero MF, Goldman ID. The functional roles of the His²⁴⁷ and His²⁸¹ residues in folate and proton translocation mediated by the human proton-coupled folate transporter SLC46A1. *J Biol Chem* 284: 17846–17857, 2009.
502. Valiyaveetil FI, Fillingame RH. Transmembrane topography of subunit a in the *Escherichia coli* F₁F₀ ATP synthase. *J Biol Chem* 273: 16241–16247, 1998.
503. Van Helden D, Hamill OP, Gage PW. Permeant cations alter endplate channel characteristics. *Nature* 269: 711–713, 1977.
504. Venkataraman P, Lamb RA, Pinto LH. Chemical rescue of histidine selectivity filter mutants of the M2 ion channel of influenza A virus. *J Biol Chem* 280: 21463–21472, 2005.
505. Venosa RA, Kotsias BA, Horowicz P. Frog striated muscle is permeable to hydroxide and buffer anions. *J Membr Biol* 139: 57–74, 1994.
506. Vissers MC, Winterbourn CC. Oxidation of intracellular glutathione after exposure of human red blood cells to hypochlorous acid. *Biochem J* 307: 57–62, 1995.
507. Von Ballmoos C, Wiedenmann A, Dimroth P. Essentials for ATP synthesis by F₁F₀ ATP synthases. *Annu Rev Biochem* 78: 649–672, 2009.
508. Von Dassow P, Latz MI. The role of Ca²⁺ in stimulated bioluminescence of the dinoflagellate *Lingulodinium polyedrum*. *J Exp Biol* 205: 2971–2986, 2002.
509. Vulcu SD, Liewald JF, Gillen C, Rupp J, Nawrath H. Proton conductance of human transient receptor potential-vanilloid type-1 expressed in oocytes of *Xenopus laevis* and in Chinese hamster ovary cells. *Neuroscience* 125: 861–866, 2004.
510. Wain HM, Bruford EA, Lovering RC, Lush MJ, Wright MW, Povey S. Guidelines for human gene nomenclature. *Genomics* 79: 464–470, 2002.
511. Wang C, Lamb RA, Pinto LH. Activation of the M2 ion channel of influenza virus: a role for the transmembrane domain histidine residue. *Biophys J* 69: 1363–1371, 1995.
512. Wang Y, Li SJ, Pan J, Che Y, Yin J, Zhao Q. Specific expression of the human voltage-gated proton channel Hv1 in highly metastatic breast cancer cells, promotes tumor progression and metastasis. *Biochem Biophys Res Commun* 412: 353–359, 2011.
513. Wang Y, Li SJ, Wu X, Che Y, Li Q. Clinicopathological and biological significance of human voltage-gated proton channel Hv1 over-expression in breast cancer. *J Biol Chem* 287: 13877–13888, 2012.
514. Warner JA, MacGlashan DW Jr. Signal transduction events in human basophils. A comparative study of the role of protein kinase C in basophils activated by anti-IgE antibody and formyl-methionyl-leucyl-phenylalanine. *J Immunol* 145: 1897–1905, 1990.
515. Weidema AF. *Ion Channels and Ion Transport in Chicken Osteoclasts* (PhD dissertation). Leiden, The Netherlands: Rijksuniversiteit te Leiden, 1995.
516. Weiss SJ, Klein R, Slivka A, Wei M. Chlorination of taurine by human neutrophils. Evidence for hypochlorous acid generation. *J Clin Invest* 70: 598–607, 1982.
517. Wicke E, Eigen M, Ackermann T. über den Zustand des Protons (Hydroniumions) in wässriger Lösung. *Z physikalische Chemie* 1: 340–364, 1954.
518. Wikström M, Verkhovsky MI, Hummer G. Water-gated mechanism of proton translocation by cytochrome c oxidase. *Biochim Biophys Acta* 1604: 61–65, 2003.
519. Winterbourn CC. Reconciling the chemistry and biology of reactive oxygen species. *Nat Chem Biol* 4: 278–286, 2008.
520. Winterbourn CC, Hampton MB, Livesey JH, Kettle AJ. Modeling the reactions of superoxide and myeloperoxidase in the neutrophil phagosome: implications for microbial killing. *J Biol Chem* 281: 39860–39869, 2006.
521. Wood ML, Schow EV, Freitas JA, White SH, Tombola F, Tobias DJ. Water wires in atomistic models of the Hv1 proton channel. *Biochim Biophys Acta* 2011.
522. Woodward OM, Willows AO. Dopamine modulation of Ca²⁺ dependent Cl⁻ current regulates ciliary beat frequency controlling locomotion in *Tritonia diomedea*. *J Exp Biol* 209: 2749–2764, 2006.
523. Wraight CA. Chance and design—proton transfer in water, channels and bioenergetic proteins. *Biochim Biophys Acta* 1757: 886–912, 2006.
524. Wu B, Steinbronn C, Alsterfjord M, Zeuthen T, Beitz E. Concerted action of two cation filters in the aquaporin water channel. *EMBO J* 28: 2188–2194, 2009.
525. Wu LJ, Wu G, Sharif MR, Baker A, Jia Y, Fahey FH, Luo HR, Feener EP, Clapham DE. The voltage-gated proton channel Hv1 enhances brain damage from ischemic stroke. *Nat Neurosci* 15: 565–573, 2012.
526. Wu Y, Ilan B, Voth GA. Charge delocalization in proton channels. II: the synthetic LS2 channel and proton selectivity. *Biophys J* 92: 61–69, 2007.
527. Yagisawa M, Yuo A, Yonemaru M, Imajoh-Ohmi S, Kanegasaki S, Yazaki Y, Takaku F. Superoxide release and NADPH oxidase components in mature human phagocytes: correlation between functional capacity and amount of functional proteins. *Biochem Biophys Res Commun* 228: 510–516, 1996.
528. Yamashita T, Someya A, Hara E. Response of superoxide anion production by guinea pig eosinophils to various soluble stimuli: comparison to neutrophils. *Arch Biochem Biophys* 241: 447–452, 1985.
529. Yang N, George AL Jr, Horn R. Molecular basis of charge movement in voltage-gated sodium channels. *Neuron* 16: 113–122, 1996.
530. Yang N, George AL Jr, Horn R. Probing the outer vestibule of a sodium channel voltage sensor. *Biophys J* 73: 2260–2268, 1997.
531. Yang N, Horn R. Evidence for voltage-dependent S4 movement in sodium channels. *Neuron* 15: 213–218, 1995.
532. Yang S, Cui Q. Glu-286 rotation and water wire reorientation are unlikely the gating elements for proton pumping in cytochrome c oxidase. *Biophys J* 101: 61–69, 2011.
533. Yarov-Yarovoy V, DeCaen PG, Westenbroek RE, Pan CY, Scheuer T, Baker D, Catterall WA. Structural basis for gating charge movement in the voltage sensor of a sodium channel. *Proc Natl Acad Sci USA* 109: E93–102, 2012.
534. Yatsuyanagi J, Ogiso T. Zinc inhibition of respiratory burst in zymosan-stimulated neutrophils: a possible membrane action of zinc. *Chem Pharm Bull* 36: 1035–1040, 1988.
535. Yazdanbakhsh M, Eckmann CM, De Boer M, Roos D. Purification of eosinophils from normal human blood, preparation of eosinoplasts and characterization of their functional response to various stimuli. *Immunology* 60: 123–129, 1987.
536. Yusaf SP, Wray D, Sivaprasadarao A. Measurement of the movement of the S4 segment during the activation of a voltage-gated potassium channel. *Pflügers Arch* 433: 91–97, 1996.
537. Zhou HX. A theory for the proton transport of the influenza virus M2 protein: extensive test against conductance data. *Biophys J* 100: 912–921, 2011.
538. Zhou J, Sharp LL, Tang HL, Lloyd SA, Billings S, Braun TF, Blair DF. Function of protonatable residues in the flagellar motor of *Escherichia coli*: a critical role for Asp 32 of MotB. *J Bacteriol* 180: 2729–2735, 1998.